The University Of Sheffield.

UK Atomic Energy Authority

Employing Additive Manufacturing for Fusion High Heat Flux Structures

A. David L. Hancock

A thesis submitted in partial fulfilment of the requirements
for the degree of Doctor of Philosophy

The University of Sheffield
Faculty of Engineering
Department of Materials Science and Engineering

United Kingdom Atomic Energy Authority

26th June 2018

The more the words, the less the meaning,
and how does that profit anyone?

Ecclesiastes 6:11 [NIV]

Wisdom, like an inheritance, is a good thing
and benefits those who see the sun.

Ecclesiastes 7:11 [NIV]

Abstract

The commercial realisation of nuclear fusion power will require advanced engineering solutions including high heat flux components with higher performance, greater reliability, and longer lifetimes. Additive manufacturing (AM) provides opportunities to produce components with previously unachievable geometries in new and hard-to-manufacture materials. This project introduces the state of the art of fusion high heat flux components and AM and then focusses on applying laser powder bed fusion to high temperature divertor designs. Much of the work was carried out in parallel to the EU FP7 AMAZE project (Additive Manufacturing Aiming towards Zero waste and Efficient production of high-tech metal products).

A review of material selection for divertor applications is carried out with an emphasis on the cooled substructure. A parallel, strengths-based approach is undertaken concluding in a series of SWOT (strengths, weaknesses, opportunities, threats) analyses rather than a traditional linear downselection. Material properties including strength, ductility, thermal expansion, and thermal conductivity are graphically presented as well as derived figures of merit for thermal stress and thermal mismatch with tungsten armour. Radiation damage and compatibillity with operational and manufacturing environments are considered and historical summaries of availability and cost are given. By emphasising high temperature operation and acknowledging the inevitability of some nuclear activation beyond the usual 100 year limit, refractory metals and their alloys present themselves as promising candidates, particularly those based on vanadium, tantalum, and molybdenum. A shortage of data for these materials is highlighted, particularly under fusion neutron irradiation, as well as the need for greater understanding of corrosion under relevant conditions.

Two novel divertor cooling schemes are then presented and evaluated via concept-level tile-type geometries. The first is a design with multiple small pipes fed from the rear of the component via an in-built manifold and the second employs an enclosed pin-fin array drawing inspiration from the electronics industry. Both highlight features made feasible only by employing AM and use tantalum as the structural material to demonstrate the effect of high-temperature operation on performance. 1D analytical calculations and simple finite element modelling with 150 °C and 600 °C coolant and up to 10 MW m^{-2} heat flux loading demonstrate improved heat transfer coefficients and more uniform temperature distributions. Performance improvement over conventional designs is likely to be marginal without significant further design optimisation, but the up to 80% reduction in material use compared with conventional concepts, higher thermal efficiency, and opportunity to reduce or relocate pipe joints are highlighted as more significant advantages.

Work to develop laser powder bed fusion of tungsten, molybdenum, and tantalum is then presented. First, a summary of context and recent related work is given. A through-lifecycle approach to component development is detailed with the aim of giving an insight into critical issues related to supply chain, process development, material testing, and component build trials. Basic characterisation of size, morphology, and flowability of a selection of powders is used to demonstrate the high variability of current supply. This is followed by determination of first-order build parameters and energy density required for consolidation. Persistent cracking is found, particularly in tungsten and molybdenum, and causes including oxidation and residual stress are posited with suggestions for possible approaches to mitigating these. The results of material testing of small samples are given, including dilatometry, laser flash, and small punch. Small sample numbers and high variablity prevent definitive conclusions from being drawn, but trends towards increased brittleness and decreased thermal conductivity are shown and there are indications that the extreme thermal conditions during processing produce β and ω phases of tantalum.

Finally a description of a new facility is given, HIVE (Heating by Induction to Verify Extremes), as well as the results of comparative high heat flux testing of two simple copper components - one produced by electron beam melting (EBM) and the other conventionally manufactured. HIVE can apply a constant 10 MW m^{-2} to a 30 mm x 30 mm testpiece in vacuum which can be cooled using a 200 °C cooling water supply. Thermocouples, thermography, and water calorimetry provide instrumentation. This facility acts as a strategic and previously unavailable intermediate concept validation step between analytical modelling and plasma-surface interaction testing or in-situ qualification. The results presented suggest that convective heat transfer is enhanced by the rough surface of the AM copper part, but that the component's lower thermal conductivity through the AM copper and across the brazed joint compared to the conventional results in a higher bulk temperature for the same input power indicating a lower overall heat flux handing capability.

The project concludes with a summary of key findings and suggestions for future work.

Acknowledgements

This work has been carried out within the framework of the EUROfusion Consortium and has received funding from the Euratom research and training programme 2014-2018 under grant agreement No 633053. This project has also received funding from the European Union's Seventh Framework Programme for research, technical development, and demonstration under the AMAZE project (Additive Manufacturing Aiming towards Zero waste and Efficient production of high-tech metal Products) [grant agreement no 313781].
The views and opinions expressed herein do not necessarily reflect those of the European Commission.
This work has also been part- funded by the RCUK Energy Programme [grant number EP/P012450/1].
To obtain further information on the data and models underlying this document please contact publicationsmanager@ukaea.uk.

Personal Thanks

I am sincerely thankful for the wealth of support and encouragement I have received throughout the last few years. While I could not possibly include a full list of all those people to whom I am indebted, I would particularly like to thank a few explicitly:

- Those in senior management at UKAEA who agreed to release me full-time to work on this myself, rather than recruiting a "real" student (as originally intended!)
- AMAZE partners who agreed my taking the lead in direction and publication of much of what follows. The ability to tie this thesis to a concrete application and draw on a wide range of collaborative efforts has enriched the work immeasurably beyond what I could have achieved alone.
- Members of the Birmingham University AMPLab, for generously providing access to their facilities and giving up valuable time and wisdom to support experimental work which would not have been otherwise possible.
- UKAEA colleagues who graciously and uncomplainingly liberated me from the bulk of AMAZE and HIVE project administration.
- Iain Todd, Brad Wynne, Mike Porton, and Dave Homfray as supervisors have variously fought my battles, stoked and tempered my frequently over-ambitious aspirations and expectations, corrected my follies (and my grammar), and have never failed to reassure me that the end was in sight.
- Last, and most of all, my family who have borne with me through the long days, frequent frustrations, and ever receding deadlines.

Contents

1

Introduction: Thesis Context and Structure

1 Introduction and research motivation

Since the dawn of the nuclear age in the 1930s, nuclear fusion has been sought after as the cleaner, safer, and more fuel-abundant counterpart to nuclear fission as a source of energy. The realisation of controlled fusion reactions for sufficient durations and at physical scales suitable for use in power stations was among the greatest physics challenges of the 20$^{\text{th}}$ century. In turn, the harnessing of these reactions for the production of electricity, within the constraints of designing practical, safe, and economically viable power plants has now become one of the greatest engineering and materials science challenges of the 21$^{\text{st}}$ century. This move from the research to the delivery phase of development requires advanced engineering solutions, novel materials, and new manufacturing methods if fusion electricity on the grid is to be viable. Chief among these challenges is the need for high heat flux components for the fusion reactor first wall with higher performance, greater reliability, and longer lifetimes.

One such technology with the potential for widening the design window for fusion components is additive manufacturing (AM). AM is by no means a new technology, with the earliest commercial systems available as early as the late 1980s, but recent years have been marked by a significant growth in the volume of research into AM, accompanied by a shift from use as primarily a prototyping tool to increased adoption as a manufacturing option where complex geometries, efficient use of feedstock material, or low lead times for small part counts are a priority. Much of this industrial effort has been focussed on medical, aerospace, and automotive applications (and to a much lesser extent fission); seeking to deploy standards for the use of a small number of historically conventional materials. The timing is right, however, to engage stakeholders across the AM component lifecycle; namely material suppliers, AM platform manufacturers, end users, and regulatory bodies; if the interests of additional industries are to be well represented.

Both fusion energy research and AM are fields undergoing rapid transition; the former from a predominantly plasma physics dominated pure science exercise to one in which engineering, industrial, and increasingly commercial considerations are the driving force; the latter from a niche (if highly publicised) technical curiosity to a mainstream tool in manufacturer's arsenal across a range of applications. This includes tightly regulated industries such as the nuclear and aerospace sectors which require very well characterised material and part performance with a large body of supporting evidence available before adopting new manufacturing techniques or materials. Both the AM and fusion fields consist of disparate networks of researchers with (in most cases) limited resources. Fusion has its home in academia and public sector laboratories worldwide, which, although historically better than average for their extensive collaborative history, is still prone to either duplication of effort or over-adherence to pet projects. AM's best resourced effort is carried out in siloed and competing corporate R&D departments with a specific product or sales strategy in mind. As AM becomes more established as an industrial process, the less well resourced academics are fighting against the movement from an open and investigative methodology for process development and innovative materials towards the sale of closed, packaged "AM solutions" tailored to those industries prepared to pay for them.

The confluence of the need for advanced engineering solutions for fusion to facilitate commercialisation and the opportunities that AM provides at this strategic point in its adoption provide the motivation for this project — namely to apply AM to the problem of fusion, and specifically to apply AM of refractory metals to fusion high heat flux components. Both the application and the proposed solution are highly integrated and cross-disciplinary problems requiring a holistic approach drawing on historical wisdom and the current state of the art. At the same time, the increased freedom of component geometry and material provided by AM allows a fresh re-evaluation of accepted conventions and design priorities. This project therefore aims to investigate the application of additive manufacturing to fusion high heat flux components. To this end, the following outcomes will be pursued:

- Re-evaluate material choices for fusion high heat flux component design. This will be done with a focus on improving component performance through high temperature operation but will also consider manufacturing processes.
- Assess the benefits of novel concepts enabled by additive manufacturing. This will include thermal and stress analysis of representative thermal management geometries but will also consider other criteria including manufacturability, weight reduction, and material usage.
- Contribute to the maturity of AM processing of the candidate high temperature materials selected above. This will include determining the influence of build parameters on consolidation and investigating the resulting thermal and mechanical properties.
- Validate the concepts and materials developed through the project via testing. This will include high heat flux testing of any prototypes produced and will compare their performance with conventionally manufactured alternatives.

Throughout the project, tools and processes will be developed to support these objectives. These will assist the future development of concept designs as well as helping to identify the most strategic research opportunities

2 Project Structure

Having identified the need for improved high heat flux component designs and the potential for AM to contribute to the realisation of these designs, the project follows this route:

Research Context:
Introductions to fusion, to fusion high heat flux components, and to AM technologies.

Paper 1:
Refractory Metals as Structural Materials for Fusion High Heat Flux Components
The work begins with a re-examination of the material options available to fusion engineers with a focus on the structural part of the component, high temperature operation, and a broader, parallel, strengths-based evaluation methodology. This has the aim of identifying potential candidate elements and alloys and directing future research to fill in gaps in required knowledge rather than making a fixed recommendation, though a number of refractory metals are identified as particularly promising.

Paper 2:
Exploring Complex High Heat Flux Geometries for Fusion Applications Enabled by Additive Manufacturing
Using the outcomes of the material selection exercise, novel cooling geometries are proposed and analysed, focussing on features and materials made available by AM and heretofore unfeasible. Using two preliminary designs, the potential benefits of AM are highlighted, paving the way to more optimised concept development.

Paper 3:
Additive Manufacturing of High Temperature Materials for Fusion: A Review of Recent Work, Strategies, and Future Outlook
The acceptance of these concepts depends not only on their design, however, as the AM of refractory metals for fusion is still very much in its infancy. The current state of the art is therefore summarised, and the results of work are presented towards progressing the field which have been carried out as part of a wider collaborative effort. This work enables a strategic assessment of weaknesses in the supply chain and lifecycle, including feedstock supply, platform functionality, and material testing.

Paper 4:
Testing Advanced Divertor Concepts for Fusion Power Plants Using a Small High Heat Flux Facility
Finally, the results of early prototype testing are presented, including a description of a new facility developed for the purpose which provides a much needed intermediate step between analytical modelling and costly and time consuming in-situ qualification or plasma-surface interaction testing.

Conclusions and further research:
The research is summarised and a collection of proposals for follow-on projects is given which acts as a broad blueprint for moving forward in this exciting and complex field.

Throughout the project there have been four core fundamentally interrelated activities, the interactions between which are broadly visualised in figure 1. Each activity is informed by at least two others. As labelled, "objectives" define the aims and scope of the activity, and "limits" provide quantitative boundaries and requirements within which the task must be carried out.

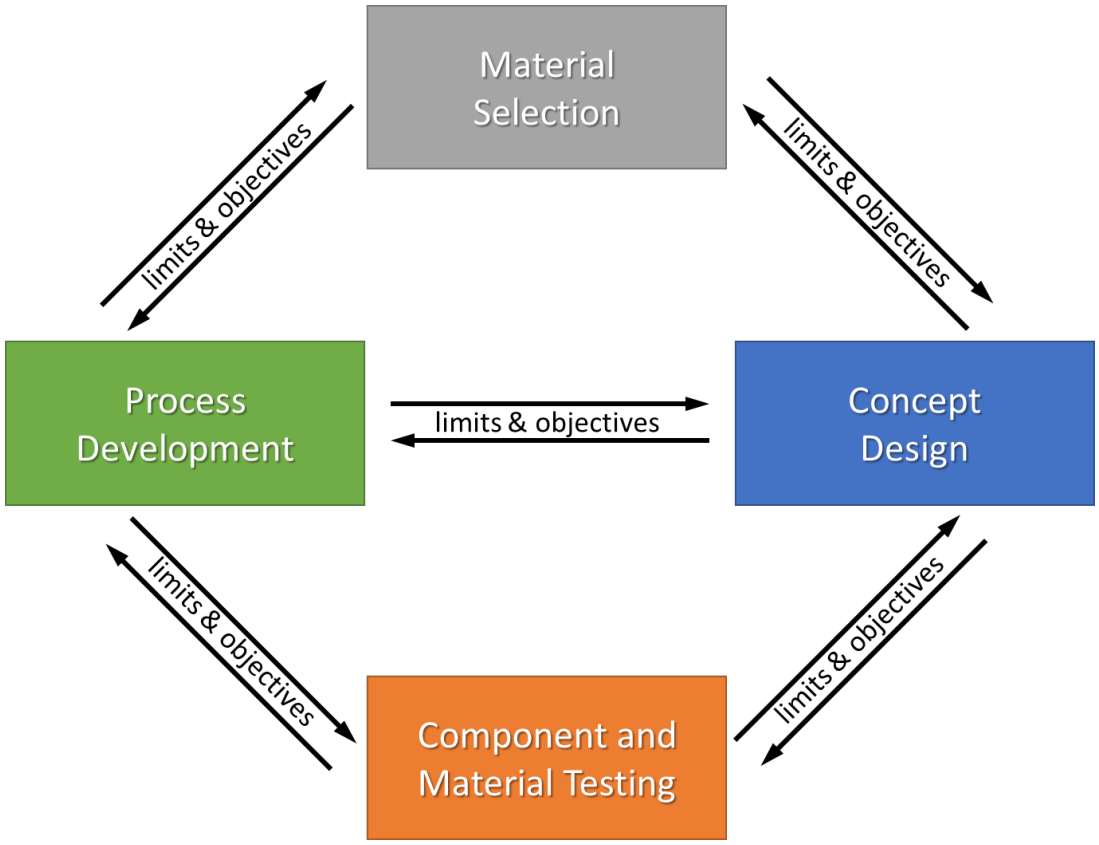

Figure 1: Relationships between project activities

A few examples of these interactions are given below:

- The **objective** of high temperature operation is fed from concept design to the material selection, which in turn provides both a candidate material and the **limits** at which it can operate.
- The **objective** of complex internal geometry for heat transfer enhancement informs the choice of AM technology process development which in turn provides design guide **limits** such as wall thickness and overhang size.
- The results of component and material testing provide design **limits** for concept design and provide **objectives** for strategic process development.
- The success or failure of process development on a particular material provides **limits** to the material selection process which in turn can supply alternative **objectives** for alloy development.

This complex web of relationships lends itself to an iterative and parallel design and development process rather than a sequential progression. The outcome of the project is therefore as much to highlight the challenges and propose a methodology for attacking the problem it as to solve the problem itself.

3 Research Context: Nuclear Fusion

3.1 Overview of nuclear fusion and the tokamak

In the context of increasing global demand for energy (figure 2) and an increasingly overwhelming global consensus that our dependance on fossil fuels for energy must change, nuclear fusion promises clean, safe, and abundant electricity via the combination of small nuclei to release large amounts of energy with only non-toxic helium and limited quantities of short-lived low and medium level nuclear waste as byproducts [1].

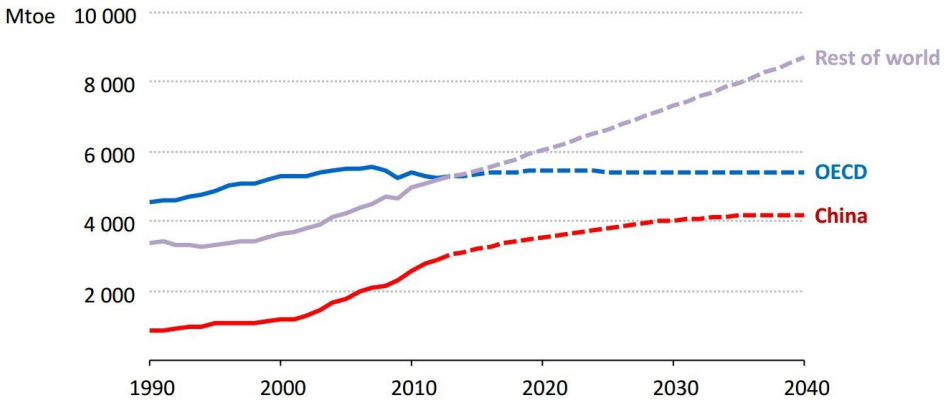

Figure 2: Predicted global energy consumption [2]

The main fusion reaction studied for use in power generation uses two hydrogen isotopes, deuterium and tritium, due to the reaction's relatively high cross section, low Coulomb threshold, and high gain [3]. When deuterium and tritium fuse, they release a high energy 14 MeV neutron and a lower, 3.5 MeV helium nucleus as shown in figure 3.

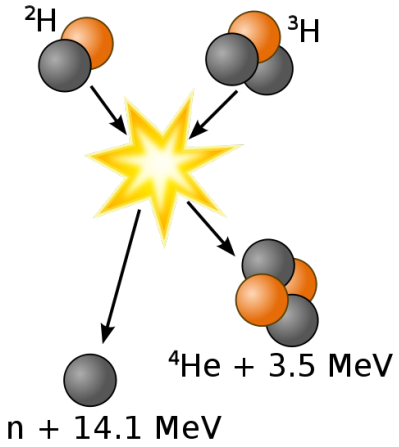

Figure 3: Schematic representation of a deuterium-tritium reaction.

One of the leading technologies aiming towards the commercial harnessing of fusion energy is magnetic confinement fusion, whereby a plasma of deuterium and tritium fuel is held within a cage of magnetic coils and heated to a point where the nuclei fuse. The most developed of a number of magnetic confinement configurations is the tokamak [4]. As shown in figure 4, the tokamak is a toroidal or donut-shaped machine consisting of a vacuum vessel surrounded by an arrangement of coils as follows:

Toroidal field coils are D-shaped coils wrapped poloidally around the vacuum vessel generating a toroidal field which confines the charged particles of the plasma.

A central solenoid acts as the primary coil of a transformer, the secondary coil being the single turn of plasma. Current induced in the plasma by the central solenoid provides ohmic heating and produces a poloidal field, twisting the field lines into a spiral within the vessel and further confining and compressing the plasma.

Poloidal field coils are wrapped toroidally, either inside or outside the D-shaped toroidal field coils and vacuum vessel to further shape and control the plasma.

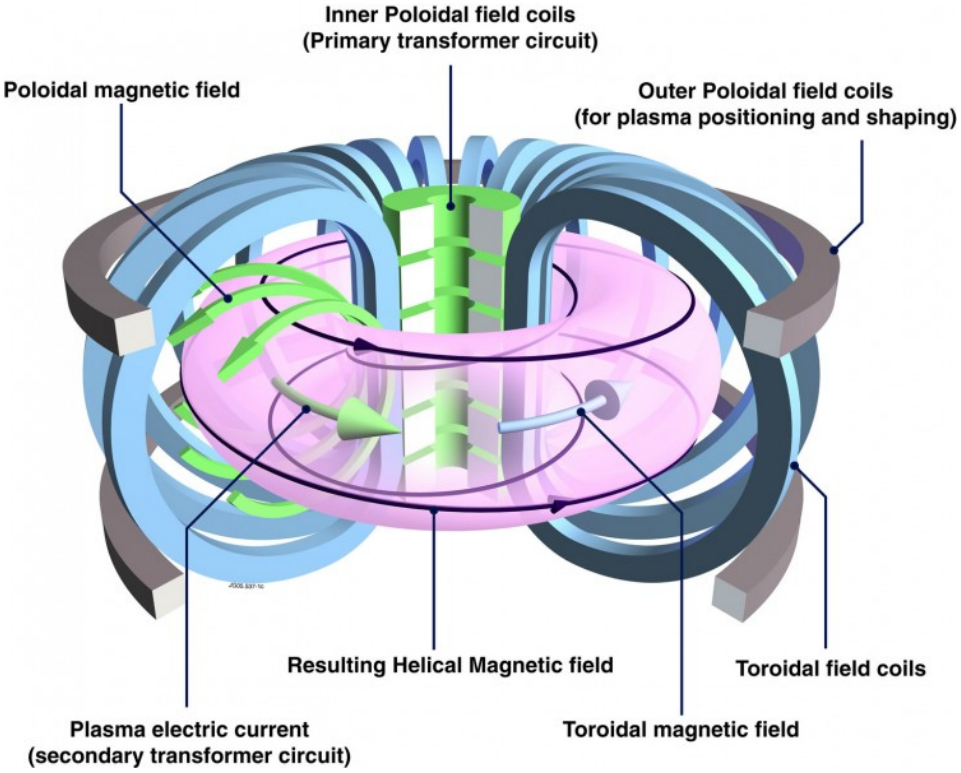

Figure 4: Schematic representation of a tokamak [5]

Additional smaller coils placed inside the vessel may also be used for diagnostics or fine control.

The neutrons generated by the fusion reactions, being uncharged, escape the magnetic confinement and are absorbed in lithium-rich blanket modules around the walls of the vessel where they deposit their energy, heating a primary coolant for a power cycle.

Tritium does not occur naturally in nature due to its relatively short 12.3 year half-life. Estimates of global resource place the quantity of tritium available for fusion as somewhere between 20 kg and 50 kg, enough to operate a 1 GW fusion plant around a month [6, 7]. Serendipitously, lithium, as well as being an excellent absorber of high energy neutrons, can be used to produce tritium via a secondary fission reaction, as shown in figure 5.

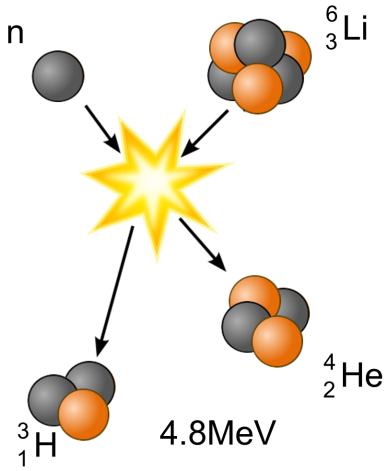

Figure 5: Schematic representation of a neutron-lithium tritium breeding reaction.

The raw fuel materials for a fusion power station are, therefore, deuterium and lithium, both of which are abundantly available and easily extracted from seawater [8, 9]. Estimates of the precise quantity of these fuels required vary somewhat, but the European Union fusion research organisation Eurofusion states that, *"A fusion power station could produce as much electricity from the lithium of one laptop battery and half a bath of water as burning 40 tons of coal."* This corresponds to a 1 GW fusion power station using 20 g of tritium and 13 g of deuterium per hour [10].

Past and current machines have made significant progress over the last six decades demonstrating the physics and

technological feasibility of fusing the raw constituents of deuterium and tritium at 200 million°C in a well controlled and sustainable way [4]. The Joint European Torus (JET) in Oxfordshire, UK, for example, has produced up to 16 MW of fusion power over a short period of time [11]; ToreSupra, in France, has operated at high power for several minutes; [12] and SST-1 in India is designed to operate for over 1000 seconds [13].

ITER (latin for "the way [to fusion power]") is the result of a global consortium effort, and is currently under construction in Caderache, France. ITER is designed to produce significant 500MW of fusion power for up to 600s and demonstrate the technical and physics basis for fusion power [14]. Figure 6 shows an image of the ITER design with some of the key components labelled.

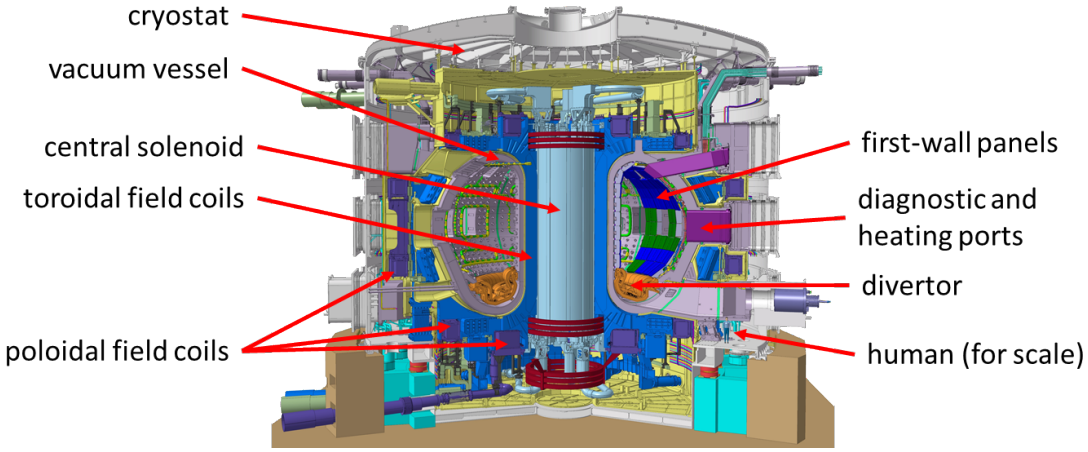

Figure 6: Schematic diagram of ITER [14]

The next step for fusion scientists and engineers is to develop and realise a design for a machine that will demonstrate the viability of commercial electricity production by fusion power. This machine is generically referred to as "DEMO" (an abbreviation of DEMOnstration Power Plant) within the European fusion community [1]. An artist's impression of such a facility is shown in figure 7.

Development, qualification, and utilisation of materials for use in DEMO and subsequent fusion power plants is probably the most significant hurdle to overcome for commercialisation of fusion power [15, 16]. At the same time, there is a particular need to develop improved components to handle the high heat fluxes imposed on the inner walls of the vessel, particularly in the divertor region, as explained in the following sections.

3.2 Fusion high heat flux components: the divertor

As explained in section 3.1, most of the energy released from the fusion reactions is in the form of high energy neutrons and it is this which will primarily be used to drive the power cycle of a fusion power plant [17]. The remainder is imparted to the helium nuclei (also referred to as alpha particles) formed in the reaction. These alpha particles perform an essential function as they, themselves, provide heating to sustain the reaction, but this process is not 100% efficient and unused power from these high energy particles must also be managed. In addition, in order for the fusion reaction to be sustained, stable, and efficient, this helium and other waste products such as dust and impurities from the inner walls of the machine must be removed from the plasma.

These goals are achieved by allowing the plasma to contact the vessel walls at set locations, either by using "limiters" at the mid-plane or shaping the magnetic field into what is known as a "divertor" configuration. For reasons beyond the scope of this report, machines with divertor configurations allow higher performance plasma operations [18, 19], and as such most currently operational and all planned tokamaks use variations on this arrangement. One such configuration, the most commonly used, known as "single-null" is shown in figure 8. More massive particles drift outwards from the core of the plasma into a region known as the "scrape-off-layer" or "SOL" and are then transported along the outermost field lines and impact on specialised regions of the vessel wall, the divertor "target" plates, from where they are pumped out of the vessel either to be recycled or disposed of.

Alternative divertor configurations are also possible and some are currently under investigation for use in DEMO [20]. Some of these focus on lengthening the distance between the x-point and the divertor targets or modifying the field in this region to allow particles to lose more energy by radiative processes before striking the target [21, 22]. Other configurations include multiple x-points to share the deposited power between them [23, 24]. The primary goal of all of these alternative configurations is to reduce the peak power deposition on the divertor target, with a secondary benefit often being to shield the divertor targets from some of the neutron flux from the core plasma. Although the final choice of divertor configuration will have a significant impact on the peak and steady-state particle and heat flux on the divertor targets, the core requirements as outlined in the following sections remain the same.

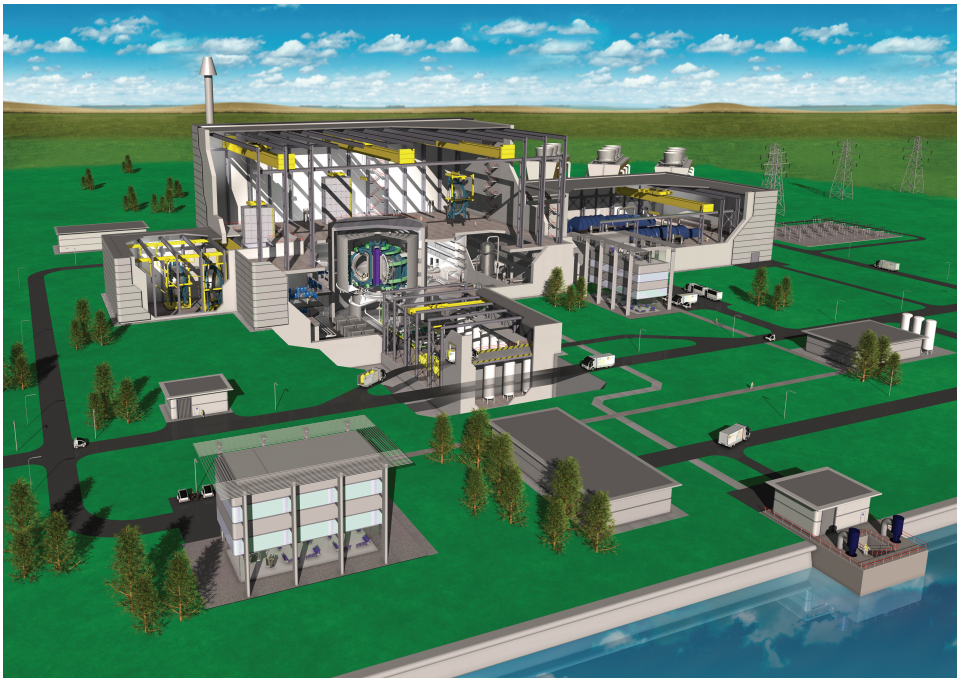

Figure 7: An artist's impression of a fusion power plant [5].

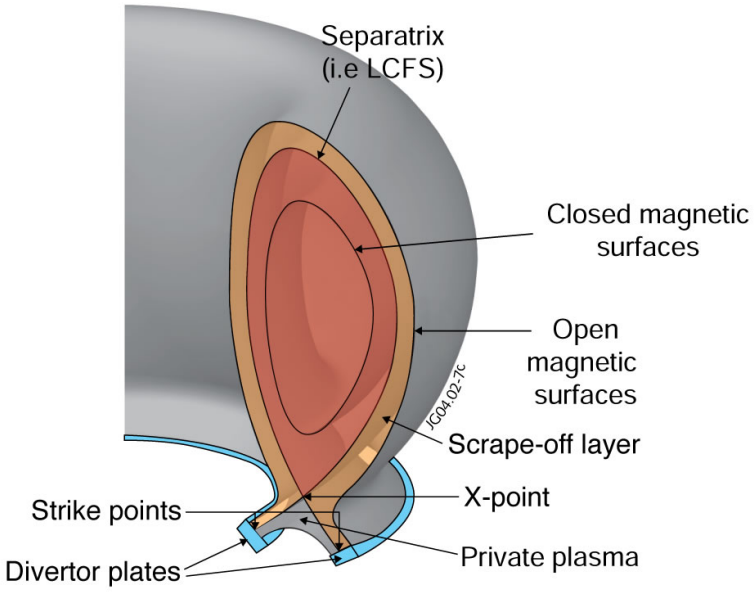

Figure 8: "Single-null" divertor configuration [5].

3.3 Divertor target design requirements

This section outlines the key design requirements and covers the priorities for divertor target design. These are also outlined in more detail in the 2012 EFDA PEX report [25].

Temperature

Temperature limits of in-vessel components are currently largely set by material limitations [15]. Lower bounds are usually set above the ductile to brittle transition temperatures (DBTT) for structural materials and upper bounds are set either by the onset of significant creep effects or, for non-structural materials, by temperatures at which functional properties such as thermal or electrical conductivity are degraded. In the case of tungsten armour on divertor target tiles, for example, an upper bound of 1300 °C was previously set due to the onset of recrystallisation. More recently, following as yet unpublished results, this has been relaxed to allow up to 1700°C on the heated face [26].

Vacuum

In common with all in-vessel fusion components, the divertor must be suitable for use in ultra high vacuum ($< 10^{-9} mbar$). This places constraints on material outgassing and absorption, as well as on methods of joining and manufacturing techniques [27].

Particle flux and erosion

The divertor target is subject to high fluences of high-energy particles. These particles impart energy to the surface, generating heat, but also cause sputtering of surface atoms [28]. This will cause erosion and redeposition of the target surface. The current baseline value for the rate of tungsten erosion is 2 mm per full-power year of operation [29] but this is highly dependant on plasma parameters and unknown neutron irradiation impact and may prove optimistic. Solutions are therefore being sought for ways to replace the tungsten armour in-situ [30, 31, 32]. As well as causing erosion, high energy particle flux embeds ions in the armour material and can cause additional surface modifications and potential material property degradation including the generation of tungsten "fuzz" [33].

Radiation

As well as being subject to significant high-energy ion fluence, the divertor region is subject to neutron and electromagnetic radiation [34]. 14 MeV neutrons from the fusion reactions cause material damage due to induced dislocations, helium production, and transmutation as well as generating internal heating. These damage mechanisms cause changes in DBTT, increased hardness, swelling, and decreases in thermal conductivity. [35, 36]. Electromagnetic radiation imposes an additional surface and volumetric heat flux. Plasma parameters and divertor geometry have a significant effect on the size of these effects as outlined in section 3.2 so current designs use parameters from centrally agreed baseline DEMO designs [37].

Tritium absorption and retention

Tritium, as previously stated, is both a scarce resource and a radioactive isotope. This creates both cost and safety requirements. Controls must therefore be in place to strictly control the tritium inventory on site at a power station, imposing challenging requirements on the recycling plant requirements [38], and on the tritium absorbed into the in-vessel components [39]. For the divertor target, this means selecting materials into which tritium does not easily diffuse or in which tritium is not tightly held. Where tritium does diffuse through the target structure into the coolant, the feasibility of detritiation must be considered.

Maintenance and lifetime

Cost and availability modelling for a baseline DEMO design has placed a requirement on the lifetime of divertor components of two full power years [40]. This makes the divertor target a regularly replaced component over the lifetime of a fusion power plant. Activation within the vessel means that all such maintenance tasks must be performed via remote handling [41]. The divertor target (or a cassette assembly carrying the target) must therefore be removable and replaceable remotely, and this must be considered at every stage of design.

3.4 State of the art of divertor target design

3.4.1 Past and present machines

Compared to the latest research machines and future fusion reactors, the design and materials selection requirements on divertors in past fusion devices have been significantly less stringent due to relatively low heat loads and neutron fluences and shorter pulse durations, eliminating the need for actively cooled components, and allowing inertial cooling between pulses.

Early machines used bare steel walls, gradually upgrading to carbon in the form of graphite [42, 21] or carbon fibre composites (CFC) as heat fluxes increased. As reducing tritium absorption and dust generation became increasingly critical, metallic beryllium and tungsten have become the materials of choice [18]. When the first wall of JET, the largest operating fusion experiment, was replaced in 2011 [43] a passively cooled tungsten divertor target was chosen as shown in figure 9 with the remaining in-vessel components either beryllium or tungsten-coated CFC.

More recently, in order to test plasmas with more representative divertor power fluxes and in preparation for ITER, a number of machines have installed water cooled divertor targets; most notably the WEST upgrade to ToreSupra in France and EAST in China [45, 46]. Experiments have also been undertaken with liquid plasma facing components, e.g. [47].

3.4.2 ITER

The ITER divertor target design is a water-cooled tungsten monoblock with a copper-chrome-zirconium pipe and compliant copper interlayer, as shown in figure 10. Sintered tungsten blocks are plated with a 0.5 mm copper layer on the inner face and then threaded onto the pipe, before being joined using hot radial pressing [48].

The path to this design is well documented in Hirai et al. [50], Pitts et al, [51] and elsewhere.

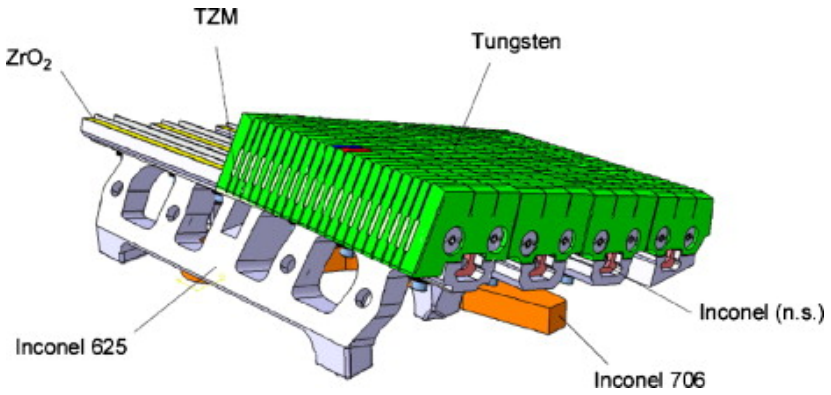

Figure 9: JET bulk tungsten divertor [44].

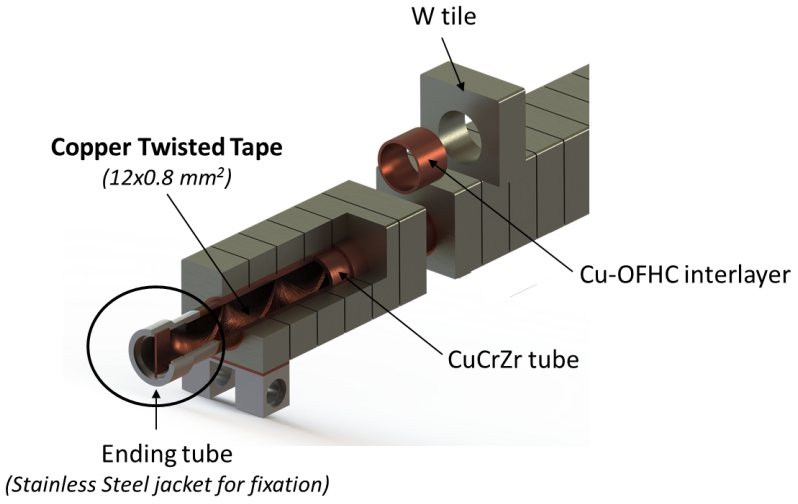

Figure 10: ITER divertor target design [49].

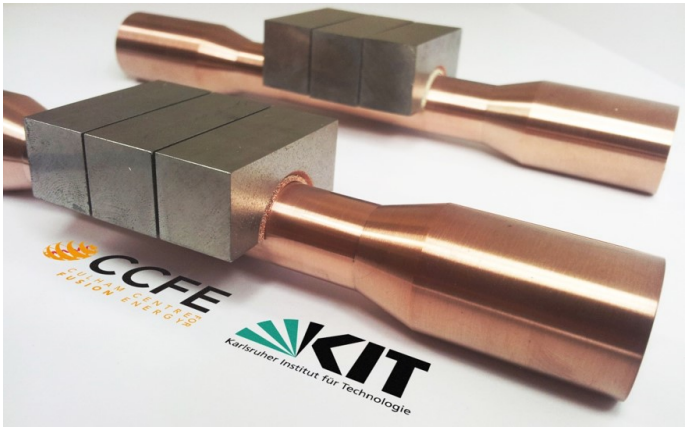

Figure 11: Feltmetal "thermal-break" concept test samples [59].

Copper-chrome-zirconium and tungsten have significantly different thermal expansion coefficients, and so their selection as structural and armour materials respectively means that a significant thermal mismatch stress develops between the two in operation, potentially leading to failure. A monoblock design ensures that the tungsten armour is captive, and if delamination between armour and structure occurs (as it has during testing [52]), although performance will be degraded, loose pieces of material will not immediately be released into the vessel. The use of small ∼20 mm tiles also reduces the stress due to thermal expansion, at the expense of a large part count and large number of joints to be qualified. Water cooling at 120°C and 3.3 MPa provides a low-risk technology with a high performance. A twist-tape inserted into the pipe aids uniformity of heating and increases critical heat flux [53].

3.4.3 DEMO divertor concept design

The divertor target in DEMO will be subject to similar steady state heat loads as ITER, but will be subject to a significantly higher neutron flux and total fluence causing material property degradation, in particular to the copper chrome zirconium inner pipe [54, 55, 56]. The ITER divertor design, unmodified, is therefore unsuitable for use in DEMO and an alternative design is needed [1]. Within the European EUROfusion consortium and elsewhere, a range of tasks are seeking to explore a number of proposed concepts that can be broadly grouped into the following categories:

Water cooled or "ITER-like"
Modifying the ITER baseline design is seen as the lowest risk approach to designing a divertor for DEMO [25]. Using materials qualified for ITER and water as a coolant with fission pressurised water reactor conditions, concepts have sought to optimise the original copper interlayer geometry, use Eurofer95 reduced activation ferritic martensitic (RAFM) steel or copper-tungsten laminate pipe, or reduce the interlayer stress through compliant or "thermal break" interlayers [57, 58, 59]. Most of these concepts have remained "pipe in monoblock" designs, though some related designs using tile geometries have been considered [60]. Figure 11 shows sample-pieces constructed to test one variant of the compliant thermal break concept.

Helium cooled
Helium provides an attractive high temperature alternative to water cooling and a number of helium cooled jet impingement concepts have been extensively developed [61, 62, 63, 54, and others]. These concepts offer heat flux handling capabilities in excess of $20\,\mathrm{MW\,m^{-2}}$ but suffer from very high part counts and significant manufacturing challenges, as well as the inherent risk of less well developed helium power cycle technology. Figure 12 shows one such concept.

Liquid divertors
With the extent of anticipated erosion a significant uncertainty in divertor design, an additional research stream seeks to use liquid lithium as plasma facing material [64, 65]. These concepts face the challenges of pumping liquid metal in large magnetic fields and of ensuring that excessive liquid is not released into the vessel. The significant advantages of self-healing, large heat flux handling capability, and low or zero maintenance make this a high-risk but high-gain strategy.

One or two other concepts have been discussed outside these core concept families. Figure 13 shows the normalised pressure drop through a low temperature water-cooled high-pressure laminate jet impingement concept developed with Oxford University and Rolls-Royce which has focused on optimisation of thermofluid aspects of the system. One concept uses cascades of silicon carbide pebbles as the plasma-facing surface [66, 67]. Heat pipes have also been proposed as a candidate technology for plasma facing components since at least 1998 [68], although the first practical

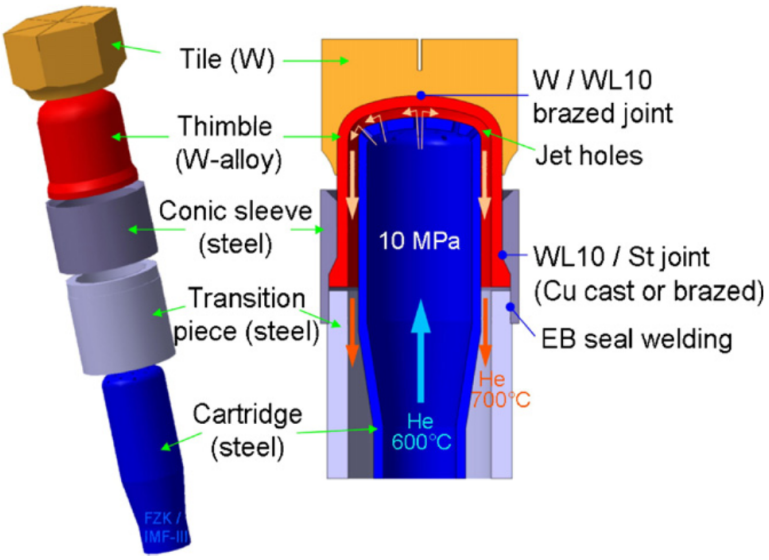

Figure 12: Helium cooled HEMJ concept [61].

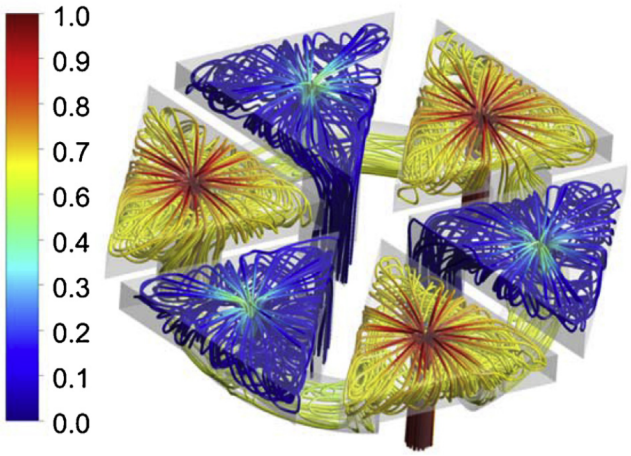

Figure 13: Normalised pressure drop through a low temperature water jet impingement concept [70].

demonstration of high heat flux performance by a liquid lithium cooled tantalum heat pipe under fusion relevant conditions was only demonstrated in 2018 by Matthews et al. [69]. Notably, the authors reporting the outcomes of this testing propose AM of refractory metals including tungsten or tantalum as a promising next step for developing the complex internal structures required for heat pipe concepts for fusion.

More recently, work at CCFE has begun to consider alternatives using AM — one significant prompt for this PhD project.

4 Research Context: Additive Manufacturing

4.1 Introduction to Additive Manufacturing

The history of AM is considered to begin in 1987 [71] with the commercialisation of stereolithography. In recent years, however, commercial and consumer interest has grown significantly, as highlighted by the hype curve produced by Gartner shown in figure 14.

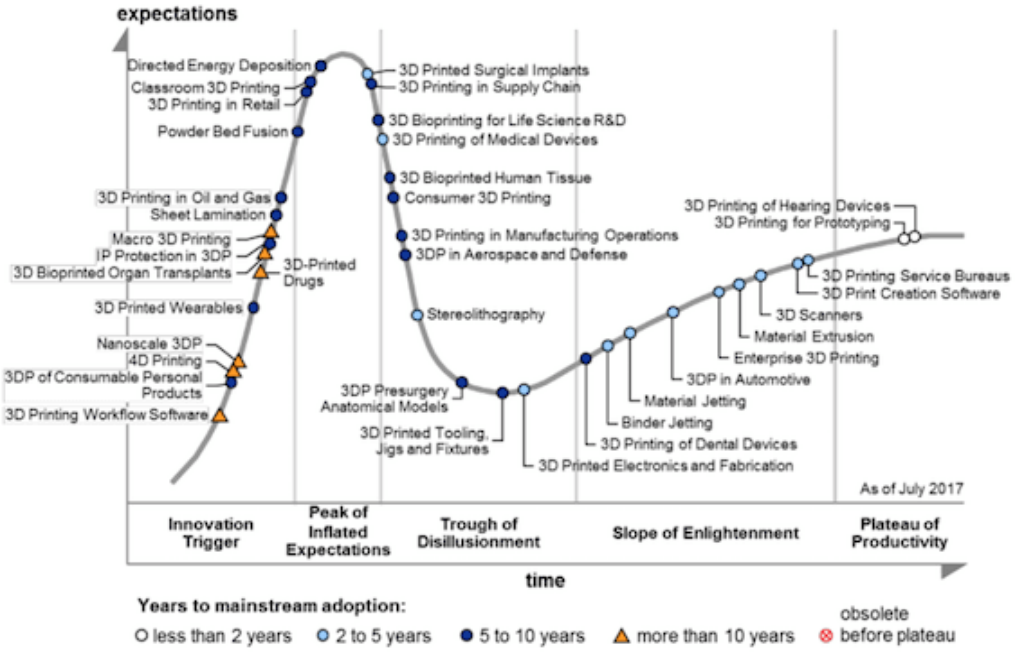

Figure 14: 3D printing hype curve [72]

This shows that industrial-scale manufacturing is still in the early "innovation trigger" phase and is therefore likely to face future challenges of over-expectation followed by disillusionment, but smaller scale "enterprise" and prototyping applications are well established and growing in maturity. Global use in industry has, however grown significantly as illustrated by the increase in sales of metal additive manufacturing systems shown in figure 15.

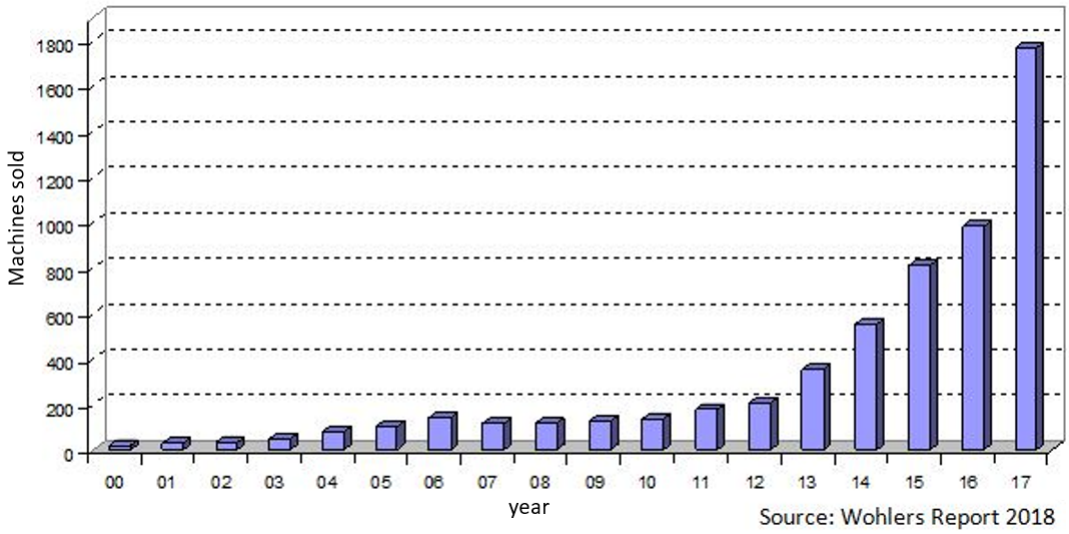

Figure 15: Global sales of metal AM systems between 2000 and 2017 [73]

A number of broad reviews of AM are available (e.g. [74, 75]). The following sections give high-level details of a range of AM processes relevant to the types of materials likely to be used for high-heat flux applications. Some processes such as stereolithography or continuous liquid interface production [76] have deliberately been excluded for clarity and brevity due to being polymer-specific or too early in their development. These sections are then followed

by a comparison summary of the processes discussed giving examples of advantages and disadvantages of each with the goal of selecting the most appropriate for the focus of this project. This is then followed by a brief outline of some additively manufactured high heat-flux concepts being developed outside the fusion community and a review of the state of the art of AM of refractory metals — a class of alloys of particular interest.

4.2 Directed Energy Deposition

Directed energy deposition (DED) processes enable the creation of parts by melting material as it is being deposited [77]. Polymer parts are typically produced using filament extruded through an electrically heated nozzle, while metal parts can be produced using a range of DED processes, using wire or powder feedstock.

4.2.1 Wire

Wire fed DED processes are also known as fused deposition modelling (FDM) or fused filament fabrication (FFF). They use a range of heating methods, including electrical arc, laser, induction, and heated nozzle, to melt the end of the filament which is then deposited on the part being built [78]. A wide range of consumer to industrial scale FDM platforms are readily available for polymer part production while metal processing has largely focused on steel or lightweight alloys for aerospace [79, 80, 81]. Figure 16 shows a schematic of the Wire + Arc Additive Manufacturing (WAAM) process for metal DED.

Wire-fed additive manufacturing has the advantage of a high build rate and the ability to deposit material in 3D. By including multiple filaments, material composition can be tailored during a single build to create functionally graded parts or to produce tailored or experimental alloys [82]. Material properties have been shown to be comparable to parent material [83]. Dimensional tolerances and surface finish on as-built parts are lower than powder based processes, however and the process is typically used to produce "near net shape" components which are then machined to the required final geometry [84].

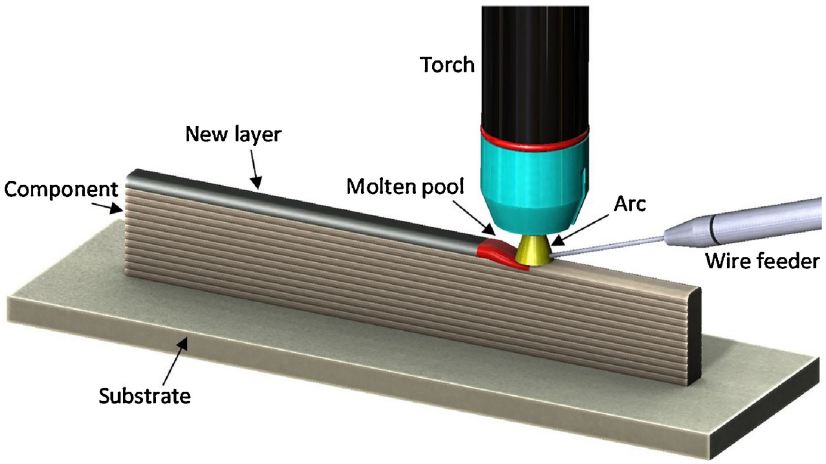

Figure 16: Illustration of the WAAM process [85]

4.2.2 Powder

Powder-based DED processes including Laser Engineered Net Shaping (LENS), Laser Metal Deposition (LMD), blown powder AM, Direct Laser Deposition (DLD), or laser cladding deliver material to a part being built in the form of powder driven by a compressed inert gas. The powder is then melted using a laser [86]. See figure 17 for a schematic representation.

This process is more widely used for cladding and repair than to produce parts from scratch, but has been used in a range of relevant engineering materials [87, 88]. Powder based DED has the advantage of finer geometry than wire-based processes, but is more limited in part complexity than powder bed processes, as outlined below, particularly with respect to overhanging features — a key requirement for structures with cooling channels.

4.3 Powder-bed fusion

Powder-bed fusion processes all share a similar methodology but vary heat input source and application. For all powder bed processes, a 3D CAD model is generated, supports are added to the model where needed, and the model is then sliced into thin layers the thickness of which is decided based on the material and geometry being used e.g. [89, 90]. A layer of powder is then spread using a roller or scraper onto a baseplate and the heat is applied in a pattern

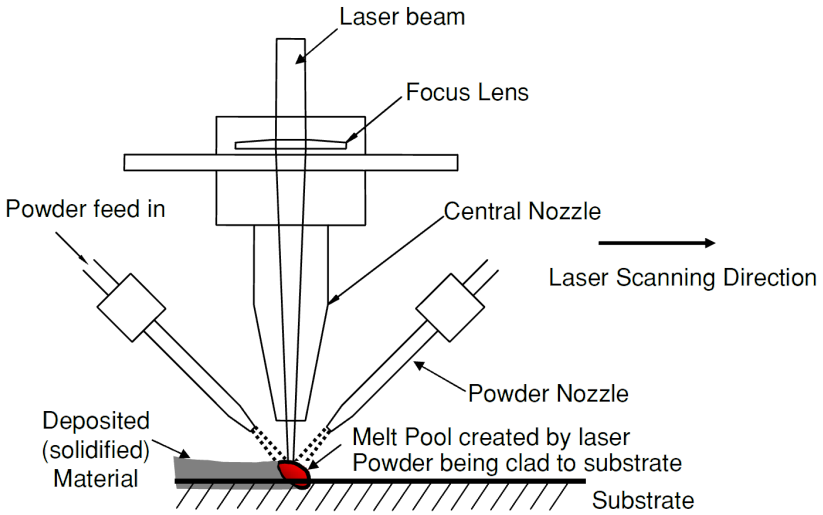

Figure 17: Schematic representation of blown powder DED [86].

corresponding to the layer of the CAD model. The baseplate is lowered by an amount corresponding to the thickness of the layer of the model, and the process is repeated. The following sections outline the significant differences between the major families of powder-bed processes.

4.3.1 Laser Powder Bed Fusion (LPBF)

LPBF uses a laser as the input source and melts the build material directly. The material can be completely melted and consolidated without the need for binder or post-sintering (though hot isostatic pressing may aid densification in some cases). This is also termed selective laser melting (SLM). Alternatively, the powder can be partially sintered with or without binder material (termed selective laser sintering (SLS) or direct metal laser sintering (DMLS)) to create a green part which can be fully densified using conventional powder metallurgy heat treatments. Kumar [91] provides a comprehensive overview. See figure 18 for a schematic of the LPBF process.

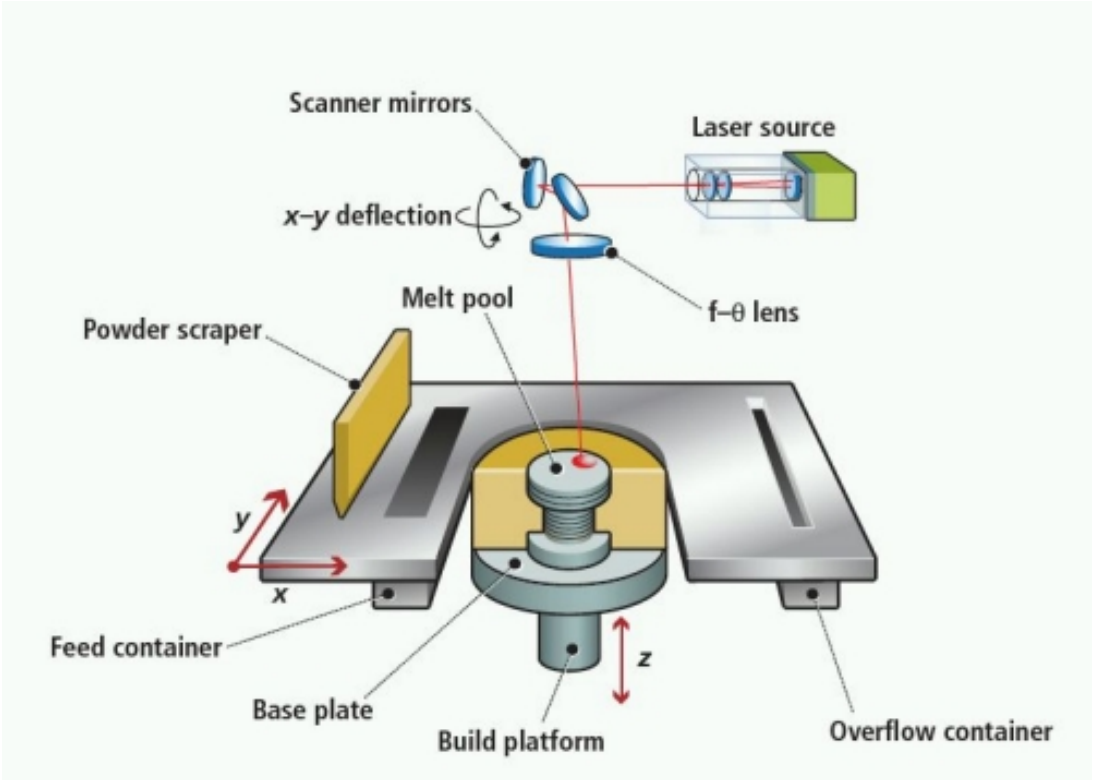

Figure 18: SLM process

4.3.2 Electron beam melting (EBM)

EBM uses an electron beam rather than a laser as heat source, as shown in figure 19. Unlike SLM, each layer is pre-heated, partially sintering the powder before the melting phase. This allows for a more uniform temperature gradient in the part, reducing residual stresses, and allows more significant overhangs than SLM, since the partially sintered powder is able to support the build throughout the process. This powder must, however, be removed in an additional post-processing step. Small cooling channels are therefore more difficult to produce. Gong et al. [92] provides a thorough review of this process.

4.4 Comparison of additive processes

Table 1 provides a summary of the advantages and disadvantages identified in the previous sections as well as highlighting a number of additional strengths and weaknesses of each process seen to be particularly relevant to this project.

Table 1: Summary comparison of AM processes

Process	Advantages	Disadvantages
Directed Energy Deposition		
Wire	high build rate, well developed for a range of materials, good material properties	only near-net shape, post processing is needed, material must be available in wire form, hard to generate overhanging structures and internal channels
Powder	can create shapes in 3D directly, high build rates	better for cladding, poor final properties, not able to generate empty spaces and channels
Powder Bed Fusion		
Laser	good geometric tolerance, able to produce relevant shapes, tested with some candidate materials	higher residual stress, harder to produce unsupported shapes, full consolidation and impurities due to binder are concerns for SLS
Electron beam	good geometric tolerance, easier to create unsupported structures, low residual stress	difficult to remove powder from small channels due to partially sintered powder

4.5 Additive manufacturing for high heat-flux applications

AM has already been identified as a potential tool for industrial cooling applications but has been applied only in a limited way to high-heat flux components. A broad view outlining potential applications of metal additive manufacturing to cooling channels can be found in [94]. Applications to the automotive industry are extensively discussed in [95]. Conformal cooling channels have been designed for injection moulding, but these operate at significantly lower temperatures and heat fluxes. Electronics heat sinks and heat exchangers have begun to explore alternative geometries for pin-fin arrangements, but conventional or electrical discharge machining (EDM) have remained the manufacturing techniques of choice for many of these. Beyond this, one optimised additively manufactured heat transfer component for motorsport has been identified [96] and one "showcase" heat exchanger design has been developed [97] and although this is described as being "optimised", it appears that it has not been designed for any particular application as yet and operational regimes are unpublished.

4.6 Additive manufacturing of refractory metals

A large proportion of metallic AM development has focused either on alloys for aerospace applications such as particularly titanium and nickel superalloys or on mainstream steels or inconel. There has been an increasing interest, however, in recent years, in a wider range of materials including those for high temperature applications or materials which are more difficult to form. For reasons more fully explained in subsequent chapters, refractory metals are of particular interest to the fusion community, particularly tungsten, molybdenum, and tantalum.

There are a significant number of reports of laser powder bed fusion of pure tungsten (e.g. [98, 99, 100, 101, 102, 103]) and tungsten with small additions of tantalum [104]. Both polyhedral and spherical powders with D_{50} between 16.76 µm and 30 µm have been used. Laser powers between 90 W and 500 W have been employed and while all studies

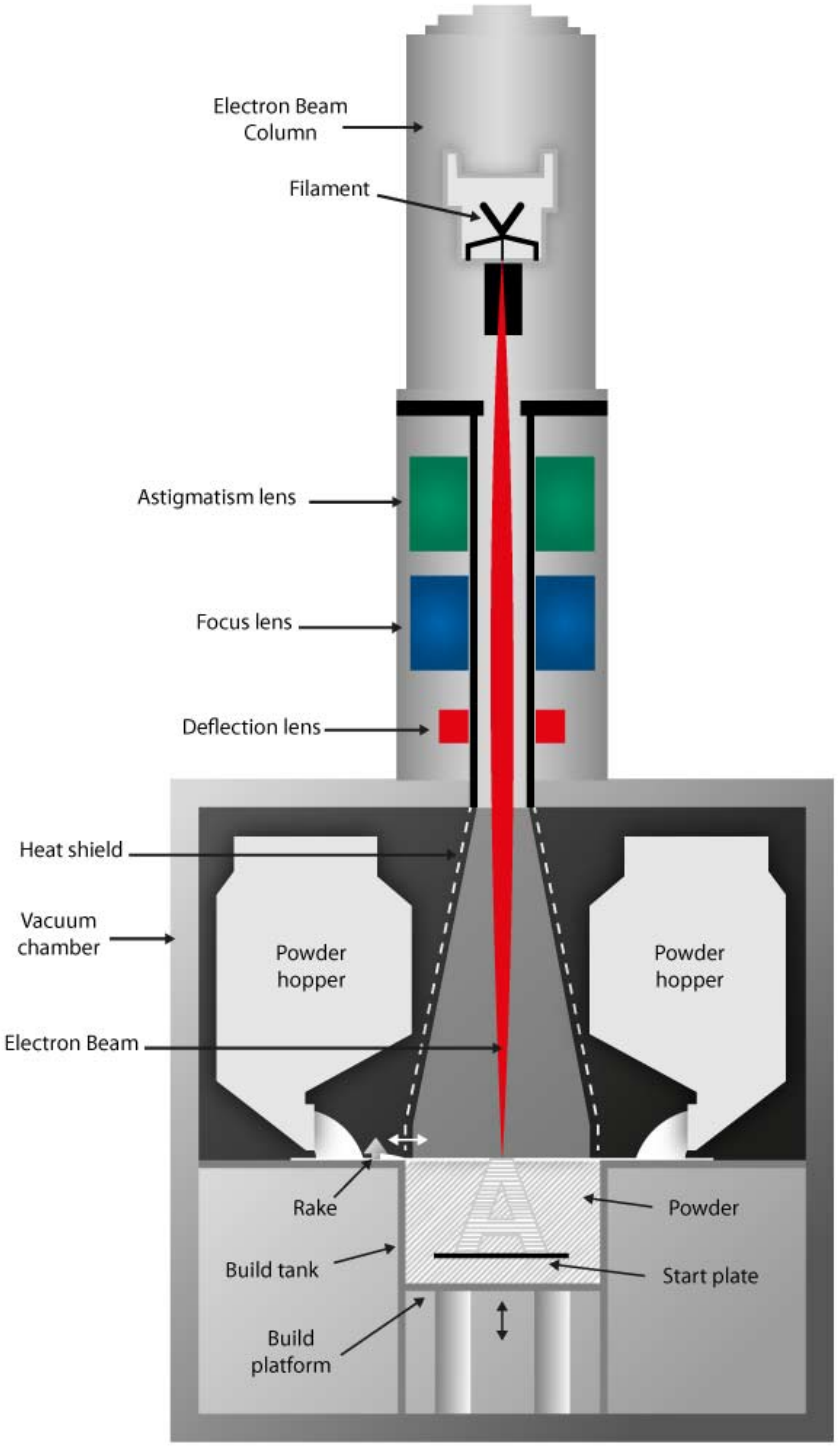

Figure 19: Schematic of an EBM machine [93]

identify an energy threshold for consolidation above which near complete densification can be achieved, this threshold and the parameters used vary widely. Layer thicknesses are mostly of the order of powder size, scan speeds between $100\,\mathrm{m\,s^{-1}}$ and $1400\,\mathrm{m\,s^{-1}}$, and hatch spacings are between 1 and 1.5 times the laser spot size (45 µm to 90 µm). A common and persistent challenge reported is fine cracking in pure tungsten, and although a heated build platform and reduced build chamber oxygen content appear to somewhat mitigate this, only the addition of tantalum appears to eliminate it completely. Unpublished reports of electron beam melting of pure tungsten suggest that the elevated build temperature and almost oxygen-free vacuum build atmosphere may provide a more successful alternative to laser-based processes.

Faidel et al. [105] achieved a maximum value of 82.5 % of full density while investigating LPBF of pure molybdenum for fusion applications, using a 200 W laser. Multiphysics modelling and supporting experiments by Leitz et al. [106] suggested that laser processing should be a feasible route for dense part fabrication, however. Wang et al. [107] subsequently achieved 99.1 % dense material using a reported linear energy density of $1142\,\mathrm{J\,m^{-1}}$ and manged to largely suppress crack growth by interlocked scanning strategies and building at high temperature — achieved by insulating the parts from the baseplate using a support structure.

The low availability of fusion-relevant vanadium alloys in any form has prevented extensive investigation for AM, but there have been some attempts to produce and process V-6Cr-6Ti powder [108, 109], resulting in promising microstructure and early indications of strength, albeit without details of the processing parameters used.

Processing of tantalum, though less widely reported, has proved more successful. Livescu et al. [110] achieved porosity of 0.018 % and similar mechanical properties to wrought material using a blend of D_{50} 25 µm and 45 µm plasma spherodized powder. Volumetric energy density of $840\,\mathrm{J\,m^{-3}}$ was applied with a laser power of 370 W, scan speed of $550\,\mathrm{mm\,s^{-1}}$, layer thickness of 20 µm, and hatch spacing of 40 µm. Similar results have been reported [111, 112, 113], though all noted the sensitivity of microstructure to choice of parameters, even if volumetric energy density remained constant at the value required for densification.

References

[1] F. Romanelli, Fusion Electricity: A roadmap to the realisation of fusion energy, Tech. rep., EDFDA (2012). doi:ISBN978-3-00-040720-8.

[2] International Energy Agency, World Energy Outlook 2014 - Press presentation (2014).

[3] G. W. C. Kaye, T. H. Laby, Kaye & Laby Tables of Physical & Chemical Constants, National Physical Laboratory, 2005.

[4] J. Wesson, D. J. Campbell, Tokamaks, 4th Edition, International Series of Monographs on Physics, Oxford University Press, Oxford, 2011.

[5] EUROfusion website.
URL https://www.euro-fusion.org/

[6] M. Ni, Y. Wang, B. Yuan, J. Jiang, Y. Wu, Tritium supply assessment for ITER and DEMOnstration power plant, Fusion Eng. Des. 88 (9-10) (2013) 2422–2426. doi:10.1016/j.fusengdes.2013.05.043.

[7] D. Maisonnier, I. Cook, S. Pierre, B. Lorenzo, B. Edgar, B. Karin, D. P. Luigi, F. Robin, G. Luciano, H. Stephan, N. Claudio, N. Prachai, P. Aldo, T. Neill, W. David, The European power plant conceptual study, Fusion Eng. Des. 75-79 (SUPPL.) (2005) 1173–1179. doi:10.1016/j.fusengdes.2005.06.095.

[8] D. Fasel, M. Tran, Availability of lithium in the context of future D–T fusion reactors, Fusion Eng. Des. 75-79 (2005) 1163–1168. doi:10.1016/j.fusengdes.2005.06.345.

[9] A. Miller, H. van Alstyne, Heavy water: a distinctive and essential component of CANDU.

[10] EUROfusion, Availability: Research for tomorrow's energy supply.

[11] M. Keilhacker, A. Gibson, C. Gormezano, P. Lomas, P. Thomas, M. Watkins, P. Andrew, B. Balet, D. Borba, C. Challis, I. Coffey, G. Cottrell, H. D. Esch, N. Deliyanakis, A. Fasoli, C. Gowers, H. Guo, G. Huysmans, T. Jones, W. Kerner, R. König, M. Loughlin, A. Maas, F. Marcus, M. Nave, F. Rimini, G. Sadler, S. Sharapov, G. Sips, P. Smeulders, F. Söldner, A. Taroni, B. Tubbing, M. von Hellermann, D. Ward, J. Team, High fusion performance from deuterium-tritium plasmas in JET, Nucl. Fusion 39 (2) (1999) 209–234. doi:10.1088/0029-5515/39/2/306.

[12] D. van Houtte, G. Martin, A. Bécoulet, J. Bucalossi, G. Giruzzi, G. Hoang, T. Loarer, B. Saoutic, o. b. o. t. T. S. Team, Recent fully non-inductive operation results in Tore Supra with 6 min, 1 GJ plasma discharges, Nucl. Fusion 44 (5) (2004) L11–L15. doi:10.1088/0029-5515/44/5/L01.

[13] Y. Saxena, S.-. Team, Present status of the SST-1 project, Nucl. Fusion 40 (6) (2000) 1069–1082. doi:10.1088/0029-5515/40/6/305.

[14] ITER Website.
URL www.iter.org

[15] S. Zinkle, N. M. Ghoniem, Operating temperature windows for fusion reactor structural materials, Fusion Eng. Des. 51-52 (52) (2000) 55–71. doi:10.1016/S0920-3796(00)00320-3.

[16] S. J. Zinkle, J. P. Blanchard, R. W. Callis, C. E. Kessel, R. J. Kurtz, P. J. Lee, K. A. McCarthy, N. B. Morley, F. Najmabadi, R. E. Nygren, G. R. Tynan, D. G. Whyte, R. S. Willms, B. D. Wirth, Fusion materials science and technology research opportunities now and during the ITER era, Fusion Eng. Des. 89 (7-8) (2014) 1579–1585. doi:10.1016/j.fusengdes.2014.02.048.

[17] M. Porton, H. Latham, Z. Vizvary, E. Surrey, Balance of plant challenges for a near-term EU demonstration power plant, in: 2013 IEEE 25th Symp. Fusion Eng., IEEE, 2013, pp. 1–6. doi:10.1109/SOFE.2013.6635331.

[18] J. Wesson, The Science of Jet, European Fusion Development Agreement, 2000.

[19] ASDEX Team, The H-Mode of ASDEX, Nucl. Fusion 29 (11) (1989) 1959–2040. doi:10.1088/0029-5515/29/11/010.

[20] M. Turnyanskiy, R. Neu, R. Albanese, R. Ambrosino, C. Bachmann, S. Brezinsek, T. Donne, T. Eich, G. Falchetto, G. Federici, D. Kalupin, X. Litaudon, M. Mayoral, D. McDonald, H. Reimerdes, F. Romanelli, R. Wenninger, J.-H. You, European roadmap to the realization of fusion energy: Mission for solution on heat-exhaust systems, Fusion Eng. Des.doi:10.1016/j.fusengdes.2015.04.041.

[21] A. W. Morris, MAST: Results and Upgrade Activities, IEEE Trans. Plasma Sci. 40 (3) (2012) 682–691. doi:10.1109/TPS.2011.2181540.

[22] Annual Report of the EURATOM/CCFE Fusion Programme 2013, Tech. rep., CCFE/EURATOM association (2013).

[23] T. Petrie, N. Brooks, M. Fenstermacher, M. Groth, A. Hyatt, R. Isler, C. Lasnier, A. Leonard, G. Porter, M. Schaffer, J. Watkins, M. Wade, W. West, Comparison of radiating divertor behaviour in single-null and double-null plasmas in DIII-D, Nucl. Fusion 48 (4) (2008) 045010. doi:10.1088/0029-5515/48/4/045010.

[24] F. Piras, S. Coda, I. Furno, J.-M. Moret, R. A. Pitts, O. Sauter, B. Tal, G. Turri, A. Bencze, B. P. Duval, F. Felici, A. Pochelon, C. Zucca, Snowflake divertor plasmas on TCV, Plasma Phys. Control. Fusion 51 (5) (2009) 055009. doi:10.1088/0741-3335/51/5/055009.

[25] J. Milnes, R. Bamber, G. Fishpool, W. Fundamenski, D. Hancock, W. Morris, A. Muir, Fusion Power Plant Divertors, a Physics and Technology Gap Analysis (WP11-PEX-01-ACT4-01/CCFE), Tech. rep., EFDA (2012).

[26] J.-H. You, Private Communication (2015).

[27] N. S. Harris, Modern vacuum practice, 3rd Edition, McGraw-Hill, London, 2007.

[28] G. Federici, C. Skinner, J. Brooks, J. Coad, C. Grisolia, A. Haasz, A. Hassanein, V. Philipps, C. Pitcher, J. Roth, W. Wampler, D. Whyte, Plasma-material interactions in current tokamaks and their implications for next step fusion reactors, Nucl. Fusion 41 (12) (2001) 1967–2137. doi:10.1088/0029-5515/41/12/218.

[29] P. Norajitra, L. Boccaccini, E. Diegele, V. Filatov, A. Gervash, R. Giniyatulin, S. Gordeev, V. Heinzel, G. Janeschitz, J. Konys, W. Krauss, R. Kruessmann, S. Malang, I. Mazul, A. Moeslang, C. Petersen, G. Reimann, M. Rieth, G. Rizzi, M. Rumyantsev, R. Ruprecht, V. Slobodtchouk, Development of a helium-cooled divertor concept: design-related requirements on materials and fabrication technology, J. Nucl. Mater. 329-333 (2004) 1594–1598. doi:10.1016/j.jnucmat.2004.04.137.

[30] D. Zhu, J. Chen, Thermal stress analysis on chemical vapor deposition tungsten coating as plasma facing material for EAST, J. Nucl. Mater. 455 (1-3) (2014) 185–188. doi:10.1016/j.jnucmat.2014.05.054.

[31] T. Hirai, A. Kreter, J. Linke, J. Malzbender, T. Ohgo, V. Philipps, G. Pintsuk, A. Pospieszczyk, Y. Sakawa, G. Sergienko, T. Tanabe, Y. Ueda, M. Wada, Critical heat flux loading experiments on CVD-W coating in the TEXTOR tokamak, Fusion Eng. Des. 81 (1-7) (2006) 175–180. doi:10.1016/j.fusengdes.2005.08.053.

[32] M. Taniguchi, K. Sato, K. Ezato, K. Yokoyama, M. Akiba, Disruption tests on repaired tungsten by CVD coating, J. Nucl. Mater. 307-311 (2002) 719–722. doi:10.1016/S0022-3115(02)01041-3.

[33] F. Sefta, K. D. Hammond, N. Juslin, B. D. Wirth, Tungsten surface evolution by helium bubble nucleation, growth and rupture, Nucl. Fusion 53 (7) (2013) 073015. doi:10.1088/0029-5515/53/7/073015.

[34] G. Federici, G. Giruzzi, C. Lowry, R. Kemp, D. Ward, R. Wenninger, H. Zohm, EU DEMO design and R&D studies, in: 2013 IEEE 25th Symp. Fusion Eng., IEEE, 2013, pp. 1–8. doi:10.1109/SOFE.2013.6635288.

[35] J. Linke, Plasma facing materials and components for future fusion devices—development, characterization and performance under fusion specific loading conditions, Phys. Scr. T123 (T123) (2006) 45–53. doi:10.1088/0031-8949/2006/T123/006.

[36] J. Linke, High Heat Flux Performance of Plasma Facing Materials and Components Under Service Conditions in Future Fusion Reactors, Fusion Sci. Technol. 57 (2T) (2010) 293–302.

[37] D. Maisonnier, I. Cook, S. Pierre, B. Lorenzo, D. P. Luigi, G. Luciano, N. Prachai, P. Aldo, DEMO and fusion power plant conceptual studies in Europe, Fusion Eng. Des. 81 (8-14 PART B) (2006) 1123–1130. doi:10.1016/j.fusengdes.2005.08.055.

[38] S. Konishi, M. Glugla, T. Hayashi, Fuel cycle design for ITER and its extrapolation to DEMO, Fusion Eng. Des. 83 (7-9) (2008) 954–958. doi:10.1016/j.fusengdes.2008.06.060.

[39] H. Bolt, V. Barabash, G. Federici, J. Linke, A. Loarte, J. Roth, K. Sato, Plasma facing and high heat flux materials - Needs for ITER and beyond, J. Nucl. Mater. 307-311 (1 SUPPL.) (2002) 43–52.

[40] O. Crofts, J. Harman, Maintenance duration estimate for a DEMO fusion power plant, based on the EFDA WP12 pre-conceptual studies, Fusion Eng. Des. 89 (9-10) (2014) 2383–2387. doi:10.1016/j.fusengdes.2014.01.038.

[41] D. Carfora, G. Di Gironimo, J. Järvenpää, K. Huhtala, T. Määttä, M. Siuko, Preliminary concept design of the divertor remote handling system for DEMO power plant, Fusion Eng. Des. 89 (11) (2014) 2743–2747. doi:10.1016/j.fusengdes.2014.07.016.

[42] M. Cox, The Mega Amp Spherical Tokamak, Fusion Eng. Des. 46 (2-4) (1999) 397–404. doi:10.1016/S0920-3796(99)00031-9.

[43] G. F. Matthews, M. Beurskens, S. Brezinsek, M. Groth, E. Joffrin, A. Loving, M. Kear, M.-L. Mayoral, R. Neu, P. Prior, V. Riccardo, F. Rimini, M. Rubel, G. Sips, E. Villedieu, P. de Vries, M. L. Watkins, JET ITER-like wall—overview and experimental programme, Phys. Scr. T145 (T145) (2011) 014001. doi:10.1088/0031-8949/2011/T145/014001.

[44] T. Hirai, H. Maier, M. Rubel, P. Mertens, R. Neu, E. Gauthier, J. Likonen, C. Lungu, G. Maddaluno, G. Matthews, R. Mitteau, O. Neubauer, G. Piazza, B. Riccardi, C. Ruset, I. Uytdenhouwen, R&D on full tungsten divertor and beryllium wall for JET ITER-like wall project, Fusion Eng. Des. 82 (15-24) (2007) 1839–1845. doi:10.1016/j.fusengdes.2007.02.024.

[45] J. Bucalossi, M. Missirlian, P. Moreau, F. Samaille, E. Tsitrone, D. van Houtte, T. Batal, C. Bourdelle, M. Chantant, Y. Corre, X. Courtois, L. Delpech, L. Doceul, D. Douai, H. Dougnac, F. Faïsse, C. Fenzi, F. Ferlay, M. Firdaouss, L. Gargiulo, P. Garin, C. Gil, A. Grosman, D. Guilhem, J. Gunn, C. Hernandez, D. Keller, S. Larroque, F. Leroux, M. Lipa, P. Lotte, A. Martinez, O. Meyer, F. Micolon, P. Mollard, E. Nardon, R. Nouailletas, A. Pilia, M. Richou, S. Salasca, J.-M. Travère, The WEST project: Testing ITER divertor high heat flux component technology in a steady state tokamak environment, Fusion Eng. Des. 89 (7-8) (2014) 907–912. doi:10.1016/j.fusengdes.2014.01.062.

[46] X. Liu, S. Du, D. Yao, J. Wei, The design, analysis and alignment of EAST divertor, Fusion Eng. Des. 84 (1) (2009) 78–82. doi:10.1016/j.fusengdes.2008.11.011.

[47] S. Mirnov, V. Evtikhin, The tests of liquid metals (Ga, Li) as plasma facing components in T-3M and T-11M tokamaks, Fusion Eng. Des. 81 (1-7) (2006) 113–119. doi:10.1016/j.fusengdes.2005.10.003.

[48] E. Visca, S. Libera, A. Mancini, G. Mazzone, A. Pizzuto, C. Testani, Hot radial pressing: An alternative technique for the manufacturing of plasma-facing components, Fusion Eng. Des. 75-79 (2005) 485–489. doi:10.1016/j.fusengdes.2005.06.123.

[49] CEA WEST project website.
URL http://west.cea.fr

[50] T. Hirai, F. Escourbiac, S. Carpentier-Chouchana, A. Fedosov, L. Ferrand, T. Jokinen, V. Komarov, A. Kukushkin, M. Merola, R. Mitteau, R. Pitts, W. Shu, M. Sugihara, B. Riccardi, S. Suzuki, R. Villari, ITER tungsten divertor design development and qualification program, Fusion Eng. Des. 88 (9-10) (2013) 1798–1801. doi:10.1016/j.fusengdes.2013.05.010.

[51] R. A. Pitts, A. Kukushkin, A. Loarte, A. Martin, M. Merola, C. E. Kessel, V. Komarov, M. Shimada, Status and physics basis of the ITER divertor, Phys. Scr. T138 (T138) (2009) 014001. doi:10.1088/0031-8949/2009/T138/014001.

[52] G. Pintsuk, M. Bednarek, P. Gavila, S. Gerzoskovitz, J. Linke, P. Lorenzetto, B. Riccardi, F. Escourbiac, Characterization of ITER tungsten qualification mock-ups exposed to high cyclic thermal loads, Fusion Eng. Des.doi:10.1016/j.fusengdes.2015.01.037.

[53] P. Gavila, B. Riccardi, S. Constans, J. L. Jouvelot, I. B. Vastra, M. Missirlian, M. Richou, High heat flux testing of mock-ups for a full tungsten ITER divertor, Fusion Eng. Des. 86 (9-11) (2011) 1652–1655. doi:10.1016/j.fusengdes.2011.02.012.

[54] P. Norajitra, S. I. Abdel-Khalik, L. M. Giancarli, T. Ihli, G. Janeschitz, S. Malang, I. V. Mazul, P. Sardain, Divertor conceptual designs for a fusion power plant, Fusion Eng. Des. 83 (7-9) (2008) 893–902. doi:10.1016/j.fusengdes.2008.05.022.

[55] V. Barabash, G. Kalinin, S. Fabritsiev, S. Zinkle, Specification of CuCrZr alloy properties after various thermo-mechanical treatments and design allowables including neutron irradiation effects, J. Nucl. Mater. 417 (1-3) (2011) 904–907. doi:10.1016/j.jnucmat.2010.12.158.

[56] S. Fabritsiev, S. Zinkle, B. Singh, Evaluation of copper alloys for fusion reactor divertor and first wall components, J. Nucl. Mater. 233-237 (1996) 127–137. doi:10.1016/S0022-3115(96)00091-8.

[57] A. Li-Puma, M. Richou, P. Magaud, M. Missirlian, E. Visca, V. P. Ridolfini, Potential and limits of water cooled divertor concepts based on monoblock design as possible candidates for a DEMO reactor, Fusion Eng. Des. 88 (9-10) (2013) 1836–1843. doi:10.1016/j.fusengdes.2013.05.114.

[58] T. Barrett, S. McIntosh, M. Fursdon, D. Hancock, W. Timmis, M. Coleman, M. Rieth, J. Reiser, Enhancing the DEMO divertor target by interlayer engineering, Fusion Eng. Des. 98-99 (2015) 1216–1220. doi:10.1016/j.fusengdes.2015.03.031.

[59] D. Hancock, T. Barrett, J. Foster, M. Fursdon, G. Keech, S. McIntosh, W. Timmis, M. Rieth, J. Reiser, Testing candidate interlayers for an enhanced water-cooled divertor target, Fusion Eng. Des. (2015) 501045doi:10.1016/j.fusengdes.2014.12.026.

[60] J. Linke, F. Escourbiac, I. V. Mazul, R. Nygren, M. Rödig, J. Schlosser, S. Suzuki, High heat flux testing of plasma facing materials and components - Status and perspectives for ITER related activities, J. Nucl. Mater. 367-370 (SPEC. ISS.) (2007) 1422–1431. doi:10.1016/j.jnucmat.2007.04.028.

[61] A. R. Raffray, R. Nygren, D. G. Whyte, S. Abdel-Khalik, R. Doerner, F. Escourbiac, T. Evans, R. J. Goldston, D. T. Hoelzer, S. Konishi, P. Lorenzetto, M. Merola, R. Neu, P. Norajitra, R. A. Pitts, M. Rieth, M. Roedig, T. Rognlien, S. Suzuki, M. S. Tillack, C. Wong, High heat flux components—Readiness to proceed from near term fusion systems to power plants, Fusion Eng. Des. 85 (1) (2010) 93–108. doi:10.1016/j.fusengdes.2009.08.002.

[62] P. Norajitra, He-Cooled Divertor for DEMO: Technological Study on Joining Tungsten Components with Titanium Interlayer, Fusion Sci. Technol. 66 (1). doi:10.13182/FST13-739.

[63] M. Tillack, A. Raffray, X. Wang, S. Malang, S. Abdel-Khalik, M. Yoda, D. Youchison, Recent US activities on advanced He-cooled W-alloy divertor concepts for fusion power plants, Fusion Eng. Des. 86 (1) (2011) 71–98. doi:10.1016/j.fusengdes.2010.08.015.

[64] R. Nygren, T. Rognlien, M. Rensink, S. Smolentsev, M. Youssef, M. Sawan, B. Merrill, C. Eberle, P. Fogarty, B. Nelson, D. Sze, R. Majeski, A fusion reactor design with a liquid first wall and divertor, Fusion Eng. Des. 72 (1-3) (2004) 181–221. doi:10.1016/j.fusengdes.2004.07.007.

[65] S. Mirnov, V. Dem'yanenko, E. Murav'ev, Liquid-metal tokamak divertors, J. Nucl. Mater. 196-198 (1992) 45–49. doi:10.1016/S0022-3115(06)80010-3.

[66] G. Voss, A. Bond, S. Davis, M. Harte, R. Watson, The cascading pebble divertor for the spherical tokamak power plant, Fusion Eng. Des. 81 (1-7) (2006) 327–333. doi:10.1016/j.fusengdes.2005.08.090.

[67] N. Gierse, J. Coenen, C. Thomser, A. Panin, C. Linsmeier, B. Unterberg, V. Philipps, Conceptual study of ferromagnetic pebbles for heat exhaust in fusion reactors with short power decay length, Nucl. Mater. Energy 2 (2015) 12–19. doi:10.1016/j.nme.2015.01.001.

[68] A. Makhankov, A. Anisimov, A. Arakelov, A. Gekov, N. Jablokov, V. Yuditskiy, I. Kirillov, V. Komarov, I. Mazul, A. Ogorodnikov, A. Popov, Liquid metal heat pipes for fusion application, Fusion Eng. Des.doi:10.1016/S0920-3796(98)00216-6.

[69] G. F. Matthews, R. E. Nygren, T. W. Morgan, S. A. Silburn, P. R. Cooper, R. Otin, A. Tallarigo, Testing of a high temperature radiatively cooled Li/Ta heat pipe in Magnum-PSI, Fusion Eng. Des.doi:10.1016/j.fusengdes.2018.12.096.

[70] J. R. J. Nicholas, P. Ireland, D. Hancock, D. Robertson, Development of a high-heat flux cooling element with potential application in a near-term fusion power plant divertor, Fusion Eng. Des. 96-97 (2015) 136–141. doi:10.1016/j.fusengdes.2015.03.033.

[71] T. T. Wohlers, Wohlers Report 2015: Additive Manufacturing and 3D Printing State of the Industry: Annual Worldwide Progress Report, Tech. rep. (2015).

[72] The 2014 Gartner Hype Cycle Special Report, Tech. rep., Gartner Inc. (2014).

[73] T. Wohlers, W. Associates, I. Campbell, T. Caffrey, O. Diegel, J. Kowen, Wohlers Report 2018: 3D Printing and Additive Manufacturing State of the Industry : Annual Worldwide Progress Report, Wohlers Associates, 2018.

[74] K. V. Wong, A. Hernandez, A Review of Additive Manufacturing (2012).

[75] W. E. Frazier, Metal Additive Manufacturing: A Review, J. Mater. Eng. Perform. 23 (6) (2014) 1917–1928. doi:10.1007/s11665-014-0958-z.

[76] J. R. Tumbleston, D. Shirvanyants, N. Ermoshkin, R. Janusziewicz, A. R. Johnson, D. Kelly, K. Chen, R. Pinschmidt, J. P. Rolland, A. Ermoshkin, E. T. Samulski, J. M. DeSimone, Continuous liquid interface production of 3D objects, Science (80-.). 347 (6228) (2015) 1349–1352. doi:10.1126/science.aaa2397.

[77] I. Gibson, D. Rosen, B. Stucker, Additive manufacturing technologies: 3D printing, rapid prototyping, and direct digital manufacturing, second edition, Springer New York, New York, NY, 2015. arXiv:arXiv:1011.1669v3, doi:10.1007/978-1-4939-2113-3.

[78] D. Ding, Z. Pan, D. Cuiuri, H. Li, Wire-feed additive manufacturing of metal components: technologies, developments and future interests, Int. J. Adv. Manuf. Technol.doi:10.1007/s00170-015-7077-3.

[79] D. Clark, M. Bache, M. Whittaker, Shaped metal deposition of a nickel alloy for aero engine applications, J. Mater. Process. Technol. 203 (1-3) (2008) 439–448. doi:10.1016/j.jmatprotec.2007.10.051.

[80] E. Brandl, A. Schoberth, C. Leyens, Morphology, microstructure, and hardness of titanium (Ti-6Al-4V) blocks deposited by wire-feed additive layer manufacturing (ALM), Mater. Sci. Eng. A 532 (2012) 295–307. doi:10.1016/j.msea.2011.10.095.

[81] F. Ribeiro, 3D printing with metals, Comput. Control Eng. J. 9 (1) (1998) 31. doi:10.1049/cce:19980108.

[82] ACCMET website.
URL http://www.accmet-project.eu/

[83] B. Baufeld, O. V. der Biest, R. Gault, Additive manufacturing of Ti–6Al–4V components by shaped metal deposition: Microstructure and mechanical properties, Mater. Des. 31 (2010) S106–S111. doi:10.1016/j.matdes.2009.11.032.

[84] J. Ding, P. Colegrove, J. Mehnen, S. Ganguly, P. Sequeira Almeida, F. Wang, S. Williams, Thermo-mechanical analysis of Wire and Arc Additive Layer Manufacturing process on large multi-layer parts, Comput. Mater. Sci. 50 (12) (2011) 3315–3322. doi:10.1016/j.commatsci.2011.06.023.

[85] A. R. McAndrew, M. Alvarez Rosales, P. A. Colegrove, J. R. Hönnige, A. Ho, R. Fayolle, K. Eyitayo, I. Stan, P. Sukrongpang, A. Crochemore, Z. Pinter, Interpass rolling of Ti-6Al-4V wire + arc additively manufactured features for microstructural refinement, Addit. Manuf. 21 (February) (2018) 340–349. doi:10.1016/j.addma.2018.03.006.

[86] H. Qi, M. Azer, A. Ritter, Studies of Standard Heat Treatment Effects on Microstructure and Mechanical Properties of Laser Net Shape Manufactured INCONEL 718, Metall. Mater. Trans. A 40 (10) (2009) 2410–2422. doi:10.1007/s11661-009-9949-3.

[87] K. Ng, H. Man, F. Cheng, T. Yue, Laser cladding of copper with molybdenum for wear resistance enhancement in electrical contacts, Appl. Surf. Sci. 253 (14) (2007) 6236–6241. doi:10.1016/j.apsusc.2007.01.086.

[88] L. Sexton, S. Lavin, G. Byrne, A. Kennedy, Laser cladding of aerospace materials, J. Mater. Process. Technol. 122 (1) (2002) 63–68. doi:10.1016/S0924-0136(01)01121-9.

[89] I. Yadroitsev, P. Bertrand, I. Smurov, Parametric analysis of the selective laser melting process, Appl. Surf. Sci. 253 (19) (2007) 8064–8069. doi:10.1016/j.apsusc.2007.02.088.

[90] J. Kruth, L. Froyen, J. Van Vaerenbergh, P. Mercelis, M. Rombouts, B. Lauwers, Selective laser melting of iron-based powder, J. Mater. Process. Technol. 149 (1-3) (2004) 616–622. doi:10.1016/j.jmatprotec.2003.11.051.

[91] S. Kumar, Selective laser sintering: A qualitative and objective approach, JOM 55 (10) (2003) 43–47. doi:10.1007/s11837-003-0175-y.

[92] X. Gong, T. Anderson, K. Chou, Review on powder-based electron beam additive manufacturing technology, Manuf. Rev. 1 (2014) 2. doi:10.1051/mfreview/2014001.

[93] ARCAM website.
URL www.arcam.com

[94] M. Lindqvist, Metal additive manufacturing of internal flow channels with powder bed fusion processes, Tech. rep., Lappeenranta University of Technology (2015).

[95] A. B. Kair, K. Sofos, Additive Manufacturing and Production of Metallic Parts in Automotive Industry, Ph.D. thesis, KTH (2014).

[96] R. Neugebauer, B. Müller, M. Gebauer, T. Töppel, Additive manufacturing boosts efficiency of heat transfer components, Assem. Autom. 31 (4) (2011) 344–347. doi:10.1108/01445151111172925.

[97] Within Lab website.
URL www.withinlab.com

[98] S. Bai, J. Liu, P. Yang, M. Zhai, H. Huang, L.-M. Yang, Femtosecond Fiber Laser Additive Manufacturing of Tungsten, in: Proc. SPIE 9738, Laser 3D Manuf. III, 97380U, 2016. doi:10.1117/12.2217551.

[99] D. Wang, C. Yu, X. Zhou, J. Ma, W. Liu, Z. Shen, Dense Pure Tungsten Fabricated by Selective Laser Melting, Appl. Sci. 7 (4) (2017) 430. doi:10.3390/app7040430.

[100] R. K. Enneti, R. Morgan, T. Wolfe, Direct Metal Laser Sintering (Dmls) / Selective Laser Melting (Slm) of Tungsten Powders 9–13.

[101] R. K. Enneti, R. Morgan, T. Wolfe, A. Harooni, S. Volk, Direct Metal Laser Sintering/Selective Laser Melting of Tungsten Powders, Int. J. Powder Metall. 53 (4) (2017) 23–31.

[102] A. Sidambe, P. Fox, Investigation of the Selective Laser Melting process with tungsten metal powder, Addit. Manuf. 8 (2015) 88–94. arXiv:arXiv:1011.1669v3, doi:10.1016/j.addma.2015.09.002.

[103] C. Tan, K. Zhou, W. Ma, B. Attard, P. Zhang, T. Kuang, Selective laser melting of high-performance pure tungsten: parameter design, densification behavior and mechanical properties, Sci. Technol. Adv. Mater. 19 (1). doi:10.1080/14686996.2018.1455154.

[104] A. Ivekovic, N. Omidvari, B. Vrancken, K. Lietaert, L. Thijs, K. Vanmeensel, J. Vleugels, J.-P. Kruth, A. Iveković, N. Omidvari, B. Vrancken, K. Lietaert, L. Thijs, K. Vanmeensel, J. Vleugels, J.-P. Kruth, Selective laser melting of tungsten and tungsten alloys, in: Int. J. Refract. Met. Hard Mater., Vol. 72, 2018, pp. 1–11. doi:10.1016/j.ijrmhm.2017.12.005.

[105] D. Faidel, D. Jonas, G. Natour, W. Behr, Investigation of the selective laser melting process with molybdenum powder, Addit. Manuf. 8 (2015) 88–94. arXiv:arXiv:1011.1669v3, doi:10.1016/j.addma.2015.09.002.

[106] K. H. Leitz, P. Singer, A. Plankensteiner, B. Tabernig, H. Kestler, L. S. Sigl, Multi-physical simulation of selective laser melting, Met. Powder Rep. 72 (5) (2017) 331–338. doi:10.1016/j.mprp.2016.04.004.

[107] D. Wang, C. Yu, J. Ma, W. Liu, Z. Shen, Densification and crack suppression in selective laser melting of pure molybdenum, Mater. Des. 129 (2017) 44–52. doi:10.1016/J.MATDES.2017.04.094.

[108] Y. Jialin, Selective laser melting additive manufacturing of advanced nuclear materials V-6Cr-6Ti, Mater. Lett. 209 (2017) 268–271. doi:10.1016/j.matlet.2017.08.014.

[109] J. Yang, J. Li, Fabrication and Analysis of Vanadium-Based Metal Powders for Selective Laser Melting, J. Miner. Mater. Charact. Eng. 06 (01) (2018) 50–59. doi:10.4236/jmmce.2018.61005.

[110] V. Livescu, C. M. Knapp, G. T. Gray, R. M. Martinez, B. M. Morrow, B. G. Ndefru, Additively manufactured tantalum microstructures, Materialia 1 (2018) 15–24. doi:10.1016/j.mtla.2018.06.007.
URL https://linkinghub.elsevier.com/retrieve/pii/S2589152918300310

[111] L. Zhou, T. Yuan, R. Li, J. Tang, G. Wang, K. Guo, Selective laser melting of pure tantalum: Densification, microstructure and mechanical behaviors, Mater. Sci. Eng. A 707 (September) (2017) 443–451. doi:10.1016/j.msea.2017.09.083.

[112] G. T. Gray, C. M. Knapp, D. R. Jones, V. Livescu, S. Fensin, B. M. Morrow, C. P. Trujillo, D. T. Martinez, J. A. Valdez, Structure/property characterization of spallation in wrought and additively manufactured tantalum, AIP Conf. Proc. 1979. doi:10.1063/1.5044799.

[113] R. Wauthle, J. Van Der Stok, S. A. Yavari, J. Van Humbeeck, J. P. Kruth, A. A. Zadpoor, H. Weinans, M. Mulier, J. Schrooten, Additively manufactured porous tantalum implants, Acta Biomater. 14 (2015) 217–225. doi:10.1016/j.actbio.2014.12.003.

2

Paper: "Refractory Metals as Structural Materials for Fusion High Heat Flux Components"

Context within thesis

This paper provides an introduction to the argument for using AM of refractory metals for fusion high heat flux components by beginning with a new approach to the material selection process. It also highlights new comparative techniques and includes new data in comparisons.

Novelty

- applying new and previously identified requirements as a set to a fuller range of materials for this application
- considering suitability over a wider operating temperature range rather than at a single point
- applying a more strengths and weaknesses based approach rather than a sequential "pass or fail" sequence of criteria.
- using newly developed tools to present material data and performance metrics
- contributing to the corpus of tools for deciding on the suitability of materials for fusion high heat flux components

Lead author contributions

- consolidation of a number of previous literature reviews and addition of additional references
- extension and formalisation of arguments for revised material selection methodology based on AMAZE project work
- all data selection and presentation
- all writing

Publication status

This paper was published in "Journal of Nuclear Materials", vol. 512, pp. 169–183, Sep. 2018.
`https://doi.org/10.1016/j.jnucmat.2018.09.052`
It has been re-typeset and additional material included for thesis submission

Approval status

Co-authors and supervisors:	Internal	(REVIEWED)	External	(REVIEWED)
UKAEA:	C. Waldon	(CLEARED)	E. Surrey	(CLEARED)
EUROfusion:	K. Gal	(ENDORSED)	T. Donne	(CLEARED)
AMAZE (notification only):	D. Wimpenny	(RELEASED)	M. Holden	(RELEASED)

Refractory Metals as Structural Materials for Fusion High Heat Flux Components

David Hancock[a,b,*], David Homfray[a], Michael Porton[a], Iain Todd[b], Brad Wynne[a,b]

[a] *Culham Centre for Fusion Energy, Culham Science Centre, Abingdon, Oxon, OX14 3DB*
[b] *University of Sheffield, Department of Materials Science and Engineering, Sir Robert Hadfield Building, Mappin Street, Sheffield, S1 3JD*

Abstract

Tungsten is the favoured armour material for plasma facing components for future fusion reactors, but studies examining the use of tungsten or other refractory metals in the underlying cooled structures have historically excluded them, leaving current concepts heavily dependent on copper alloys such as copper chrome zirconium. This paper first outlines the challenge of selecting an appropriate alternative material for this application, with reference to historical selection methodology and design solutions, and then re- examines the use of refractory metals in the light of current design priorities and manufacturing techniques.

The rationale for considering refractory alloys as structural materials is discussed, showing how this is the result of relatively small changes to the logic previously applied, with a greater emphasis on high temperature operation, a re-evaluation of current costs, a relaxation of absolute activation limits, and the availability of advanced manufacturing techniques such as additive manufacturing. A set of qualitative and quantitative assessment criteria are proposed, drawing on the requirements detailed in the first section; including thermal and mechanical performance, radiation damage tolerance, manufacturability, and cost and availability. Considering these criteria in parallel rather than sequence gives a less binary approach to material selection and instead provides a strengths and weaknesses based summary from which more nuanced conclusions can be drawn.

Data on relevant material properties for a range of candidate materials, including elemental refractory metals and a selection of related alloys are gathered from a range of sources and collated using a newly developed set of tools written in the python language. These tools are then used to apply the aforementioned assessment criteria and display the results. The lack of relevant data for a number of promising materials is highlighted, and although a conclusive best material cannot be identified, refractory alloys in general are proposed as worthy of further investigation.

Keywords: fusion, high heat flux, divertor, materials, refractory

1. Introduction

1.1. The divertor problem

Energy from controlled nuclear fusion promises clean, safe, and abundant electricity and significant advances have been made in recent history, particularly in the field of magnetic confinement fusion, employing the tokamak reactor design. Significant technical challenges remain, however, and commercial viability has yet to be proven. One of the most significant challenges faced by designers of fusion power plants, whatever the technology used, will be extracting heat and exhaust gasses efficiently.

For the tokamak concept, a core element of the power exhaust system is the divertor, where magnetic field lines are directly incident on a region of the vessel wall (the divertor target) and which is subject to steady state heat fluxes in the form of radiation and high energy particles in excess of $10\,\mathrm{MW\,m^{-2}}$ with excursions due to off-normal events producing transient loads an order of magnitude higher. There is currently no divertor target design suitable for use in a demonstration fusion power plant, either due to insufficient heat handling capability, thermal efficiency, or component lifetime [1]. Significant effort is being spent reducing the heat and particle fluxes incident on the target by adapting the plasma geometry, e.g. [2, 3], but engineering requirements still exceed capability. When compared to designs used for ITER and other current machines, peak incident heat flux, surface material erosion, irradiation damage, and required coolant efficiency are all likely to be higher, in some cases considerably [4].

1.2. Divertor target state of the art

Away from exposed liquid or vapour-based proposals [5] [6] which have a number of significant outstanding technical and physics challenges, leading concepts broadly fall into two categories: water cooled pipes in tungsten monoblocks similar to the design used for ITER [7] and helium cooled thimbles or pipes employing jet impingement [8].

Figure 1 shows two example divertor target designs: one ITER-like and the other a helium-cooled alternative. The former consists of a water cooled CuCrZr pipe with twisted tape insert surrounded by tungsten "monoblocks" as armour and steel mounting blocks as mechanical support. The other uses a tungsten laminate pipe with

*Corresponding Author
Email address: david.hancock@ukaea.uk (David Hancock)

Eurofer steel connections and perforated cartridge insert in place of the copper elements.

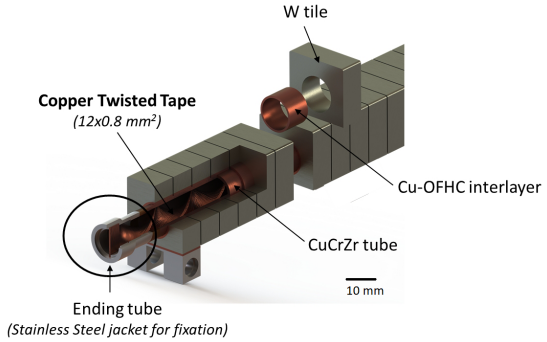

(a) ITER-like [9]

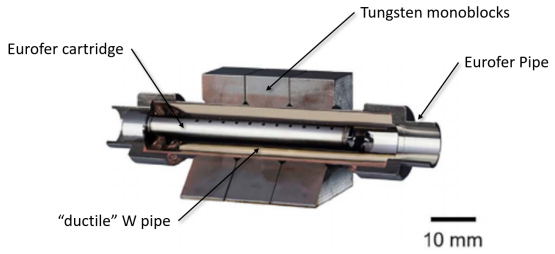

(b) Helium-cooled (adapted from [10])

Figure 1: ITER-like and Helium cooled divertor target designs

A third, high pressure cascade jet impingement concept [11] draws on elements of both of these with a focus on thermal efficiency as well as high performance, but has yet to be fully tested in a representative environment or a manufacturing route proven.

1.3. Why focus on the structural material?

As shown above, the fundamental elements of these and other divertor target concepts can broadly be divided into the following sub-components: coolant, armour, cooled structure, and mechanical support.

Pure tungsten or possibly an alloy thereof with additions for ductility or self passivation are generally understood to be the sole candidates for the armour material due to its high melting point, high sputtering resistance, vacuum compatibility, and reasonable resistance to irradiation damage [12], though alternatives including other refractory metals have been considered [13].

The supporting substructure is assumed to be steel, in keeping with divertor cassette designs for ITER [7] and the current DEMO baseline for first wall components, although the design is still evolving and alloys based on zirconium, chromium, and vanadium have also been discussed [14].

Leading candidate coolants include water and helium, with supercritical CO_2, liquid metals, and molten salts considered for more advanced concepts [15]. Hydrogen is used for cooling turbine generators due to its higher thermal conductivity and specific heat, but it has historically been discounted for fusion applications because of embrittlement concerns [16].

Between the armour and mechanical support, the cooled structural material must be joined to the armour and compatible with the chosen coolant, while containing coolant pressure and conducting heat away from the armour. The choice of this material has the largest impact on overall component performance, driving operational temperature, heat flux handling capability, and integration with surrounding interfaces.

Armour material choice is therefore relatively fixed and (beyond facilitating the choice of plasma geometry) the supporting substructure does not have a significant impact on performance of the plasma facing components, but the selection of coolant and the material for the cooled structure remain much more open to innovation and as such provide a potentially strategic avenue to improvements in performance from current designs. In addition, advanced manufacturing techniques, including additive manufacturing (AM), may allow both the use of materials formerly difficult to form and the production of optimised geometries which further enhance performance.

2. Structural material selection process

The interfaces between the cooled substructure, the surrounding subcomponents, and the operating environment lead to a raft of somewhat conflicting selection criteria.

Recent material selection processes have focused strongly on thermal conductivity and the avoidance of brittle materials, maximising heat handling capability and ease of fabrication [17, 18]. In addition, a conservative approach to manufacturing risk and the costs of qualifying new materials have further restricted the range of options considered, leading to a narrow reliance on copper alloys such as CuCrZr for water cooled designs and tungsten for higher temperature helium cooled concepts. Refractory alloys other than tungsten have historically featured prominently in attempts to design higher power density concepts, but have ultimately been sidelined due to a strict adherence to activation limits or concerns about hydrogen compatibility [19, 20]. In addition, these studies have tended to make decisions based on performance at a single temperature point, rather than evaluating performance at a range of operating conditions.

As detailed in section 6, radiation by the high energy neutrons produced by fusion causes a wide range of damage effects. The scale and nature of these effects is in many cases specific to neutron fluence and energy spectrum. It may be, in some cases, possible to partially extrapolate trends from existing fission-based data, but the lack of a fusion specific (i.e. 14 MeV) neutron source means that there is almost no data at relevant damage levels for the materials under consideration. In an ideal case, a rigorous material selection process would compare

both irradiated and unirradiated properties for all the materials under consideration, giving manufacture to end-of-life performance. The collection of neutron irradiated data for all candidate materials is, however, both cost and time prohibitive if commercial fusion is to be achieved, and so strategic pre-selection is required to direct targeted irradiation campaigns.

A fresh approach to material selection is needed which allows a continuous re-assessment of material options based on current knowledge, technologies, and revised priorities while still seeking to learn from the large volume of relevant historical research. In the absence of an "ideal" material and complete data, a more parallel strengths and weaknesses based approach is proposed.

An initial downselection is still useful, enabling a subset of candidate elements with broadly attractive properties to be compared. After a brief examination of the historical interest in and key attributes of alloys based on these elements, each requirement is examined in turn and rather than rejecting any candidates which "fail," either on the basis of lack of data or less than ideal performance, all the materials are retained throughout. This then leaves a greater number of possible candidates from which a selection can ultimately be made based on a pragmatic choice with carefully considered compromises. This choice can either be taken immediately or, if gaps in knowledge about more promising materials are identified, can feed into irradiation campaigns and alloy development programmes.

Divertor structural material requirements have been, for this paper, grouped into five distinct but inter-related categories: thermomechanical performance, radiation damage tolerance, compatibility with operational environment (including coolant), manufacturability (incoporating forming processes and joining to armour and support substructure and pipework), and price and availability.

Despite their exclusion by the preliminary selection, current preferred structural materials including copper, CuCrZr and stainless steel 316LN (in the absence of extensive data for EUROFER) are included at each stage, giving a clearer comparison with the baseline.

3. Preliminary downselection

Figure 2 shows a flowchart for one approach to a high level downselection method with a particular emphasis on high temperature divertor operation, using a coolant operating at an arbitrary nominal bulk temperature of 600 °C, which leads to refractory metals as candidate materials.

As detailed in section 1.1, improved thermofluid efficiency will be required for commercial fusion power plants over current concepts. Selecting a coolant temperature above that achievable by the baseline concepts introduces an inherent improvement over current water-cooled baseline. This temperature is also selected to highlight the effect of altered design priorities on the core palette of materials.

The process used in this case begins with mechanical strength at high temperature as well as high thermal conductivity, before applying further restrictions based on activation and then availability, cost and mechanical performance under irradiation.

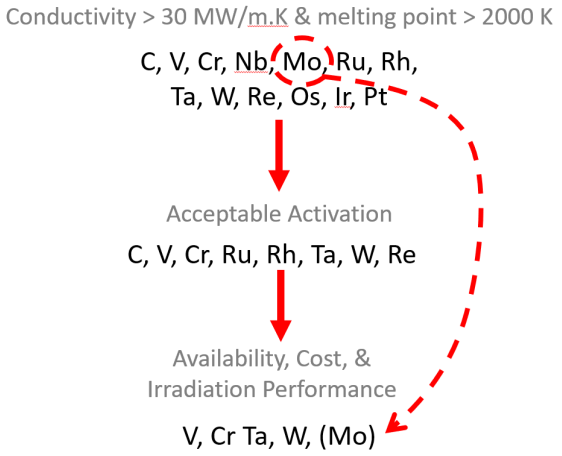

Figure 2: Material Downselection Flowchart

Melting point is used as a simple metric for high temperature operation. 2000 K (1726 °C) is chosen as a convenient threshold by taking onset of significant creep at 30% of melting point and aiming for a 600 °C coolant. Thermal conductivity is considered at room temperature as a first step. "Low" activation materials are considered to be those for which activation levels are below thresholds as defined in section 6. "Availability, cost and irradiation performance" is a more qualitative filter, enabling a pragmatic exclusion of particularly rare or costly elements or those particularly vulnerable to neutron damage.

The significant difference between this and previous methods is to allow the low ductility of chromium, and moderate thermal conductivity of vanadium, while excluding copper and steel on the basis of their lower melting points. Allowing molybdenum despite its less than favourable activation leaves it as a possible additional candidate and is retained for reasons highlighted later in this paper. It is notable at this stage that such a high-temperature focussed approach naturally lends itself to the refractory metal elements and excludes "traditional" materials including CuCrZr and steels which would otherwise remain the baseline beyond ITER.

A reduced initial threshold temperature would significantly widen the scope of the study, and so focussing on refractory metals as a group gives focus to the exercise and facilitates obtaining comparable data.

4. Overview of refractory metals

4.1. Tungsten

With tungsten as the primary candidate for plasma facing armour, including cooling directly would be an attractive option, rather than relying on joints which

have historically been the location for part failures under testing, as well as reducing the number of joints to qualify. Tungsten's inherent brittleness has thus far, however, excluded it from consideration as a structural material, particularly as the ductile to brittle temperature of traditionally manufactured bulk material is raised above 800 °C under neutron irradiation. More recently, however, cold rolled and thin laminated material, as used in the concept shown in figure 1b above, has demonstrated more ductility and toughness than conventional tungsten. Attempts to introduce alloying elements such as tantalum to increase ductility have shown additional surface modification effects under ion irradiation [21] and no suitable alternative has been discovered. High temperature helium-cooled jet impingement concepts such as the HEMJ design do employ tungsten doped with 1 wt.% La_2O_3 (WL10) as the impingement surface, though this is supported by a steel substructure [22] and this design requires an enormous number of steel to tungsten welds and a further joint between the tungsten alloy and pure tungsten armour.

4.2. Molybdenum

Molybdenum and its various alloys are used in a range of high temperature structural applications, due to their high thermal conductivity, high strength, and low thermal expansion. TZM (0.5% Ti, 0.08% Zirconium, balance Mo) is one of the most commonly used Mo alloys; its additions of titanium and zirconium act to increase strength and raise the recrystallization temperature. However, TZM in particular is not optimised for use under irradiation and the limited, exploratory irradiation experiments to date have raised concerns over embrittlement [23]. Various developmental alternatives have been proposed to mitigate these effects but are far from commercialisation. It is also important to note that traditional Mo alloys would be suitable only in selected high heat flux locations within a fusion power plant; elsewhere the higher neutron fluxes bring its activation above the permanent disposal waste (PDW) radiological dose limit. Mitigation options for this are discussed in section 6.

4.3. Tantalum

Tantalum has been discussed for fusion applications for more than 20 years [24], and is an attractive prospect for high temperature applications due to its high ductility and corrosion resistance when compared to other refractories, as well as having similarly high strength and melting point. A number of tantalum alloys were developed in the 1960s for space reactor applications, chief among them T-111 (8% W, 2% Hf, $<$ 100 ppm O, $<$ 50 ppm C, $<$ 50 ppm N, $<$ 10 ppm H) [25] which has been frequently proposed for fusion applications, most recently as a replacement for WL10 in the helium-cooled HEMJ design discussed above. A variant, T-222, with 10 wt% W and 2.5 wt.% Hf, has superior mechanical strength, though available data is less comprehensive [26]. A range of tantalum-tungsten alloys is more readily available, with tungsten percentages ranging from 2.5% (Tantaloy 63) to 10% (Tantaloy 60) with increasing hardness and yield strength and decreasing ductility. [27]

The minimum operating temperature under irradiation is estimated to be well over 1000 °C, however, providing a formidable cooling and balance of plant design challenge. Hydrogen embrittlement also remains a significant worry below 600 °C even before irradiation. Cost and stability of supply in large quantities have historically been cited as grounds for concern, but are not currently as significant.

4.4. Chromium

Chromium alloys were heavily pursued in the 60s and 70s in Australia, US and Russia as a candidate high temperature material via various alloying and thermal treatment studies [28]. Once a potential rival to the eventually dominant nickel superalloys within the aerospace industry, the chromium alloys ultimately fell out of favour and have found only limited applications in the interim. Interestingly, the fusion community undertook some coarse thermo-mechanical testing of two commercially available Plansee chromium alloys in the early 2000s, before abandoning them citing the lack of room temperature ductility as a barrier to application [29]. Given advancements in manufacturing techniques including AM, this may not remain as significant a hurdle. In addition, the alloys in question (Ducropur — a high purity near-elemental product; Ducrolloy — a 5% Fe alloy to tailor thermal expansion for specific electronic applications) were clearly not developed for to fulfil fusion requirements with the historical chromium studies clearly indicating preferential alloying and/or treatment techniques that successfully offered high temperature strengthening or room temperature ductility superior to the two commercial variants considered.

4.5. Vanadium

There has been considerable interest in using vanadium alloys in fusion applications since the 1990s [30, 31]. Vanadium alloys are inherently promising as a candidate structural material for fusion reactors because of their low irradiation-induced activity, favourable mechanical properties and good manufacturability. V-4Cr-4Ti is currently considered to be the "reference" V alloy for use in fusion reactors [32]. The nominal operating temperature range for this alloy is of order 600 °C to 800 °C. However, the supply of this reference material is limited with the largest ingots to date produced in the US, Europe and China but each only representing a few 10s kg. Further challenges are presented with respect to its heat handling and the prospective integrity of a W-V joint given the moderate thermal conductivity and dissimilar thermal expansion coefficient to tungsten.

5. Thermomechanical performance

For many of the materials under consideration only limited thermophysical data are available and so the following section gives a review of several sources, including historical studies cited above (e.g. [29, 31, 32]), material handbooks (e.g. [27]), internal ITER project technical data (e.g. [33, 34]), and data provided by material suppliers (e.g. [35]). The aim is primarily to draw preliminary performance comparisons (particularly at high temperature), demonstrate the proposed methodology, and highlight key gaps in available information using the sources above, rather than provide absolute conclusions or provide an extensive database of material property data. Graphs are plotted without extrapolation for one data source for each property, rather than averaging, and so data may be available from alternative sources where there appears to be a gap.

The influence of heat treatment and thermal history is significant for all of these materials, and values for both annealed and stress relieved conditions are not always available. Where possible, given the preference for high temperature operation, enhanced ductility over strength (in most cases), and the likelihood of extended periods of time at elevated temperature during operation, the recrystalised values are used. This has a significant impact, for example on the yield stress of tungsten, which varies by a factor of 14 between the recrystalised and stress relieved states at room temperature [34].

As stated above, one of the most significant challenges facing designers of fusion high heat flux components is the lack of fusion-neutron irradiated property data for candidate materials at suitable irradiation temperatures, durations, spectra, and fluence levels [12]. Sections 5.1 and 6 do begin to discuss some of the effects of irradiation on structural materials, but in the absence of suitable irradiated data this section will focus on unirradiated comparisons. The hope is that if promising alternative candidate materials emerge from this new selection methodology, irradiation campaigns will follow.

5.1. Operating temperature window

A temperature window can be defined as a guide to describe limits within which the structural material can best be used [36], although geometric considerations and careful assessment of failure mechanisms must also be taken into consideration. At high temperature, the structural material must retain its mechanical strength, usually limited by thermal creep or increases in environmental interactions as outlined in section 7. At lower temperatures, structural properties are usually reduced by radiation effects, particularly radiation embrittlement, which in BCC materials leads to an increase in the ductile to brittle transition temperature (DBTT) and a loss of ductility.

This window should not, however, be considered to provide absolute limits of operation. The lower limit in particular may be extended if guidance for design with brittle materials is followed, an area of active development for fusion reactor confinement boundaries [37]. Similarly, by careful design and analysis, it may be possible to have parts of a structural component operating at much higher temperature where stresses are less significant or where not exposed to damaging environmental conditions.

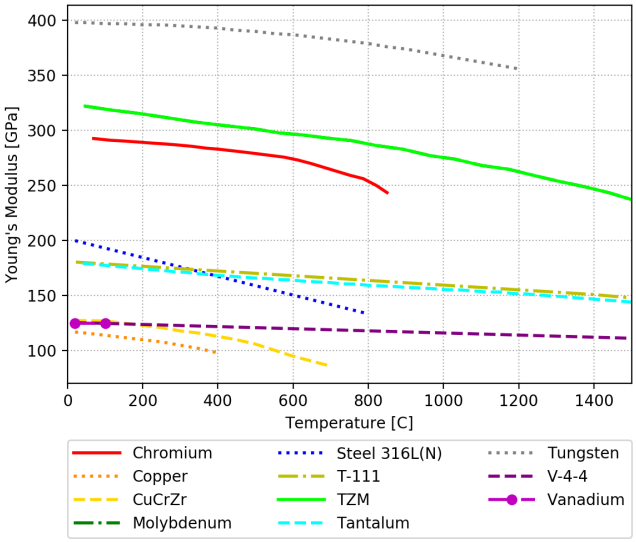

Figure 3: Young's modulus with temperature [33, 26, 35, 31]

5.1.1. High temperature strength

To properly assess high temperature strength, ultimate and yield stress and creep properties across the full temperature range of interest are required, including irradiated properties under fusion neutron irradiation.

Young's modulus is available for a relatively large number of options, however, and gives a general indication of strength. As figure 3 shows, molybdenum and vanadium are closest to tungsten in absolute terms, but only molybdenum and tantalum retain their strength at temperatures over 800 °C.

Figures 4 and 5 show yield stress and ultimate tensile strength for the materials under consideration. As justified above, annealed or recrystalised values have been taken where possible, though like-for-like comparative data for all materials is not available, hence tungsten's surprisingly low relative yield stress. When considering ultimate tensile strength, TZM's enhanced ductility over tungsten gives it significant advantages above 600 °C and T-111 also shows promise across the full temperature range.

5.1.2. Ductile to brittle transition temperature

At the other end of the temperature window, the ductile to brittle transition temperature defines a lower bound for ideal operation. Design rules for brittle materials such as ceramics in fusion structures are being considered [37]. These are preliminary, however, and ductility throughout the operational temperature range is clearly preferable.

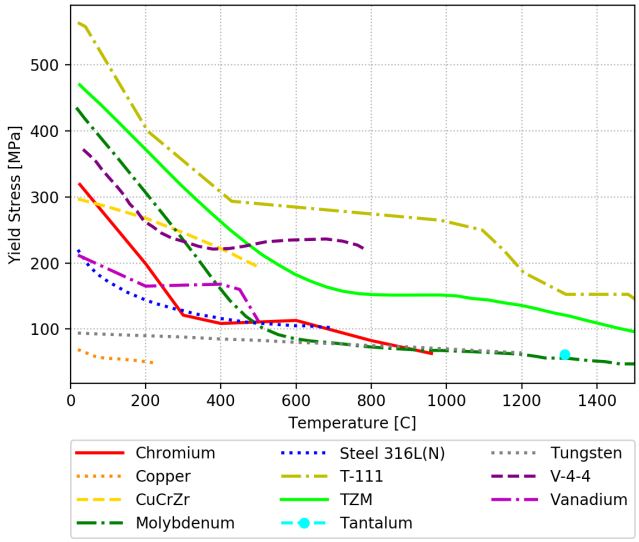

Figure 4: Yield stress with temperature [33, 26, 35, 29, 27]

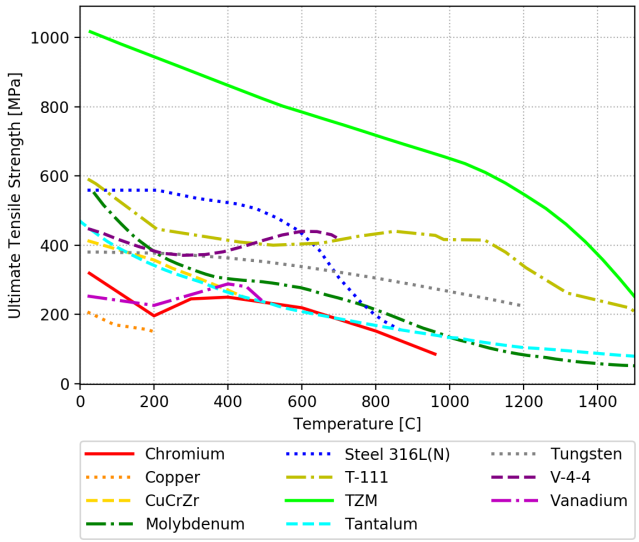

Figure 5: Ultimate tensile strength with temperature [33, 26, 35, 31]

The quantification of radiation induced embrittlement poses an additional challenge, with large uncertainties reported in the change in the DBTT of irradiated tungsten and values up to 880 °C used as the baseline [38], leading to the conclusion that at least some brittleness must be anticipated if refractory metals are to be used in the structure.

Directly comparable unirradiated data for all the materials under consideration is not available, and irradiated data is sparse. In addition, fracture toughness measurements are heavily dependent on the details of sample geometry and test conditions. Data for percentage reduction in area is somewhat more readily available and figure 6 gives values for a number of materials.

This graph shows that in the pure and unirradiated state, of the refractory elements only tantalum and vanadium have particularly attractive ductility at temperatures up to 400 °C, with molybdenum a close third. Care should be taken, however, as even moderate quantities of oxygen or other impurities and relatively low levels of irradiation damage have been shown to significantly degrade ductility [23]. In addition, DBTT (particularly of tungsten) is heavily dependent on grain size and grain refinement may provide a mitigation strategy if subsequent recrystalisation cannot be avoided [10].

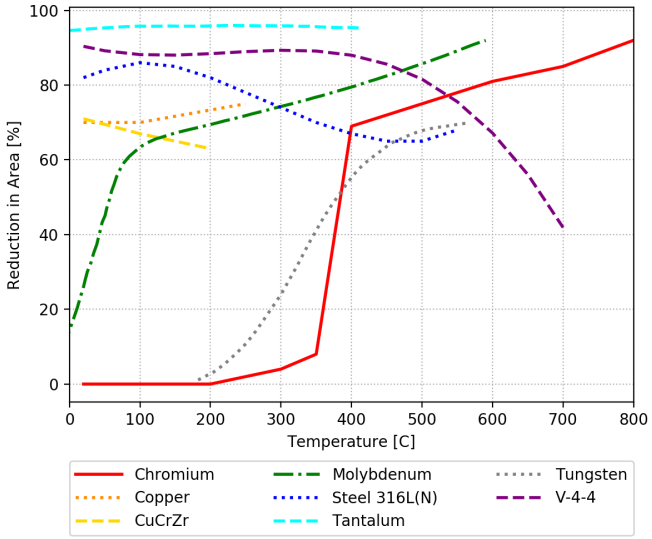

Figure 6: Percentage reduction in area with temperature [33, 27, 32]

5.2. Thermal stress

5.2.1. Thermal conductivity

With steep thermal gradients inevitable in cooled components subject to high heat flux, understanding and quantifying the interaction between thermal and mechanical performance is critical. Thermal conductivity is the primary driver of this thermal gradient but, as shown in figure 7, apart from copper and its alloys, other candidate materials become increasingly comparable at high temperature. This figure does not take into account, however, the additional factors which affect thermal conductivity such as grain size or the presence of impurities or defects, which for this application will include the production of voids or transmutation products as a result of neutron irradiation.

5.2.2. Coefficient of thermal expansion

High thermal gradients induce high thermal stresses, particularly when joints between dissimilar materials are considered. A lower thermal expansion coefficient generally means a lower thermal stress, but as figure 8 shows, differentiating clearly between candidates on this metric alone is insufficient. The challenge of joining copper or steel to tungsten armour is well highlighted however, it is possible to identify chromium and vanadium as an intermediate group, and it is clear that tantalum and molybdenum alloys are much better matched to tungsten.

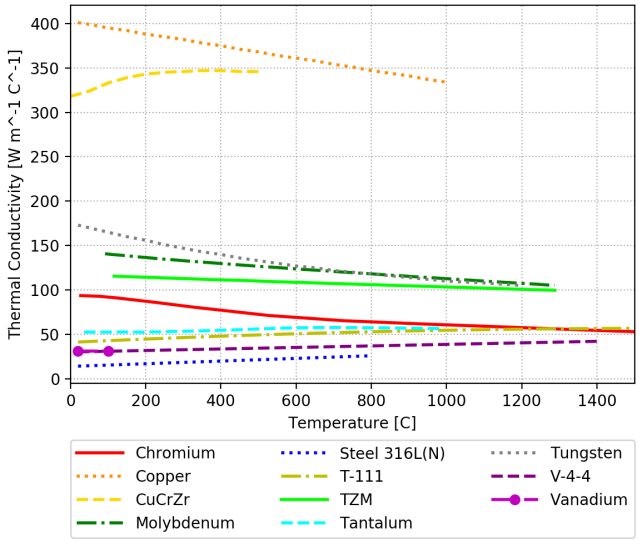

Figure 7: Thermal conductivity with temperature [33, 26, 35, 31]

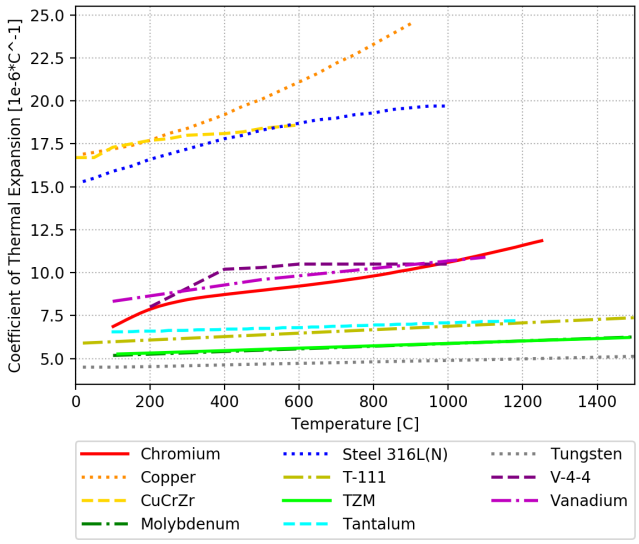

Figure 8: Thermal expansion with temperature [33, 26, 35, 31]

5.2.3. *Thermal stress figure of merit*

In order to clarify these interrelated criteria, Zinkle and Ghoneim [36] define a figure of merit for thermal stress M to qualitatively rank candidate materials in terms of maximum allowable heat flux. This value is dependent on ultimate tensile strength (σ_{UTS}), thermal conductivity (k_{th}), Young's modulus (E), coefficient of thermal expansion (α_{th}), and Poisson's ratio (ν) as shown in equation 1.

$$\phi_{qmax} \propto \frac{M}{\Delta x} = \frac{\sigma_{UTS} k_{th}(1-\upsilon)}{\alpha_{th} E \Delta x} \tag{1}$$

Here ϕ_{qmax} is the maximum allowable heat flux and Δx is the wall thickness of a constrained plate. Thus higher values of M indicate a better ability for a given material to handle high heat fluxes. Figure 9 shows a plot

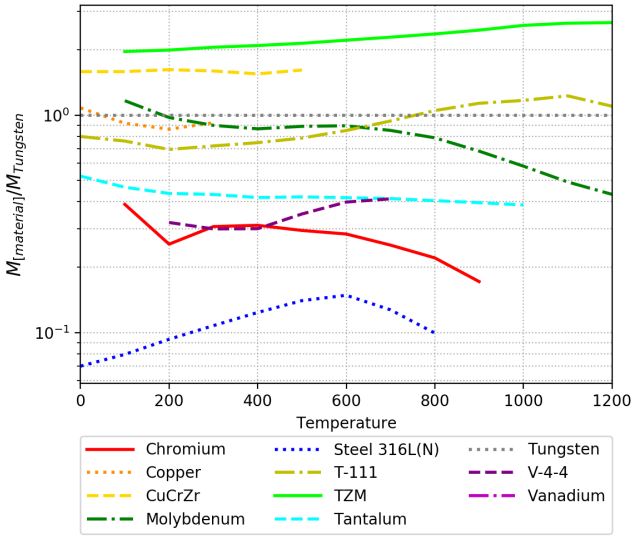

Figure 9: Thermal stress figure of merit with temperature relative to tungsten

of $M_{[material]}$ against temperature (normalised against $M_{tungsten}$ for clarity) when applied to a $5mm$ thick plate of the materials under consideration.

This graph makes it clear why CuCrZr has been such a strong candidate for high heat flux components operating at lower temperatures. However, the significant reduction in strength at high temperature (figures 4 and 5) precludes it from use above about 350 °C [38].

Notably, TZM emerges as an attractive prospect, surpassing even CuCrZr, and elemental molybdenum is comparable to pure copper. The remaining materials are much more closely grouped, with tantalum and its alloys only slightly better than chromium, vanadium or even steel.

5.2.4. *Thermal mismatch stress*

Thermal stress within the structural material due to thermal gradient is not the whole story, however. The primary cause of failure in prototype divertor components has been the interface between the structure (in most cases CuCrZr) and the tungsten armour [39]. Pure copper is used in ITER as a ductile interlayer to mitigate this, and concepts employing more complex compliant or graded structures have also been proposed for DEMO [40, 41]. At the same time, alternative materials with lower thermal mismatches are being explored, including chromium [42]. Applying a thin-walled tube approximation, the stress induced in the structural material due to the thermal expansion mismatch can be calculated using a standard

planar stress calculation as shown in equation 2.

$$\sigma_{mm} = \frac{\alpha_2(T_{2,mean} - T_{ref}) - \alpha_1(T_{1,mean} - T_{ref})}{\frac{(1-\upsilon_2)t_1}{t_2 E_2} + \frac{1-\upsilon_1}{E_1}}$$
$$T_{1,mean} = T_{coolant} + \frac{q}{h} + \frac{qt_1}{2.k_1} \quad (2)$$
$$T_{2,mean} = T_{coolant} + \frac{q}{h} + \frac{qt_1}{k_1} + \frac{qt_2}{2k_2}$$

where σ_{mm} is the mismatch stress, T_{ref} is the reference starting temperature of the component, $T_{coolant}$ is the bulk coolant temperature, q is the incident heat flux, t_1 and t_2 are the thicknesses of structure and armour respectively, $T_{1,mean}$ and $T_{2,mean}$ are the mean temperatures in each material, ν_1 and ν_2 are Poisson's ratios, α_1 α_2 are thermal expansion coefficients, and E_1 and E_2 are Young's moduli [43].

This equation can be used to indicate the degree of mismatch between tungsten armour and substructure, and so figure 10 shows a graph of the magnitude of this stress with applied heat fluxes up to 25 MW m^{-2} calculated for 1 mm of a range of materials paired with 5 mm of tungsten using 150 °C coolant. Values are not plotted once mean temperatures in the structural material are 100 °C above the maximum temperature for which material data has been provided.

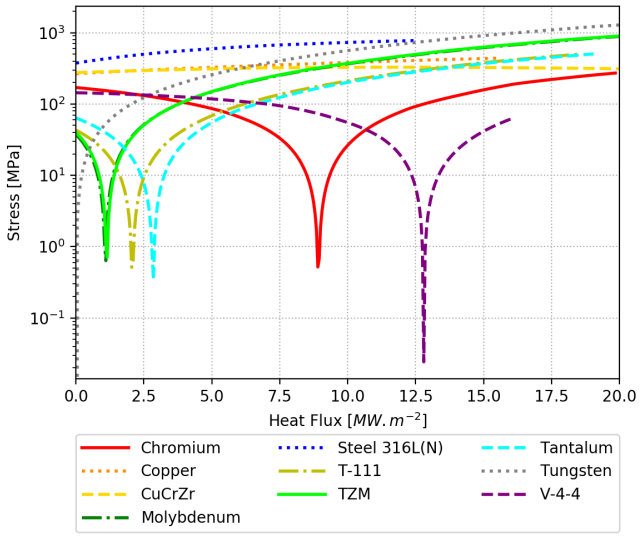

Figure 10: Thermal mismatch stress using 150 °C coolant.

Notably, at a certain combination of heat flux, material thicknesses, and thermal conductivities, using a material with a slightly larger thermal expansion coefficient and lower thermal conductivity than tungsten results in a lower stress at the interface than even a tungsten-tungsten joint, due to the large temperature gradient mitigating the thermal expansion mismatch. At heat fluxes below approximately 7 MW m^{-2} tantalum and molybdenum alloys show the best performance. At higher heat fluxes, however, chromium and vanadium become the clear favourites. The "ideal" heat flux for CuCrZr for this combination of material thicknesses, temperatures, and convective heat transfer coefficients is higher than has been plotted, but the mean material temperature at this point is sufficiently high that structural properties are significantly degraded.

Figure 11 highlights the sensitivity of material pairing to component design parameters. For example, increasing the coolant temperature to 500 °C significantly improves the performance of tantalum and molybdenum alloys, but further excludes copper alloys and moves chromium and vanadium outside their operating temperature windows.

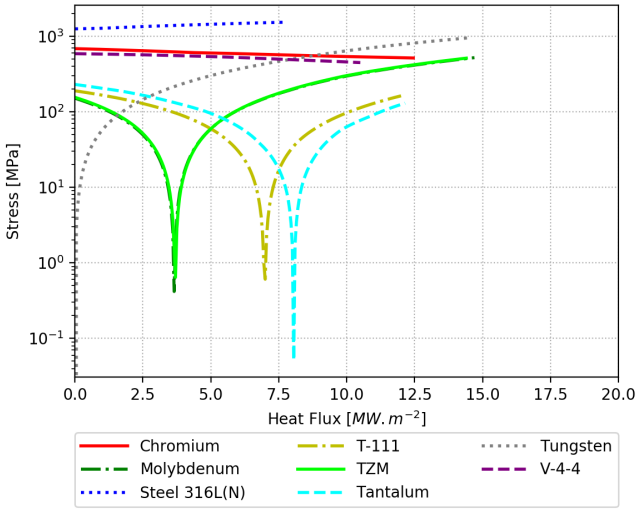

Figure 11: Thermal mismatch stress using 500 °C coolant.

The choice of T_{ref} is also a critical factor in the validity of these graphs, as bonding is usually carried out at elevated temperatures. Geometric design and variation in heat transfer coefficient or methods to remove residual stress during and post assembly (e.g. [44]) will further significantly impact these values, and so these calculations should be taken as demonstrating a figure of merit to be used as a tool for assessing coupled sets of design parameters including material choice rather than as engineering design proposals as they stand.

6. Radiation damage tolerance

As well as radiation induced loss of ductility as described in section 5.1, additional radiation damage mechanisms must be considered, namely activation and swelling.

In order to satisfy environmental responsibility and reduce decommissioning costs, the fusion community have set ambitious and stringent requirements on the activation of power plant components as follows:

As given in [45], for remote handling recycling the dose rate limit is:

$$\sum_{i=1}^{118} A(^{A}_{i}X) < 10\frac{mSv}{hr} \quad (3)$$
$$and \quad Decay\ heat < 10W/m^3$$

For hands-on recycling the dose rate limit is:

$$\sum_{i=1}^{118} A(^{A}_{i}X) < 10\frac{\mu Sv}{hr} \quad (4)$$
$$and \quad Decay\ heat < 1W/m^3$$

The above criteria are to be achieved within 100 years ex-reactor.

Combining these and other environmental concerns, IAEA guidelines define a clearance index of a material to determine if the material can be disposed of with no special precautions. If less than 1 then the material can be disposed of or 'cleared' as if it were non-radioactive [46].

Figures 12, 13, and 14 show dose rate, decay power, and clearance index plots against these limits for tungsten, molybdenum, tantalum, chromium, and vanadium calculated for a neutron spectra corresponding to the first wall of a conceptual fusion power plant [47]. Copper is also included for comparison.

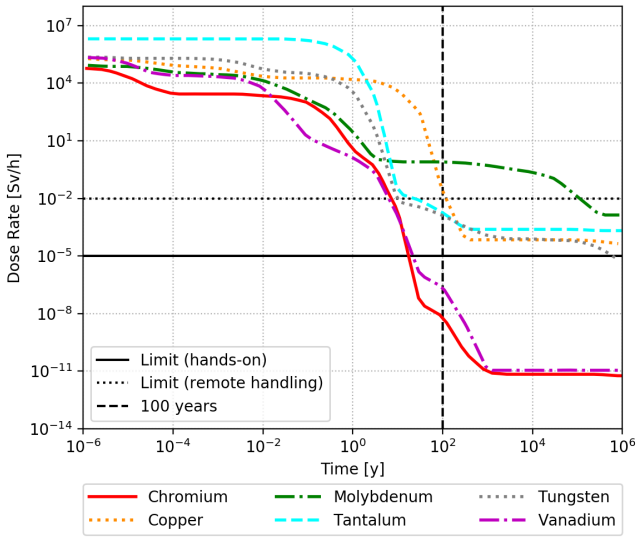

Figure 12: Activation Dose Rate

This data shows that molybdenum is significantly more activated than the other materials considered, chromium and vanadium are notably less activated, and tantalum compares favourably with tungsten and copper at the 100 year cut-off timescales.

These graphs also show that despite to the oft repeated mantra of, "everything to be recyclable in 100 years," the currently assumed first wall armour and structural materials of tungsten and copper alloys will not meet this

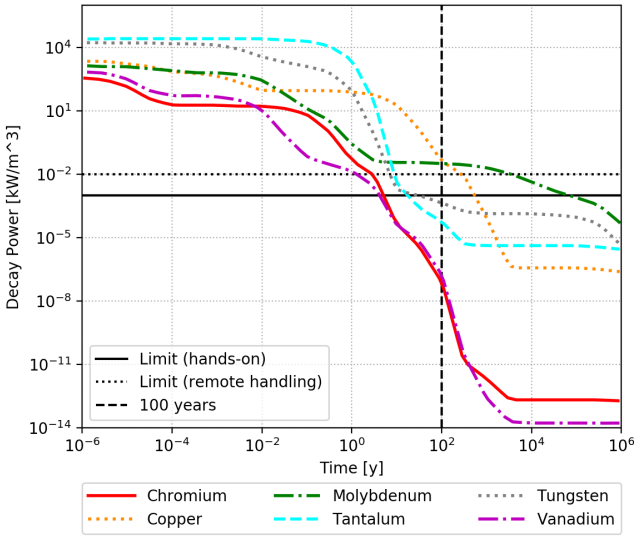

Figure 13: Activation Decay Power

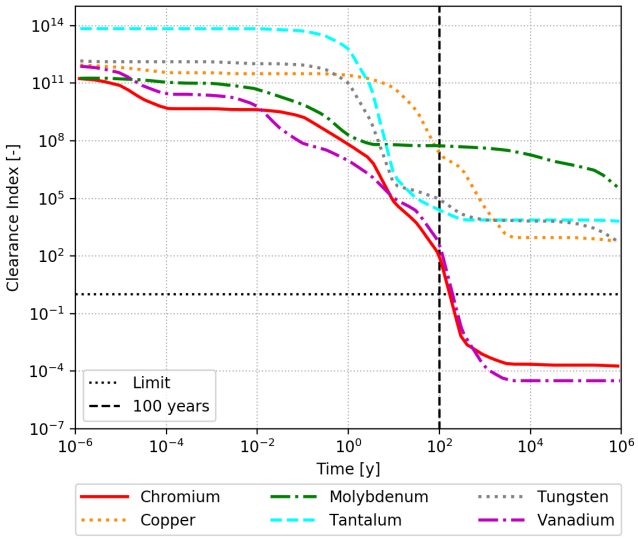

Figure 14: Activation Clearance Index

target with the baseline first wall neutron spectra. Given the apparent inevitability of a certain quantity of mid-level waste at the decommissioning stage of the first generation of fusion power plants (or at least for an engineering demonstrator such as DEMO), it seems sensible to tentatively consider the possibility of small quantities of more activated materials during this phase of fusion power development, if concepts employing them provide a route to progressing towards commercialisation and overcoming other challenges in parallel.

If even allowing modest quantities of active waste is discounted, Gilbert et al. [48] have demonstrated that isotope tailoring provides one route to using materials which would not otherwise be palatable, and have used molybdenum as an example. Seven isotopes of molybdenum occur naturally in relatively equal abundance, one

of which (Mo97) is significantly less activated than the others. Figure 15 shows that although it does not meet the dose rate requirements, it does compare favourably with tungsten after the 100 year limit.

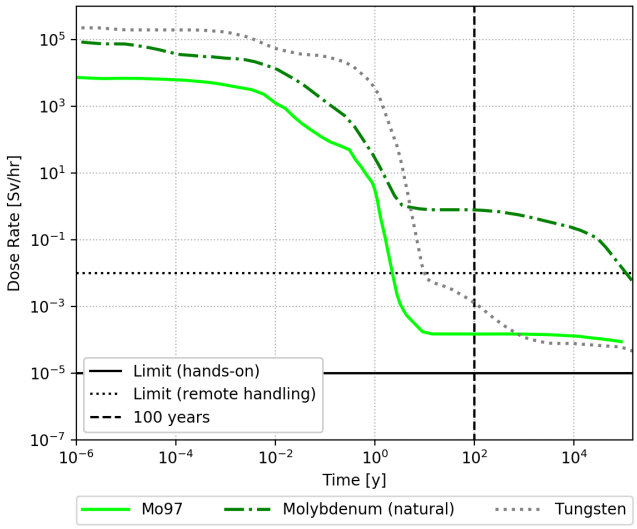

Figure 15: Isotope tailoring of molybdenum

Achieving the enrichment needed to meet this level of activation will almost certainly be prohibitively expensive for bulk elemental molybdenum, but if quantities of isotopically tailored material are small or if Mo97 is used as a minor alloying element to enhance performance in another candidate material, it may prove a worthwhile tool in the designers' arsenal and should not be immediately discounted.

The high heat flux and shallow grazing angle of incident particle fluxes on plasma facing surfaces require close geometric tolerances to be maintained throughout the lifetime of divertor components. Helium production in neutron irradiated materials causes swelling [49] which can accelerate surface erosion and induce additional stresses which in turn reduce component lifetime. Little data is available for materials other than tungsten in a fusion neutron spectrum, but the BCC crystal structure of the other refractory metals suggests that the degree of swelling will be similar.

7. Chemical compatibility with operating environment

Thermomechanical performance of structural materials for fusion must be maintained throughout the component lifetime while exposed to both the demanding rigours of the tokamak environment on the plasma-facing side and the coolant on internal surfaces. In addition, condideration must be made for manufacturing and off-normal events. A full evaluation of all the mechanisms involved is beyond the scope of this paper, particularly as comparable quantitative data for each pairing of material and reagent is not available. The following sections, therefore, highlight critical issues and present a brief summary of available knowledge.

7.1. Oxidation

During normal operation, the low concentration of oxygen in the tokamak environment prevents signifcant oxidation of exposed surfaces. This is not the case during off-normal events such as loss of coolant or air ingress, however, and self-passivating alloys are actively being developed to prevent the production of volatile tungsten oxides under these circumstances [17]. Resistance to oxidation also has a significant impact on ease of manufacture, particularly for high-temperature melt-based joining or forming processes such as welding, brazing, or additive manufacturing.

All of the refractory metals under consideration have relatively poor resistance to oxidation. As mechanisms and rate of weight loss or gain are dependent on both temperature and precise atmospheric conditions, quantitative susceptibility to oxidation is application specific, but the temperature at which the major oxide becomes volatile gives a good indication for ranking purposes.

By this measure, chromium has the highest resistance, melting at 1907 °C, well before Cr_2O_3 becomes volatile. Tantalum is next, with Ta_2O_5 becoming volatile at 1370 °C, followed by W_2O_5 at 1000 °C, MoO_3 at 800 °C, and Cr_2O_3 at 675 °C.

7.2. Tokamak gasses

The structural materials will largely be shielded from direct contact with incident particle fluxes by the tungsten armour, but will nonetheless still be exposed to the tokamak environment. Primarily, this means that vapour pressure must be low enough to maintain ultra-high-vacuum, but exposure to hydrogen isotopes and helium pose additional challenges. Tritium retention must be as low as possible in order to both minimise overall radioactive inventory in a reactor and to avoid loss of available fuel due to decay. In addition, exposure to hydrogen causes embrittlement, and this has historically been the cause of most concern (e.g. [16, 20]). The degree of embrittlement, particularly when combined with radiation effects, depends heavily on partial pressure of hydrogen and operating temperature of the component. In addition, hydrogen can, in some cases, be sufficiently removed by holding the component at an elevated temperature [50].

7.3. Coolant

Proposed high temperature coolants for fusion high heat flux applications fall broadly into four categories: gasses, supercritical fluids, liquid metals, and molten salts. The choice of pairing of structural material and coolant is an integrated decision closely tied to the geometry and is based on multiple interdependent factors. Comparisons of

thermofluid performance, based on bulk coolant temperature, heat transfer coefficient, and critical heat flux have been reported elsewhere, e.g. [15, 51]. Wider balance of plant and reactivity considerations are less connected to the choice of structural material and are also well debated, e.g. [52]. Information is less well collated on issues of corrosion, erosion, and embrittlement in the context of specifically high temperature fusion applications and refractory materials, and so the following sections will focus primarily on these for each type of coolant, while highlighting gaps in knowledge, where necessary.

7.3.1. Gasses

The pressure inside cooling channels will be significantly different from that outside, but compatibility with the leading candidate gas coolants, helium and hydrogen, has been covered above. Other than the embrittlement previously discussed, significant concerns regarding the use of these are generally material independent, and are more operational issues such as leak tightness, cost, thermal efficiency, and safety.

7.3.2. Supercritical fluids

Supercritical water has been proposed as a coolant for both fission and fusion, is currently used in state of the art high temperature fossil fuel power plants up to 600 °C, and has been proposed for applications up to 700 °C [53]. Despite this, the focus of corrosion studies has been on a relatively small number of conventional materials with less information available on refractory alloys. At first inspection, the high corrosion resistance of refractory alloys suggests that this may not be a significant concern, but the release of both oxygen and hydrogen due to radiolysis under neutron exposure raises the possibility of reaction from both.

There is also some experience of using supercritical CO_2 for gas-cooled fission reactors and it has been proposed for the secondary coolant loop of fusion power plants [54, 55], but its use as a primary coolant has not been fully explored.

In summary, both supercritical water and CO_2 promise high heat transfer coefficients at high temperature at the expense of very high pressure operation and unknown corrosion performance.

7.3.3. Liquid metals

Liquid metals, particularly lithium, lead-lithium, and sodium have persistently been considered as coolants for both fission [56] and fusion [5]. For fusion, this has included use as both coolant and as plasma facing material for blanket and divertor applications (e.g. [57, 6, 58, 59]), to the extent that a lead-lithium divertor was included as the baseline of the most advanced of the European powerplant conceptual study concepts [45].

Dual cooled lithium lead blanket (DCLL) concepts exist for both ITER and DEMO [60, 61]. Liquid metals have very high boiling temperature and high heat transfer capability, even at low pressure, and, if lithium or lead-lithium is used, can perform multiple-duty as coolant, neutron multiplier, and tritium breeder. These significant benefits must be balanced with numerous challenges, however. Magnetohydrodynamic (MHD) effects due to flow in the presence of tokamak magnetic fields increase pumping power significantly, even at low velocities and when care is taken with the orientation of flow channels. Where water is used as a secondary coolant, reactivity in the event of leakages is a significant risk.

As with molten salts, corrosion and erosion are of significant concern. Compatibility with tantalum is well established, but corrosion [62] and other interactions such as wetting properties [63] require further characterisation under fusion-relevant conditions.

7.3.4. Molten salts

Corrosion is the driving factor affecting compatibility between structural material and molten salts. Corrosivity depends heavily on impurities present in the salt used, and so quantitative assessments of compatibility are subject to the need for careful chemistry control. Reviews of the literature suggest that historical studies have mainly been limited to a subset of nickel based superalloys [64], but these give indications of the susceptibility of various alloying elements which can be used to infer relative performance of alloys based on these.

For fluoride salts chromium is the most readily corroded element among the most common constituents of nickel alloys, but tantalum fluoride has an even lower energy of formation suggesting yet greater vulnerability. Molybdenum, vanadium, and tungsten on the other hand are more comparable to iron and nickel, suggesting performance comparable to alloys previously studied, with molybdenum alloys historically listed as the most favourable for fusion applications (e.g. [24]). Trials using FLiBe with vanadium alloys have also identified tritium permeation and retention as a significant challenge which needs careful control measures [65]

Results for chloride salts reported in the above reviews suggest that they may be more corrosive than their fluoride counterparts, though studies on relevant materials are even more limited.

Although internal coatings can be used to allow use of a wider range of materials, if complex cooling geometries are to be employed, both the application of these coatings and the verification of their efficacy become increasingly challenging.

8. Manufacturing process

Purely selecting a structural material for a high heat flux component on its thermomechanical properties and chemical merits is not sufficient, however: the concept must be manufactured. The cooled structure must be formed into the desired geometry, whether tube or more

complex shape, and it must be joined to the armour either directly or using an interlayer. Throughout these processes, the mechanical properties must be maintained — typically meaning the maintenance (or generation) of suitable grain structure.

8.1. Forming

The inherent hardness and high melting points of refractory metals makes them very difficult to form and fragile if complex shapes are used. Drawing for tubes or forging requires high ductility and very high temperature tooling. Tungsten, in particular, is difficult to machine, and cutting using electrode discharge machining is time consuming and expensive. Traditional powder metallurgy including pressing and sintering is limited to relatively simple shapes and does not lend itself to pressure-retaining geometries.

More recent work has focused on tungsten, examining the use of multilayered foils, powder injection moulding, and fibre reinforced composites and seeks to solve some of these problems, particularly striving for increased ductility [66].

Additive manufacturing opens the possibility of employing complex geometries not achievable by conventional manufacturing techniques as well as significantly more efficient use of raw material reducing both wastage and remote handling mass [67]. Figure 16 shows as an example the level of complexity that can be achieved in powder bed additive layer manufacturing, though robust consistency of material properties has yet to be established for a full range of refractory materials, with tantalum and vanadium as the most promising so far [68].

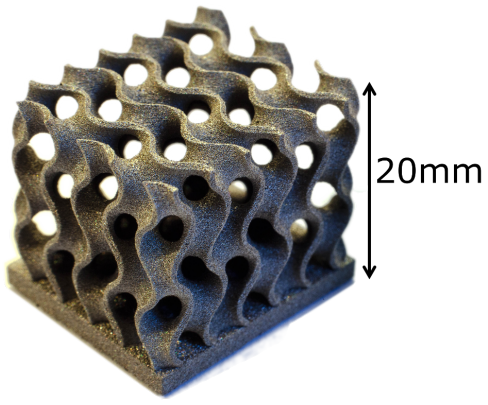

Figure 16: additively manufactured tungsten gyroid

8.2. Joining

As stated in section 5.2.4, The joint between tungsten armour and copper alloy substructure has historically been the primary point of failure for high heat flux components, due to the high thermal expansion mismatch. For these dissimilar metal joints, ductility is a desirable characteristic as detailed above, and the inclusion of a ductile pure copper interlayer is the usual mitigation technique. Newer concepts involving compliant structures have also shown the ability to survive large numbers of cycles at elevated heat fluxes [40]. Novel thermal cycling methods for brazing dissimilar materials [44] have also been proposed for reducing these stresses in operation.

One of the most active areas of investigation is that of functionally grading the joint. For copper and tungsten, this has been attempted using a range of methods, including plasma spray techniques [69], melt infiltration [70], spark plasma sintering [71], and laminated foils [72]. For refractory metals, wire arc additive manufacturing has been used to produce a promising three layer joint between tantalum, molybdenum, and tungsten, though this work is unpublished at the time of writing.

The mutual solubility of the two materials and any intermetallic phases formed between them are critical factors in the ease of joining, as well as proximity of melting point, if direct melt-based joining processes are to be used without e.g. braze filler. Of the materials under consideration in this paper, tantalum in particular has excellent solubility with tungsten and with its high melting point lends itself well to powder based grading processes.

9. Price and availability

Figure 17 shows the historical price of a number of refractory elements, with copper included for comparison. Price has been an argument for excluding tantalum for consideration, and while costs have fluctuated significantly in recent years, it is certainly an ongoing concern, being nearly an order of magnitude more costly than tungsten. Notably, chromium has remained significantly cheaper than even copper, and molybdenum and vanadium have shown a marked downward trend over the last few years making them worthy of monitoring.

Of ongoing concern is the future availability of candidate materials for fusion applications. Figure 18 shows relative stability over the last 50 years for all materials under consideration, with similar levels of production for tungsten, molybdenum, and vanadium. Tantalum's relative scarcity and chromium's significance (e.g. as an alloying element in steel) are also clearly shown.

Concepts based around additive manufacturing require the supply of suitable feedstock. Elemental tungsten, tantalum, molybdenum, and vanadium powders for laser powder bed fusion have been sourced in small quantities and trials are ongoing with the use of both blended and pre-alloyed tungsten-tantalum ratios but quality has been highly variable between suppliers and cost remains high.

In addition, as shown in the proceeding sections, alloys of candidate elements are likely to show better performance overall than the elements alone, and supply chain for fusion-relevant (and in some cases novel) refractory alloys would need to be fully established, including a

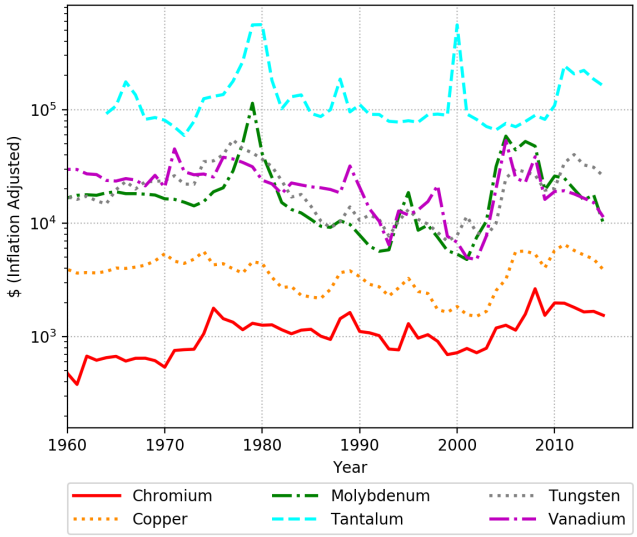

Figure 17: Historical refractory metal prices [USGS]

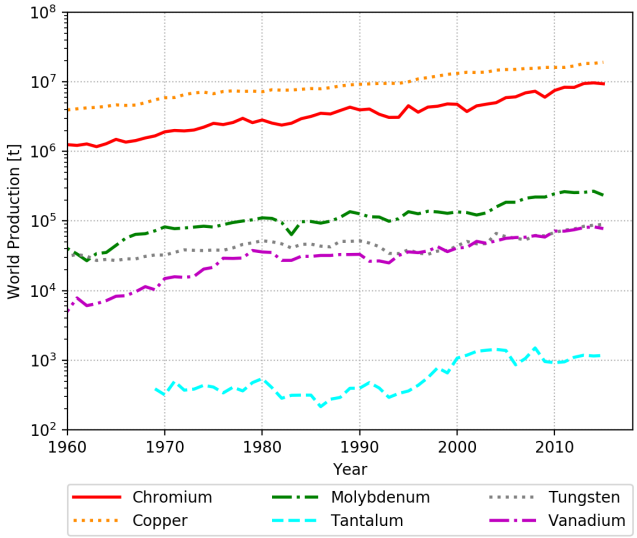

Figure 18: World Production of candidate materials [USGS]

programme of characterisation and testing, before they could be considered for inclusion as structural material candidates.

10. SWOT analyses

Tables 1 to 5 show one approach for assessing the results detailed above. Each element is subjected to a SWOT analysis summarising the strengths, weaknesses, opportunities, and threats associated with choosing alloys based on it. In this case, **"strengths"** and **"weaknesses"** are taken to be inherent properties of the material which are advantageous or disadvantageous for their use. On the other hand, **"opportunities"** and **"threats"** are external; being either possible research avenues which might prove the material to be useful or factors where there is large uncertainty either due to lack of available data or unknown future priorities.

Table 1: Tungsten SWOT analysis

Strengths • Current baseline material • No joint to armour needed	**Weaknesses** • Brittleness • Oxidation • Significant loss in strength when recrystalised
Opportunities • Advanced manufacturing may allow cooled structures • Alloy development may increase ductility	**Threats** • Lack of irradiated data • Variability in quality of supplied material

Table 2: Molybdenum SWOT analysis

Strengths • TZM has excellent high temperature strength • High thermal conductivity • Low thermal expansion	**Weaknesses** • Activation • Oxidation • Brittleness
Opportunities • Isotope tailoring may permit some use • Fusion specific alloys may be possible which are more suitable than TZM under irradiation	**Threats** • Lack of irradiated data • Lack of corrosion data

Table 3: Tantalum SWOT analysis

Strengths • Alloys have excellent high temperature performance • Excellent corrosion and oxidation resistance • Proven compatibility with liquid metals • Good low temperature ductility	**Weaknesses** • High cost • Must be operated at very high temperature to avoid embrittlement • Poor compatibility with molten salts
Opportunities • Exploration of historical alloys such as T-111 • Results of additive manufacturing trials are promising	**Threats** • Lack of irradiated data • Uncertain availability

Lack of available relevant irradiated data is a constant threat across all fusion materials and corrosion data is

Table 4: Chromium SWOT analysis

Strengths • Good thermal mismatch behaviour at lower bulk temperatures • Very low Activation • Low Cost	**Weaknesses** • Moderate yield and ultimate strength at high temperature • Brittleness • Poor thermal stress figure of merit • Poor compatibility with molten salts
Opportunities • Designs for thermal mismatch reduction • Alloy development to increase ductility	**Threats** • Lack of irradiated data • Lack of corrosion data

Table 5: Vanadium SWOT analysis

Strengths • Significant body of historical research • Very low activation • Good unirradiated ductility	**Weaknesses** • Modest strength at high temperature
Opportunities • Alloy development may improve performance • Poor thermal mismatch at high temperature	**Threats** • Lack of irradiated data • Lack of corrosion data • Limited supply of suitable alloys

almost as equally sparse. Although the inclusion in each table might seem excessive, continuing to highlight the strategic relevance of these research areas remains an important task. Similarly, the potential for developing new alloys more specifically suited to fusion applications or revisiting historical research on refractory alloys such as T-111 occurs repeatedly in the "opportunities" quadrants, particularly when seeking to employ advanced technologies such as additive manufacturing with different requirements to traditional techniques.

11. Conclusions

Historical material selection processes for fusion high heat flux structural materials have generally taken a linear sequential approach to requirements, excluding elements from the periodic table or known alloys at each stage. This, along with a prevailing conservatism within the community, has led to a very small palette of options available to component designers. Some recent work on composites of these materials has shown enhanced strength and damage tolerance, but the potential for significant performance enhancement if alternative materials can be found for cooled structures leads to a desire to re-evaluate the initial material selection process.

Recent advances in manufacturing methods, including additive manufacturing; improved analysis and testing towards design with brittle materials; progress in the practicality of designing alloys for specific applications; and a fuller assessment of the feasibility of isotope tailoring or more pragmatic approach to the rigorous application of the "recyclable in 100 years" mantra will inevitably broaden the aforementioned palette of candidate materials. Component designers must therefore make choices based on a more nuanced parallel assessment of strengths and compromises, recognising that no "ideal" material exists for any application. Such an assessment will inevitably identify gaps in knowledge and will prompt targeted research, including alloy development, material testing, and irradiation campaigns. New materials, new manufacturing techniques, and new geometric design freedom will also need new design rules for determining structural integrity for future fusion devices and although this need is already recognised for DEMO (e.g. [73]), the early identification of candidate materials and processes will allow their timely inclusion in these design guidelines.

This paper demonstrates one such assessment, focussed on high temperature operation of divertor components, looking at thermomechanical performance, radiation damage tolerance, chemical compatibility, manufacturing, and price and availability of a number of refractory metals identified as a promising group following a preliminary downselection exercise. Material properties and derived figures of merit are compared to current baseline materials and general observations are made at each stage.

Brittleness, manufacturability, and concerns about activation have historically been grounds for excluding many of these refractory alloys from consideration when designing divertor target concepts and other high heat flux components for fusion energy. Despite other issues such as availability and lack of data for alloys rather than pure elements rendering a number of these relatively unattractive at present, the value of further investigation into their development and subsequent use has been discussed.

Acknowledgements

This work has been carried out within the framework of the EUROfusion Consortium and has received funding from the Euratom research and training programme 2014-2018 under grant agreement No 633053. This project has also received funding from the European Union's Seventh Framework Programme for research, technical development, and demonstration under grant agreement no 313781. The views and opinions expressed herein do not necessarily reflect those of the European Commission. This work has also been part-funded by the RCUK Energy Programme [grant number EP/P012450/1]. To obtain further information on the data and models underlying this paper please contact publicationsmanager@ccfe.ac.uk.

The authors also gratefully acknowledge the support of the whole AMAZE project team, particularly Matti Coleman for assistance with defining requirements and Chris Harrington for his extensive knowledge of fusion relevant coolants.

References

[1] M. Turnyanskiy, R. Neu, R. Albanese, R. Ambrosino, C. Bachmann, S. Brezinsek, T. Donne, T. Eich, G. Falchetto, G. Federici, D. Kalupin, X. Litaudon, M. Mayoral, D. McDonald, H. Reimerdes, F. Romanelli, R. Wenninger, J.-H. You, European roadmap to the realization of fusion energy: Mission for solution on heat-exhaust systems, Fusion Eng. Des.doi:10.1016/j.fusengdes.2015.04.041.

[2] G. Fishpool, J. Canik, G. Cunningham, J. Harrison, I. Katramados, A. Kirk, M. Kovari, H. Meyer, R. Scannell, MAST-upgrade divertor facility and assessing performance of long-legged divertors, J. Nucl. Mater. 438 (2013) S356–S359. doi:10.1016/j.jnucmat.2013.01.067.

[3] R. Zagórski, V. Pericoli, H. Reimerdes, R. Ambrosino, H. Bufferand, Evaluation of the power and particle exhaust performance of various alternative divertor concepts for DEMO, 22nd Int. Conf. Plasma Surf. Interact. Control. Fusion Devices (2016) 39.

[4] G. Federici, W. Biel, M. Gilbert, R. Kemp, N. Taylor, R. Wenninger, European DEMO design strategy and consequences for materials, Nucl. Fusion 57 (9) (2017) 092002. doi:10.1088/1741-4326/57/9/092002.

[5] F. L. Tabarés, Present status of liquid metal research for a fusion reactor, Plasma Phys. Control. Fusion 58 (1) (2016) 014014. doi:10.1088/0741-3335/58/1/014014.

[6] R. J. Goldston, R. Myers, J. Schwartz, The lithium vapor box divertor, Phys. Scr. T167 (T167) (2016) 014017. doi:10.1088/0031-8949/T167/1/014017.

[7] T. Hirai, V. Barabash, F. Escourbiac, A. Durocher, L. Ferrand, V. Komarov, M. Merola, ITER divertor materials and manufacturing challenges (jul 2017). doi:10.1016/j.fusengdes.2017.07.009.

[8] P. Norajitra, R. Giniyatulin, T. Hirai, W. Krauss, V. Kuznetsov, I. Mazul, I. Ovchinnikov, J. Reiser, G. Ritz, H.-J. Ritzhaupt-Kleissl, V. Widak, Current status of He-cooled divertor development for DEMO, Fusion Eng. Des. 84 (7-11) (2009) 1429–1433. doi:10.1016/J.FUSENGDES.2008.11.042.

[9] Y. Huang, M. S. Tillack, N. M. Ghoniem, Tungsten monoblock concepts for the Fusion Nuclear Science Facility (FNSF) first wall and divertor (jun 2017). doi:10.1016/j.fusengdes.2017.06.026.

[10] J. Reiser, L. Garrison, H. Greuner, J. Hoffmann, T. Weingärtner, U. Jäntsch, M. Klimenkov, P. Franke, S. Bonk, C. Bonnekoh, S. Sickinger, S. Baumgärtner, D. Bolich, M. Hoffmann, R. Ziegler, J. Konrad, J. Hohe, A. Hoffmann, T. Mrotzek, M. Seiss, M. Rieth, A. Möslang, Ductilisation of tungsten (W): Tungsten laminated composites, Int. J. Refract. Met. Hard Mater. 69 (2017) 66–109. doi:10.1016/j.ijrmhm.2017.07.013.

[11] J. R. J. Nicholas, P. Ireland, D. Hancock, D. Robertson, Development of a high-heat flux cooling element with potential application in a near-term fusion power plant divertor, Fusion Eng. Des. 96-97 (2015) 136–141. doi:10.1016/j.fusengdes.2015.03.033.

[12] D. Stork, P. Agostini, J.-L. Boutard, D. Buckthorpe, E. Diegele, S. L. Dudarev, C. English, G. Federici, M. R. Gilbert, S. Gonzalez, A. Ibarra, C. Linsmeier, A. L. Puma, G. Marbach, L. W. Packer, B. Raj, M. Rieth, M. Q. Tran, D. J. Ward, S. J. Zinkle, Materials R&D for a timely DEMO: Key findings and recommendations of the EU Roadmap Materials Assessment Group, Fusion Eng. Des. 89 (7) (2014) 1586–1594. doi:10.1016/j.fusengdes.2013.11.007.

[13] J. Brooks, L. El-Guebaly, A. Hassanein, T. Sizyuk, Plasma-facing material alternatives to tungsten, Nucl. Fusion 55 (4) (2015) 043002. doi:10.1088/0029-5515/55/4/043002.

[14] T. R. Barrett, G. Ellwood, G. Pérez, M. Kovari, M. Fursdon, F. Domptail, S. Kirk, S. C. Mcintosh, S. Roberts, S. Zheng, L. V. Boccaccini, J.-H. You, C. Bachmann, J. Reiser, M. Rieth, E. Visca, G. Mazzone, F. Arbeiter, P. K. Domalapally, Progress in the engineering design and assessment of the European DEMO first wall and divertor plasma facing components, Fusion Eng. Des. 109111 (2016) 917–924. doi:10.1016/j.fusengdes.2016.01.052.

[15] W.-P. Baek, S. H. Chang, Coolant options and critical heat flux issues in fusion reactor divertor design, J. Korean Nucl. Soc. 29 (4) (1997) 348–359.

[16] R. P. Jewett, R. J. Walter, W. T. Chandler, R. P. Frohmberg, Hydrogen environment embrittlement of metals, Tech. Rep. March, NASA (1973).

[17] C. Linsmeier, M. Rieth, J. Aktaa, T. Chikada, A. Hoffmann, J. Hoffmann, A. Houben, H. Kurishita, X. Jin, M. Li, A. Litnovsky, S. Matsuo, A. von Müller, V. Nikolic, T. Palacios, R. Pippan, D. Qu, J. Reiser, J. Riesch, T. Shikama, R. Stieglitz, T. Weber, S. Wurster, J.-H. You, Z. Zhou, Development of advanced high heat flux and plasma-facing materials, Nucl. Fusion 57 (9) (2017) 092007. doi:10.1088/1741-4326/aa6f71.

[18] J.-H. You, A review on two previous divertor target concepts for DEMO: mutual impact between structural design requirements and materials performance, Nucl. Fusion 55 (11) (2015) 113026. doi:10.1088/0029-5515/55/11/113026.

[19] M. A. Abdou, Exploring novel high power density concepts for attractive fusion systems, Fusion Eng. Des. 45 (2) (1999) 145–167. doi:10.1016/S0920-3796(99)00018-6.

[20] M. Übeyli, e. Yalçin, e. Yalçın, Utilization of refractory metals and alloys in fusion reactor structures, J. Fusion Energy 25 (3-4) (2006) 197–205. doi:10.1007/s10894-006-9019-4.

[21] S. Gonderman, J. K. Tripathi, T. J. Novakowski, T. Sizyuk, A. Hassanein, Effect of dual ion beam irradiation (helium and deuterium) on tungsten-tantalum alloys under fusion relevant conditions, Nucl. Mater. Energydoi:10.1016/j.nme.2017.02.011.

[22] P. Norajitra, R. Giniyatulin, V. Kuznetsov, I. V. Mazul, G. Ritz, He-cooled divertor for DEMO: Status of development and HHF tests, Fusion Eng. Des. 85 (10-12) (2010) 2251–2256. doi:10.1016/j.fusengdes.2010.09.006.

[23] R. Konings, T. R. Allen, R. E. Stoller, S. Yamanaka, Comprehensive Nuclear Materials, Elsevier Science, 2011.

[24] D. J. Mazey, C. A. English, Role of refractory metal alloys in fusion reactor applications, J. Less-Common Met. 100 (C) (1984) 385–427. doi:10.1016/0022-5088(84)90078-X.

[25] P. E. Moorhead, P. L. Stone, Survey of Properties of T111 (1970).

[26] S. J. Zinkle, Thermophysical and mechanical properties for Ta-8% W-2% Hf, Tech. rep., Oak Ridge National Laboratory, Oak Ridge (1998).

[27] C. Campbell, Elements of Metallurgy and Engineering alloys, ASM International, 2008.

[28] W. D. Klopp, A review of chromium, molybdenum, and tungsten alloys, J. Less-Common Met. 42 (3) (1975) 261–278. doi:10.1016/0022-5088(75)90046-6.

[29] R. Wadsack, R. Pippan, B. Schedler, Chromium - A material for fusion technology, Fusion Eng. Des. 58-59 (2001) 743–748. doi:10.1016/S0920-3796(01)00554-3.

[30] B. A. Loomis, A. B. Hull, D. L. Smith, Evaluation of low-activation vanadium alloys for use as structural material in fusion reactors, J. Nucl. Mater. 179-181 (PART 1) (1991) 148–154. doi:10.1016/0022-3115(91)90030-B.

[31] D. L. Smith, M. C. Billone, K. Natesan, Vanadium-base alloys for fusion first-wall / blanket applications, Int. J. Refract. Metals Hard Mater. 18 (September 2000) (2000) 213–224. doi:10.1016/S0263-4368(00)00037-8.

[32] D. L. Smith, H. M. Chung, B. A. Loomis, H. C. Tsai, Reference vanadium alloy V-4Cr-4Ti for fusion application, J. Nucl.

Mater. 233-237 (PART 1) (1996) 356–363. doi:10.1016/S0022-3115(96)00231-0.
[33] ITER Organisation, Structural Design Criteria for In-Vessel Components (SDC-IC) v3.3, ITER Doc. G 74 MA 8 01-05-28 W0.2.
[34] ITER Organisation, ITER Material Properties Handbook, ITER Doc. G 74 MA 16.
[35] Plansee, https://www.plansee.com.
[36] S. Zinkle, N. M. Ghoniem, Operating temperature windows for fusion reactor structural materials, Fusion Eng. Des. 51-52 (52) (2000) 55–71. doi:10.1016/S0920-3796(00)00320-3.
[37] R. Bamber, R. Morrell, C. Waldon, M. Shannon, Design substantiation of ceramic materials on fusion reactor confinement boundaries (jul 2017). doi:10.1016/j.fusengdes.2017.07.001.
[38] Y. Ueda, K. Schmid, M. Balden, J. W. Coenen, T. Loewenhoff, A. Ito, A. Hasegawa, C. Hardie, M. Porton, M. Gilbert, Baseline high heat flux and plasma facing materials for fusion, Nucl. Fusion 57 (9) (2017) 92006.
[39] P. Gavila, B. Riccardi, G. Pintsuk, G. Ritz, V. Kuznetsov, A. Durocher, High heat flux testing of EU tungsten monoblock mock-ups for the ITER divertor, Fusion Eng. Des. 98-99 (2015) 1305–1309. doi:10.1016/j.fusengdes.2014.12.006.
[40] M. Fursdon, T. Barrett, F. Domptail, L. M. Evans, N. Luzginova, N. H. Greuner, J.-H. You, M. Li, M. Richou, F. Gallay, E. Visca, The development and testing of the thermal break divertor monoblock target design delivering 20 MWm^{-2} heat load capability, Phys. Scr. T170 (2017) 014042. doi:10.1088/1402-4896/aa8c8e.
[41] M. Richou, F. Gallay, I. Chu, M. Li, P. Magaud, M. Missirlian, S. Rocella, E. Visca, J.-H. You, Status on the W monoblock type high heat flux target with graded interlayer for application to DEMO divertor, Fusion Eng. Des. 124 (2017) 338–343. doi:10.1016/j.fusengdes.2017.03.087.
[42] J. H. You, G. Mazzone, E. Visca, C. Bachmann, E. Autissier, T. Barrett, V. Cocilovo, F. Crescenzi, P. K. Domalapally, D. Dongiovanni, S. Entler, G. Federici, P. Frosi, M. Fursdon, H. Greuner, D. Hancock, D. Marzullo, S. McIntosh, A. V. Müller, M. T. Porfiri, G. Ramogida, J. Reiser, M. Richou, M. Rieth, A. Rydzy, R. Villari, V. Widak, Conceptual design studies for the European DEMO divertor: Rationale and first results, Fusion Eng. Des. 109-111 (PartB) (2016) 1598–1603. doi:10.1016/j.fusengdes.2015.11.012.
[43] T. Barrett, D. Hancock, M. Kalsey, W. Timmis, M. Porton, Report for WP12-DAS02-T02-D3, Tech. rep., EFDA (2012).
[44] N. R. Hamilton, J. Wood, D. Easton, M. B. O. Robbie, Y. Zhang, A. Galloway, Thermal autofrettage of dissimilar material brazed joints, Mater. Des. 67 (2015) 405–412. doi:10.1016/j.matdes.2014.11.019.
[45] D. Maisonnier, I. Cook, S. Pierre, B. Lorenzo, D. P. Luigi, G. Luciano, N. Prachai, P. Aldo, DEMO and fusion power plant conceptual studies in Europe, Fusion Eng. Des. 81 (8-14 PART B) (2006) 1123–1130. doi:10.1016/j.fusengdes.2005.08.055.
[46] R. A. Forrest, The European Activation File: EAF-2007 biological, clearance and transport libraries, Tech. rep., UKAEA (2007).
[47] R. A. Forrest, A. Tabasso, C. Danani, S. Jakhar, A. K. Shaw, Handbook of Activation Data Calculated Using EASY-2007 (2009) 666.
[48] M. Gilbert, L. Packer, J.-C. Sublet, R. Forrest, Inventory simulations under neutron irradiation: Visualization techniques as an aid to materials design, Nucl. Sci. Eng. 177 (3) (2014) 291–306. doi:10.13182/NSE13-76.
[49] D. Stork, P. Agostini, J. L. Boutard, D. Buckthorpe, E. Diegele, S. L. Dudarev, C. English, G. Federici, M. R. Gilbert, S. Gonzalez, A. Ibarra, C. Linsmeier, A. Li Puma, G. Marbach, P. F. Morris, L. W. Packer, B. Raj, M. Rieth, M. Q. Tran, D. J. Ward, S. J. Zinkle, Developing structural, high-heat flux and plasma facing materials for a near-term DEMO fusion power plant: The EU assessment, J. Nucl. Mater. 455 (1-3) (2014) 277–291. doi:10.1016/j.jnucmat.2014.06.014.
[50] B. R. Simonovi, S. V. Mentus, R. Dimitrijevi, Kinetic and structural aspects of tantalum hydride formation, J. Serb. Chem. Soc. 68 (8-9) (2003) 657–663.
[51] S. Ishiyama, Y. Muto, Y. Kato, S. Nishio, T. Hayashi, Y. Nomoto, Study of steam, helium and supercritical CO 2 turbine power generations in prototype fusion power reactor, Prog. Nucl. Energydoi:10.1016/j.pnucene.2007.11.078.
[52] M. Porton, H. Latham, Z. Vizvary, E. Surrey, Balance of plant challenges for a near-term EU demonstration power plant, in: 2013 IEEE 25th Symp. Fusion Eng., IEEE, 2013, pp. 1–6. doi:10.1109/SOFE.2013.6635331.
[53] P. S. Weitzel, J. M. Tanzosh, B. Boring, N. Okita, T. Takahashi, N. Ishikawa, Advanced Ultra-Supercritical Power Plant (700 to 760C) Design for Indian Coal, Proc. Power-Gen Asia, Thail.
[54] J. I. Linares, L. E. Herranz, I. Fernández, A. Cantizano, B. Y. Moratilla, Supercritical CO2Brayton power cycles for DEMO fusion reactor based on Helium Cooled Lithium Lead blanket, Appl. Therm. Eng. 76 (2015) 123–133. doi:10.1016/j.applthermaleng.2014.10.093.
[55] J. I. Linares, A. Cantizano, E. Arenas, B. Y. Moratilla, V. Martín-Palacios, L. Batet, Recuperated versus single-recuperator re-compressed supercritical CO2Brayton power cycles for DEMO fusion reactor based on dual coolant lithium lead blanket, Energy 140 (2017) 307–317. doi:10.1016/j.energy.2017.08.105.
[56] V. I. Subbotin, M. N. Arnol'dov, F. A. Kozlov, A. L. Shimkevich, Liquid-metal coolants for nuclear power, At. Energy 92 (1) (2002) 29–40. doi:10.1023/A:1015050512710.
[57] F. Najmabadi, A. Abdou, L. Bromberg, T. Brown, V. C. Chan, M. C. Chu, F. Dahlgren, L. El-Guebaly, P. Heitzenroeder, D. Henderson, H. E. St. John, C. E. Kessel, L. L. Lao, G. R. Longhurst, S. Malang, T. K. Mau, B. J. Merrill, R. L. Miller, E. Mogahed, R. L. Moore, T. Petrie, D. A. Petti, P. Politzer, A. R. Raffray, D. Steiner, I. Sviatoslavsky, P. Synder, G. M. Syaebler, A. D. Turnbull, M. S. Tillack, L. M. Waganer, X. Wang, P. West, P. Wilson, The ARIES-AT advanced tokamak, Advanced technology fusion power plant, Fusion Eng. Des. 80 (1-4) (2006) 3–23. doi:10.1016/j.fusengdes.2005.11.003.
[58] S. Mirnov, V. Evtikhin, The tests of liquid metals (Ga, Li) as plasma facing components in T-3M and T-11M tokamaks, Fusion Eng. Des. 81 (1-7) (2006) 113–119. doi:10.1016/j.fusengdes.2005.10.003.
[59] R. Nygren, T. Rognlien, M. Rensink, S. Smolentsev, M. Youssef, M. Sawan, B. Merrill, C. Eberle, P. Fogarty, B. Nelson, D. Sze, R. Majeski, A fusion reactor design with a liquid first wall and divertor, Fusion Eng. Des. 72 (1-3) (2004) 181–221. doi:10.1016/j.fusengdes.2004.07.007.
[60] L. M. Giancarli, M. Abdou, D. J. Campbell, V. A. Chuyanov, M. Y. Ahn, M. Enoeda, C. Pan, Y. Poitevin, E. Rajendra Kumar, I. Ricapito, Y. Strebkov, S. Suzuki, P. C. Wong, M. Zmitko, Overview of the ITER TBM Program, in: Fusion Eng. Des., Vol. 87, North-Holland, 2012, pp. 395–402. doi:10.1016/j.fusengdes.2011.11.005.
[61] D. Rapisarda, I. Fernandez, I. Palermo, F. R. Urgorri, L. Maqueda, D. Alonso, T. Melichar, O. Frýbort, L. Vála, M. Gonzalez, P. Norajitra, H. Neuberger, A. Ibarra, Status of the engineering activities carried out on the European DCLL, Fusion Eng. Des. 124 (2017) 876–881. doi:10.1016/j.fusengdes.2017.02.022.
[62] N. Rumbaut, F. Casteels, M. Brabers, M. Soenen, H. Tas, J. De Keyser, Corrosion of Refractory Metals in Liquid Lithium, in: Mater. Behav. Phys. Chem. Liq. Met. Syst., Springer US, Boston, MA, 1982, pp. 131–139. doi:10.1007/978-1-4684-8366-6_14.
[63] P. Fiflis, A. Press, W. Xu, D. Andruczyk, D. Curreli, D. N. Ruzic, Wetting properties of liquid lithium on select fusion relevant surfaces, Fusion Eng. Des. 89 (12) (2014) 2827–2832. doi:10.1016/j.fusengdes.2014.03.060.
[64] D. Samuel, Molten Salt Coolants for High Temperature Reactors: A summary of Key R&D Activities and Challenges,

IAEA Internsh. Rep. (INPRO Cool.

[65] N. Taylor, B. Merrill, L. Cadwallader, L. Di Pace, L. El-Guebaly, P. Humrickhouse, D. Panayotov, T. Pinna, M.-T. Porfiri, S. Reyes, M. Shimada, S. Willms, Materials-related issues in the safety and licensing of nuclear fusion facilities, Nucl. Fusion 57 (9) (2017) 092003. doi:10.1088/1741-4326/57/9/092003.

[66] M. Rieth, S. Dudarev, S. Gonzalez de Vicente, J. Aktaa, T. Ahlgren, S. Antusch, D. Armstrong, M. Balden, N. Baluc, M.-F. Barthe, W. Basuki, M. Battabyal, C. Becquart, D. Blagoeva, H. Boldyryeva, J. Brinkmann, M. Celino, L. Ciupinski, J. Correia, A. De Backer, C. Domain, E. Gaganidze, C. García-Rosales, J. Gibson, M. Gilbert, S. Giusepponi, B. Gludovatz, H. Greuner, K. Heinola, T. Höschen, A. Hoffmann, N. Holstein, F. Koch, W. Krauss, H. Li, S. Lindig, J. Linke, C. Linsmeier, P. López-Ruiz, H. Maier, J. Matejicek, T. Mishra, M. Muhammed, A. Muñoz, M. Muzyk, K. Nordlund, D. Nguyen-Manh, J. Opschoor, N. Ordás, T. Palacios, G. Pintsuk, R. Pippan, J. Reiser, J. Riesch, S. Roberts, L. Romaner, M. Rosiński, M. Sanchez, W. Schulmeyer, H. Traxler, A. Ureña, J. van der Laan, L. Veleva, S. Wahlberg, M. Walter, T. Weber, T. Weitkamp, S. Wurster, M. Yar, J.-H. You, A. Zivelonghi, Recent progress in research on tungsten materials for nuclear fusion applications in Europe, J. Nucl. Mater. 432 (1-3) (2013) 482–500. doi:10.1016/j.jnucmat.2012.08.018.

[67] D. Hancock, D. Homfray, M. Porton, I. Todd, B. Wynne, Exploring Complex High Heat Flux Geometries for Fusion Applications Enabled by Additive Manufacturing, Fusion Eng. Des.doi:https://doi.org/10.1016/j.fusengdes.2018.02.097.

[68] D. Hancock, M. Curtis-Rouse, A. Field, D. Homfray, H. Lewtas, M. Porton, E. Surrey, I. Todd, S. Williams, B. Wynne, Additive Manufacturing of High Temperature Materials for Fusion: A Review of Recent Work, Strategies, and Future Outlook, (Article Prep.

[69] G. Pintsuk, S. Brünings, J.-E. Döring, J. Linke, I. Smid, L. Xue, Development of W/Cu—functionally graded materials, Fusion Eng. Des. 66-68 (2003) 237–240. doi:10.1016/S0920-3796(03)00220-5.

[70] J.-H. You, a. Brendel, S. Nawka, T. Schubert, B. Kieback, Thermal and mechanical properties of infiltrated W/CuCrZr composite materials for functionally graded heat sink application, J. Nucl. Mater. 438 (1-3) (2013) 1–6. doi:10.1016/j.jnucmat.2013.03.005.

[71] M. Galatanu, M. Enculescu, A. Galatanu, High temperature thermo-physical properties of SPS-ed W-Cu functional gradient materials, Mater. Res. Express.

[72] J. Reiser, M. Rieth, A. Möslang, B. Dafferner, J. Hoffmann, T. Mrotzek, A. Hoffmann, D. Armstrong, X. Yi, Tungsten foil laminate for structural divertor applications – Joining of tungsten foils, J. Nucl. Mater. 436 (1-3) (2013) 47–55. doi:10.1016/j.jnucmat.2013.01.295.

[73] M. Porton, B. Wynne, R. Bamber, C. Hardie, M. Kalsey, Structural integrity for DEMO: An opportunity to close the gap from materials science to engineering needs, Fusion Eng. Des.doi:10.1016/j.fusengdes.2015.12.050.

3

Paper: "Exploring Complex High Heat Flux Geometries for Fusion Applications Enabled by Additive Manufacturing"

Context within thesis

Having outlined the benefits of a wider range of materials for fusion high heat flux structures, this paper details the potential benefits of employing AM to produce complex geometries in these materials for this application. Two sample geometries are shown which include features and materials only feasible through the use of AM. The paper does not discuss the technical maturity of AM of refractories, give detailed concept designs, or justify the use of tantalum as a reference material directly, but successfully demonstrates that these types of concepts are worthy of further optimisation and investigation.

Novelty

- applying AM to new geometries and novel materials for fusion high heat flux components

Lead author contributions

- detailed component design, building on some prior AMAZE concept generation work as detailed in the text
- all modelling and analysis
- all writing

Publication status

This work was presented in paper and poster form in September 2017 at the 13$^{\text{th}}$ International Symposium on Fusion Technology (ISFNT-13) in Kyoto, Japan, and was subsequently included in the associated conference proceedings published in the peer-reviewed journal, Fusion Engineering and Design.
`https://doi.org/10.1016/j.fusengdes.2018.02.097`
This paper has been re-typeset and additional information included for thesis submission

Approval status

Co-authors and supervisors:	Internal	(REVIEWED)	External	(REVIEWED)
UKAEA:	C. Waldon	(CLEARED)	E. Surrey	(CLEARED)
AMAZE (notification only):	D. Wimpenny	(RELEASED)	M. Holden	(RELEASED)

Exploring Complex High Heat Flux Geometries for Fusion Applications Enabled by Additive Manufacturing

David Hancock[a,b,*], David Homfray[a], Michael Porton[a], Iain Todd[b], Brad Wynne[a,b]

[a] *Culham Centre for Fusion Energy, Culham Science Centre, Abingdon, Oxon, OX14 3DB, UK*
[b] *University of Sheffield, Department of Materials Science and Engineering, Sir Robert Hadfield Building, Mappin Street, Sheffield, S1 3JD, UK*

Abstract

The geometrical freedom that additive manufacturing (AM) provides enables realisation of formerly impossible design concepts for high heat flux components aimed at use in a fusion reactor. This paper demonstrates a number of these advantages using a tile-based divertor target with two examples of novel cooling geometry. To showcase the potential benefits of high temperature operation using materials newly available for AM processing, tantalum was used as the structural material. Rather than present optimised prototypes or propose specific material choices, these two concepts highlight design features enabled by this new technology. Details of AM technology and processing parameters are likewise deliberately excluded.

Simple quantitative analysis shows heat transfer improvements of 25% for a multiple small pipe concept compared to single pipe designs. Finite element analysis for both designs, including a tungsten armour, also demonstrates a more uniform temperature distribution, reducing thermal stresses below elastic limits for $5\,\mathrm{MW\,m^{-2}}$ heat flux cases, even with 600 °C coolant. At $10\,\mathrm{MW\,m^{-2}}$ yield is exceeded but the expectation is further design optimisation should enhance structural integrity.

Overall, there are modest gains in heat flux handling, lifetime, and thermal efficiency compared to existing concepts, but there are significant improvements in waste reduction and remote handling mass, using typically 80% less material. Moreover, integrated manifolding and careful location of coolant connection is suggested to facilitate repair and replaceability, which should also reduce risk associated with qualifying joints.

Keywords: Plasma facing components, Divertor, Materials, Design, Additive manufacturing, DEMO

1. Introduction

1.1. High heat flux design for nuclear fusion

Power exhaust, and specifically divertor design, has been identified as one of the most critical challenges facing the realisation of commercial fusion power [1]. Current baseline designs for engineering demonstrators such as DEMO, FSNSF, and CFETR face significant difficulties in designing divertor target components which will survive the increased surface erosion and radiation damage when compared to ITER [2, 3, 4]. Beyond these, in order to achieve commercial viability, it is likely that prototype power stations will add higher heat fluxes, higher thermal efficiency, and improved capacity for remote handling maintenance and repair to the list of requirements [5].

Overcoming this challenge requires, first of all, advances in plasma physics to reduce first wall and divertor heat loads and facilities such as MAST-U are working to this end [6]. Advanced engineering solutions will also be needed, however, to address the remaining requirements of thermal efficiency, reliability, and maintainability while simultaneously striving to handle higher powers.

The current baseline divertor target designs for DEMO-class devices employ variations on the ITER monoblock shown in Figure 1a. Due to the low thermal expansion coefficient of the tungsten armour compared to candidate structural materials (typically CuCrZr or steel), the joint between the coolant carrying pipe and tungsten armour is subject to significant stress and this has been shown to be a significant limiting factor for performance and lifetime. The identification of this interface as a major point of failure has led to a number of variations on this design specifically tailored to mitigate this stress [7].

The desire to operate at high coolant temperatures for increased thermal efficiency has driven the development of helium cooled concepts, including the jet-impingement HEMJ shown in Figure 1b, but these too face joining challenges between the multiple parts required for the complex cooling paths. Furthermore, uncertainties in tungsten erosion rates in DEMO have led to exploration of options for in-situ repair and re-coating.

*Corresponding Author
Email address: david.hancock@ukaea.uk (David Hancock)

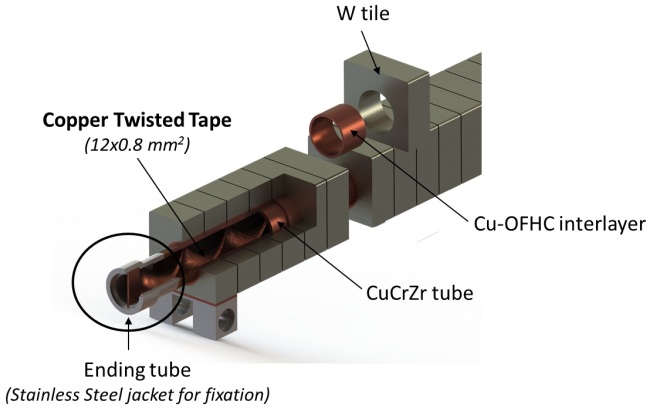

(a) ITER W monoblock divertor [8]

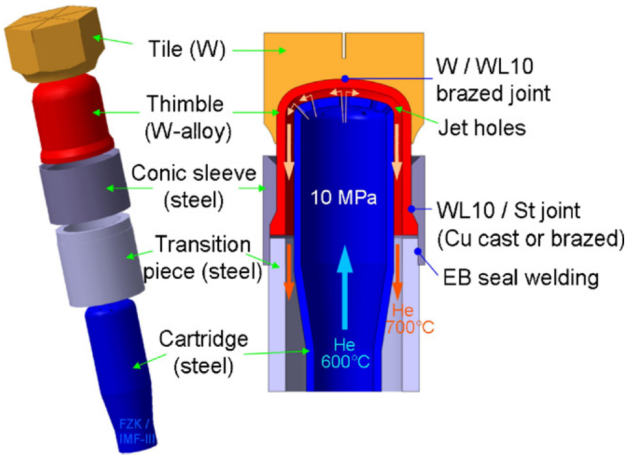

(b) He-cooled divertor for DEMO [9]

Figure 1: Divertor designs for ITER and DEMO

1.2. Potential benefits of additive manufacturing

Additive manufacturing (AM), also known as additive layer manufacturing, is a term applied to a range of techniques whereby successive layers of material are deposited to generate net shape or near net shape components. This is in contrast to subtractive techniques where material is removed from a larger piece of material or techniques such as casting or forging which deform or extrude the raw material by force.

AM provides a number of general advantages over conventional techniques. In particular, design freedom is facilitated by the ability to add potentially complex geometric features without incurring additional tooling or machining costs. AM parts, particularly those produced using powder bed processes, can also include features not otherwise possible, such as internal structures inaccessible to machining or drilling tools. This freedom of geometry enables design optimisation for weight, strength, thermal, or material usage [10].

Constant advances in AM processing of metal alloys are broadening the pallet of materials available for use, though there remain significant challenges, particularly for

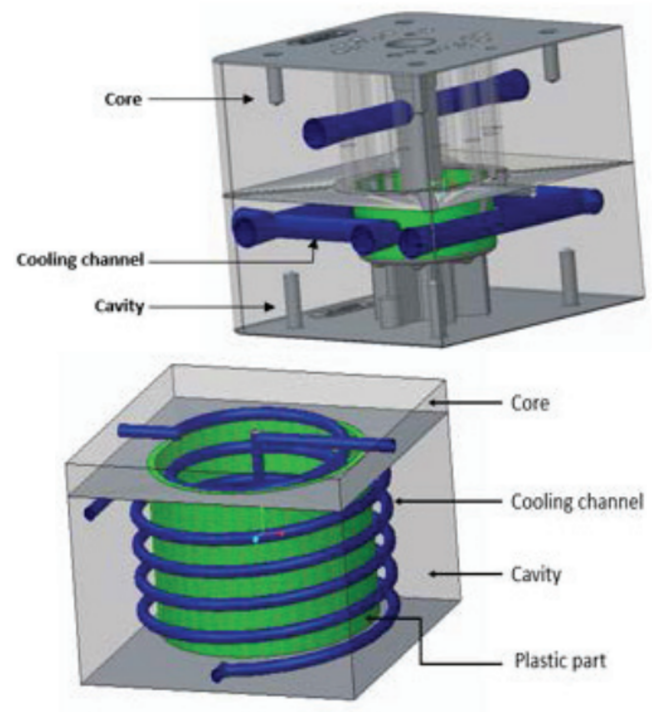

Figure 2: Conformal cooling (lower image) compared to traditional solution (upper image), as used in injection molding [15]

those materials suitable for high temperature use or those which are inherently brittle or prone to oxidation during processing [11].

Functionally graded joints between armour and structure have been investigated for use in divertor applications [12, 13] and wire-based AM has recently shown promise for refractory materials (articles in preparation). Repair of armour material in-situ using spray or wire techniques would provide a further means to extend the in-service lifetime of plasma facing surfaces [14].

In addition to and as a result of the general advantages listed above, AM provides a number of specific opportunities for enhanced high heat flux components:

Previous divertor target designs have employed single large pipes or channels, but AM allows multiple small channels either arranged in parallel to minimise pressure drop or in series to maximise heat pickup. These can be also routed and sized optimally for performance or efficiency to areas requiring the most cooling. This ideology of "conformal cooling" is increasingly being used in other industries. One such example, an injection mold for the plastics industry, is shown in figure 2.

Traditional designs have achieved high heat transfer coefficients with added turbulence enhancement features such as swirl tubes or hypervapotrons [16] in combination with high flowrates and/or nucleate boiling. The integration of these features is possible from the start using AM rather than as a subsequent assembly step. In addition, while the typically rough as-built surface finish produced by powder-based AM processes is usually

considered a disadvantage for many applications, in this case it may provide a way of improving of heat transfer coefficient. The pursuit of high heat transfer coefficients has been a significant driver of divertor design decisions and the risks associated with erosion due to the resulting high coolant flowrates and burnout due to nucleate boiling operation close to the critical heat flux limits may be able to be reduced with AM designs by exchanging high heat transfer coefficients for larger cooled surface area.

While recent research into the AM processing of refractory metals show there are significant hurdles to overcome before the realisation of high integrity cooled components is possible, these high temperature materials would facilitate high temperature coolant and hence high thermal efficiency, while at the same time having low coefficients of thermal expansion much closer to that of tungsten, reducing the mismatch stress described above.

The number of joints between parts directly affects both the cost and reliability of components, particularly in the context of qualification for nuclear applications. The ability to reduce part count through inclusion of manifolding into single printed parts or even the integration of cooling directly into armour material would provide a further advantage.

Lastly, the potential for reduced material use throughout the component lifecycle reduces costs for manufacture and disposal.

2. Concept generation

2.1. Design methodology

Concept generation has incorporated TRIZ [17] and systems engineering techniques, meaning that a clear and concise set of requirements has been generated and solutions have sought to draw upon TRIZ techniques for overcoming conflicts in these requirements. In particular the potential for small channels as described in section 3 have been identified and it has been recognised that concerns about cascade failure of tile designs for ITER could be significantly mitigated through the use of better matching of thermal expansion between armour and structure and/or the use of mechanical keying or functional grading as facilitated by AM. Throughout this process synergies with non-fusion applications have been sought, in particular aerospace and electronics applications.

Although AM does provide significant freedom of geometry and material, its capabilities are not unlimited, and design for AM is a complex integrated problem. For the purposes of this exercise a middle ground was sought between neglecting all limitations of the current technology completely and limiting design decisions to one particular manufacturing method. The complex internal structures and relatively small individual components proposed suggest that powder bed fusion is most likely to be the most appropriate method for manufacture, but details of type of AM, machine to be used, material feedstock, and process parameters are deliberately excluded at this stage. In addition, while the as stated above, the rough surfaces of as-built AM parts may prove beneficial to convective heat transfer on cooled surfaces, this is not taken into account in modelling at this stage.

2.1.1. Requirements

To demonstrate the value of AM for fusion divertor design, concepts must meet or exceed both quantitative and qualitative requirements currently accepted for DEMO. While transient loads for ITER peak at $20\,\mathrm{MW\,m^{-2}}$, recent water cooled design work has used as its benchmark $5\,\mathrm{MW\,m^{-2}}$ to $10\,\mathrm{MW\,m^{-2}}$ of heat flux in the form of high velocity ions and electrons for 6000 multi-hour cycles over a period of at least 2 full power years of operation [5]. In addition, the divertor structure must be compatible with tokamak gasses (H, D, T, He) and whatever coolant is chosen without contaminating the tokamak vacuum. Installation and maintenance must be possible via remote handling, with consideration for overall weight of components [18]. It is a generally accepted tenet of power plant design within the fusion community that materials should be chosen such that residual nuclear activation after 100 years of shutdown must be less than $10\,\mu\mathrm{Sv\,h^{-1}}$ for hands-on recycling [19].

2.1.2. Key features to demonstrate

Rather than aiming to produce final optimised, detailed designs as competing concepts for a DEMO divertor, this exercise seeks to set forth concept-level geometries which showcase a select number of specific potential advantages facilitated by the use of AM. Each will aim to incorporate a number of features which could be used in a more mature candidate design.

Firstly, concepts must have improved thermofluid performance contributing to higher heat flux handling or greater thermal efficiency. This could be achieved by increased heat transfer coefficient, higher bulk coolant temperature or lower pumping power for a given cooled area. Secondly, performance and in-service lifetime will be increased through reduction in stress due to thermal expansion mismatch between armour and structure by using lower thermal expansion materials and by employing cooling channel geometries which produce more even or tailored cooling. Overall manufacturing risk will be reduced through a reduction in part count and number of joints by employing integrated manifolding and/or ensuring that joints are further removed from high temperature high stress regions. Concepts will seek to reduce the volume of structural and armour material needed for performance comparable to current designs. This will reduce material supply costs, waste volume, and part mass for remote handling.

Divertor target tiles are inherently small, complex, high value sub-components and while large numbers will have to be produced for a full divertor assembly, the scale is well suited to current AM capability [20]. Increases in AM platform scale would enable greater numbers to be

produced in parallel and would also enable the inclusion of larger manifold sections into the additive parts, but are not required for demonstration of final-scale concepts at the tile level. In addition, the benefits of AM are likely to be less for larger, simpler parts. Therefore, single tile sections will be designed with features to allow testing in the first instance, without inclusion of the full cassette assembly.

Operation with coolants above 600 °C will require the use of a material able to operate at higher temperatures than the copper alloy or steel currently proposed. Parallel work described elsewhere in this thesis has shown that a number of refractory metals show promise and work has been carried out to develop the AM processing of molybdenum, tungsten, vanadium, and tantalum. Alloys rather than elemental metals are likely to be the final materials of choice, but elemental tantalum has used as the reference structural material for the designs presented here for the purposes of concept illustration. Tantalum's high strength at elevated temperature, low thermal expansion, full solubility with tungsten, compatibility with candidate coolants, and low activation make it an attractive candidate, but while tantalum alloys have a long heritage of being proposed for fusion high heat flux applications [21, 22], historical concerns about embrittlement, cost and availability remain relevant and would need to be considered before inclusion in a power plant.

3. Manifolded small pipe

3.1. Previous work

This concept builds on work done under the AMAZE project[1], during which a "millipipe" design was proposed which used multiple small channels in a cooled substructure rather than one single pipe embedded in armour. This design draws inspiration from biological capillary networks, applying high performance cooling in small pipes only where needed, with larger diameter manifolding connections and lower pressure drops in lower heat flux regions. The test geometry shown in figure 3 was designed to be tested in the HIVE high-heat-flux testing facility and a demonstrator component was manufactured using an electron-beam melted copper substructure, manufactured by FAU Erlangen in Germany [23], brazed to a laser powder bed fusion tungsten tile manufactured by the University of Birmingham. The predicted performance of this part was limited to low-temperature coolant (50 °C) and moderate heat fluxes ($\approx 4\,\mathrm{MW\,m^{-2}}$) due to the use of copper as the structural material.

[1] AMAZE (Additive Manufacturing Aiming Towards Zero Waste and Efficient Production of High-Tech Metal Products) was an EC FP7 collaborative research and development consortium, aiming to deliver the technological capability for rapid production of large defect-free metallic components for use in high-tech sectors.

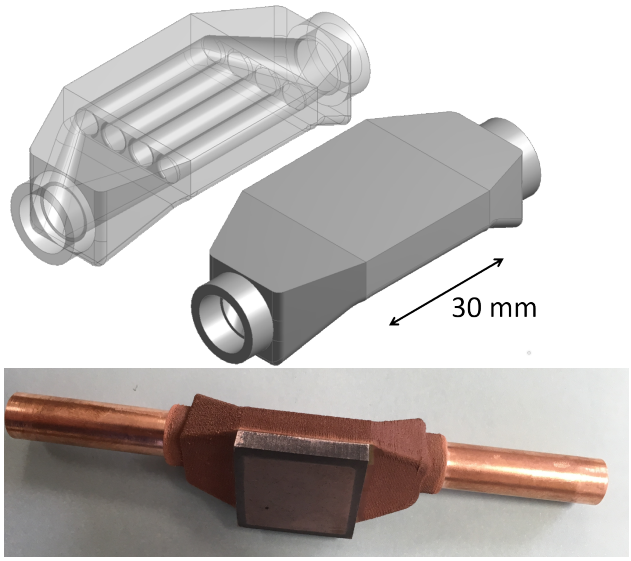

Figure 3: AMAZE "millipipe" test geometry and AM demonstrator

3.2. Empirical correlations and 2D finite element modelling

A number of thermal and mechanical benefits can be gained by using multiple small pipes in a cooled structure rather than one large one.

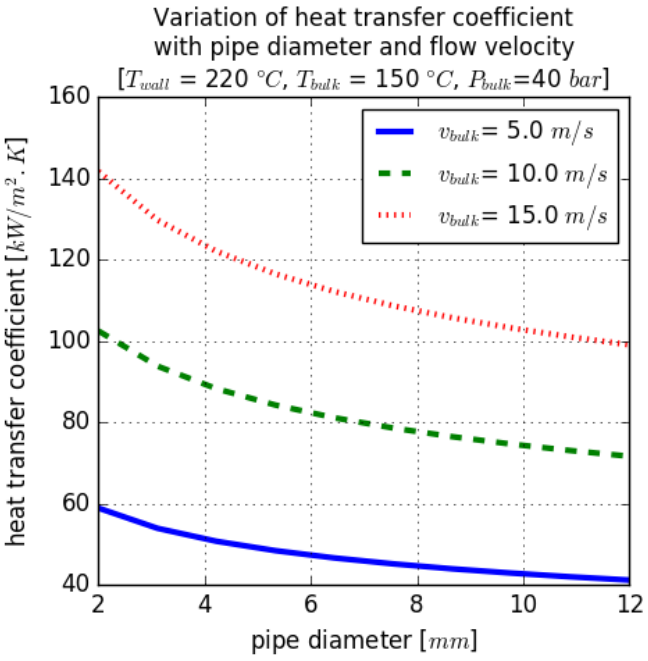

Figure 4: Increasing heat transfer coefficient with reducing pipe diameter

First, as shown in figure 4, for typical water parameters, heat transfer coefficient in a simple pipe increases with reducing diameter between 12 mm and 2 mm. These values were calculated using the Seider-Tate correlation.

The behaviour of simple 2D thermal and mechanical finite element models of an array of between 1 and 6 pipes

was assessed under a uniform 5 MW m^{-2} heat flux. A solid 30 mm wide tungsten structure was used for simplicity, maintaining constant coolant channel cross section, equivalent to a single 10 mm diameter pipe. Distance between cooling channel and heated surface (i.e. armour thickness) was kept at a constant 5 mm and vertical distance between pipe and bottom face was 2.5 mm. Heat transfer coefficients were applied uniformly and were calculated iteratively using maximum pipe wall temperature. Analysis was carried out using ANSYS Workbench 18.0, with default direct solver settings. Automated meshing was applied with component-level sizing controls adjusted to ensure a minimum of 2 elements through thickness. Minimum mechanical constraints were applied to nodes at the bottom corners to prevent bulk movement.

Figure 5 shows a selection of these geometries with contour maps of the resulting body temperature.

As shown in Figure 6, the results of this analysis show a reduction in peak wall temperature, maximum overall temperature, stress, and part cross sectional area (corresponding to an overall reduction in material and weight).

3.3. Summary of analysis of concept geometry

Figure 7 shows a concept sketch for a test-piece design which employs these principles and also demonstrates the possibility of designing the feed-pipes such that connections can be made at the rear, away from surfaces directly exposed to the plasma.

3.3.1. Pressure drop

Empirical calculations of pressure drop were carried out using the Darcy-Weisbach equation, based on 4 parallel 4mm diameter pipes with 90˚ bends at each end and internal roughness of 40 µm. For the reference water parameters from the DEMO baseline [5], connected in series with simple 10 mm internal-diameter U-bends, pressure drop for an array of these concepts is $\approx$ 0.45 MPa m^{-1}, compared to $\approx$ 0.35 MPa m^{-1} for the ITER-reference twist-tape, showing that in a series configuration, there is little to be gained from the small pipe concept in terms of pumping power efficiency. A parallel configuration, however, is foreseen for a more mature concept. Each element has only $\approx$ 0.014 MPa loss, and the integration of manifolds within the additive part would enable this to be exploited fully.

3.3.2. Thermomechanical analysis

3D finite element analysis was performed to provide first order indications of performance rather than provide fully validated qualitative assessments. Modelling was carried out using ANSYS Workbench 18.2, as above, with minimal variation from default solver and meshing settings other than to ensure more than one higher order tetrahedral element through thickness. 3-2-1 constraints were applied to three corner nodes to prevent bulk displacements rather than attempting to reproduce those which would be imposed by a more fully designed mounting scheme. A convective heat transfer coefficient of 0.1 W m^{-1} K^{-1} was applied uniformly to the small pipes, while transfer in the larger voids was neglected. Material properties were taken from ITER reference values and [24].

A summary of key findings is presented in Table 1. Four test cases are shown: two sets of coolant parameters and two heat fluxes. Lower temperature water parameters allow a direct comparison with the water-cooled monoblock concept and a 600 °C case shows the impact of a higher temperature coolant, e.g. liquid lithium. Heat fluxes compared are 5 MW m^{-2} and 10 MW m^{-2}.

Three results are used for comparison: Maximum equivalent stress in the model, maximum temperature in the armour, and maximum temperature in the structure. While simple, these show to first order that the concept operates within the limit of yield stress for recrystalised Tantalum for both the 5 MW m^{-2} cases. If stress relieved or irradiated properties from [24] are used, this falls below 2/3 yield. For the higher power cases, the peak stress is highly localised at the interface between the tungsten and tantalum and may be able to be mitigated at manufacture [25]. A reduction in armour thickness would render the higher temperature higher power case feasible but would require a means to replace eroded material.

4. Enclosed pin-fin array

While cylindrical channels provide the best geometry for minimising stress with high-pressure coolant, one alternative explored by the electronics industry is an array of pin-fins [26]. Research into forced convection in enclosed channels with various shaped fins has shown high heat transfer with low pressure drop [27] for similar heat fluxes to fusion divertor applications. The bulk of the work in this area has focussed on lower temperature gas cooled applications but extension to high temperature shows promise, as outlined below, and additive manufacturing has already been identified as a means for producing such components [28, 29].

The large coolant volume to structural material ratio shows promise for significantly reducing material use and weight for remote handling. The ability to operate at lower flow-rates would reduce both material erosion, increasing part lifetime; and pumping power, increasing plant efficiency. The ability to manufacture these components in a single part with optimised pin geometry could further improve structural integrity and performance.

4.1. Empirical correlations

Empirical or theoretical heat transfer correllations for water-cooled pin-fin arrays are not available for high temperature and high Reynolds numbers at component scales relevant for fusion high heat flux components, making direct comparisons with pipe designs difficult. Sahiti et al [30] do provide Nusselt number vs. Reynolds

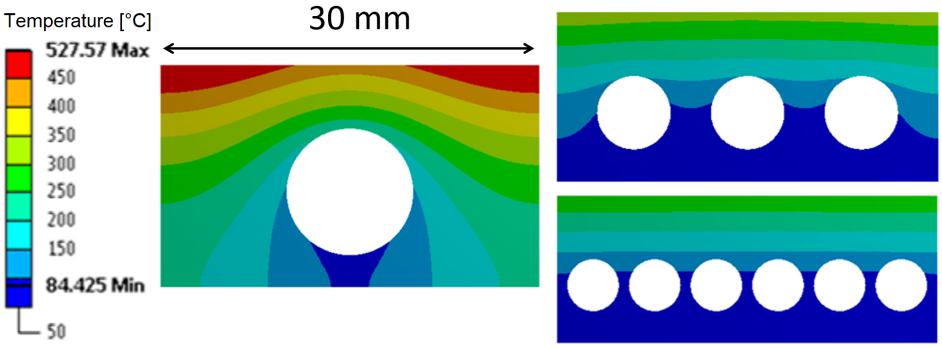

Figure 5: Thermal results of 2D finite element models for 1, 3, and 6 pipe arrays with 50 °C coolant and 5 MW m^{-2} heat flux.

Table 1: Small pipe analysis results summary

Coolant parameters	**Heat flux**	$\boldsymbol{\sigma_{max}}$	$\boldsymbol{T_{max,struct.}}$	$\boldsymbol{T_{max,armour}}$
$T_{bulk} = 150\,°C$ $P_{bulk} = 4\,MPa$ $h_{wall} = 0.1\,W\,mm^{-2}\,K^{-1}$	$5\,MW\,m^{-2}$	224 MPa	470 °C	633 °C
$T_{bulk} = 150\,°C$ $P_{bulk} = 4\,MPa$ $h_{wall} = 0.1\,W\,mm^{-2}\,K^{-1}$	$10\,MW\,m^{-2}$	484 MPa	778 °C	1162 °C
$T_{bulk} = 600\,°C$ $P_{bulk} = 5\,MPa$ $h_{wall} = 0.1\,W\,mm^{-2}\,K^{-1}$	$5\,MW\,m^{-2}$	250 MPa	899 °C	1095 °C
$T_{bulk} = 600\,°C$ $P_{bulk} = 5\,MPa$ $h_{wall} = 0.1\,W\,mm^{-2}\,K^{-1}$	$10\,MW\,m^{-2}$	441 MPa	1193 °C	1620 °C

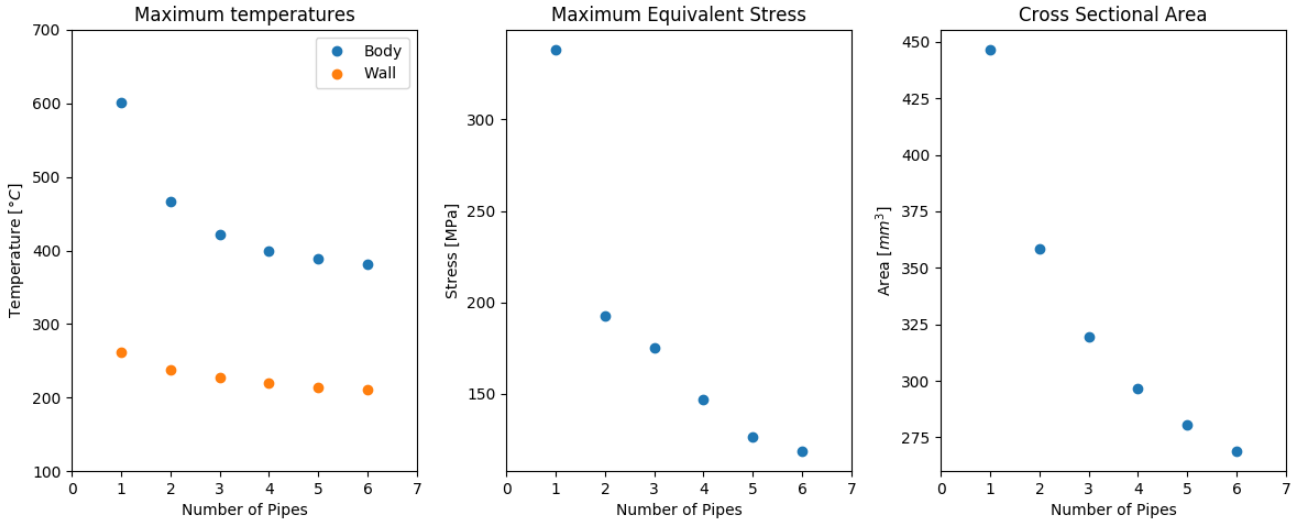

Figure 6: Results of finite element modelling of 2D array of small pipes

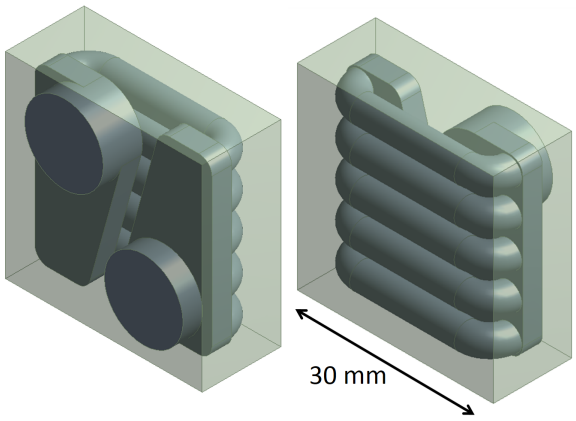

Figure 7: Rear fed, manifolded small-pipe concept geometry

number for a selection of of enclosed air-cooled pin-fin arrays with broadly appropriate dimensions and with various shapes of pin, however. Figure 8 presents these data alongside empirical values for a simple water-cooled 10 mm pipe for comparison, showing that, at low temperatures at least, pin-fin arrays significantly outperform simple pipes. The pressure drop for these geometries is significantly higher for a given Reynolds number [31] but the ability to arrange pin fin heat flux elements in parallel could mitigate this disadvantage.

4.2. Summary of analysis of test geometry

Figure 9 shows a concept sketch for a test-piece design employing these principles. This geometry is designed to be suitable for testing in the HIVE high heat flux facility at CCFE.

The sensitivity of pressure drop to pin geometry and coolant parameters and the lack of experimental data at relevant conditions precludes a quantitative assessment of pressure drop within the scope of this paper, but a set of thermomechanical analyses, using the same methodology including coolant temperatures, pressures, and heat fluxes as §3.3.2 are shown in table 2. As before, pessimistic heat transfer coefficients are included to show the effect of the increased area and even cooling on overall temperature and stress.

As with the small pipe concept, the stress in the structure remains below yield for the $5\,\mathrm{MW\,m^{-2}}$ cases. The reduction in stress for the 600 °C cases is caused by the inclusion of the feed sections at each end of the test piece and is a result of higher temperature gradients at each end of the pin-fin array section.

Notably, for the 600 °C, $5\,\mathrm{MW\,m^{-2}}$ case, the temperature of both tantalum and tungsten parts are within the limits specified by [22], enabling both materials to operate within a window defined by their creep and ductile-brittle transition temperatures, potentially even in the irradiated condition.

5. Concept assessment summary

Both the pin-fin and small pipe concept geometries show that at incident heat fluxes of $5\,\mathrm{MW\,m^{-2}}$ they are able to operate within the elastic stress regime of the bulk material. This is particularly notable when compared to the ITER-like concept which is dependent on significant plastic strain in the interlayer [7]. However, at $10\,\mathrm{MW\,m^{-2}}$, both designs exceed yield stress in the structure, though this is highly localised and is likely to be mitigated by further design optimisation. With 600 °C coolant, both the structural and armour material are within their respective operating windows for the $10\,\mathrm{MW\,m^{-2}}$ cases, according to [22]. The ability to arrange cooling elements in parallel opens the possibility of significantly reduced pressure drop and pumping

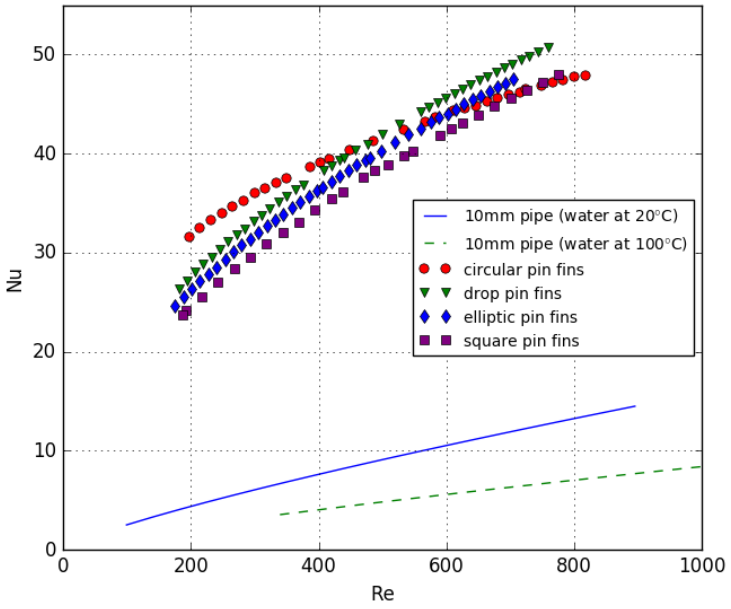

Figure 8: Nusselt numbers for a selection of pin-fin arrays compared to a simple pipe (adapted from [30])

Table 2: Pin-fin analysis results summary

Coolant parameters	**Heat flux**	$\boldsymbol{\sigma_{max}}$	$\boldsymbol{T_{max,struct.}}$	$\boldsymbol{T_{max,armour}}$
$T_{bulk} = 150\,^{\circ}\mathrm{C}$ $P_{bulk} = 4MPa$ $h_{wall} = 0.02\,\mathrm{W\,mm^{-2}\,K^{-1}}$	$5\,\mathrm{MW\,m^{-2}}$	262 MPa	342 °C	421 °C
$T_{bulk} = 150\,^{\circ}\mathrm{C}$ $P_{bulk} = 4\,\mathrm{MPa}$ $h_{wall} = 0.02\,\mathrm{W\,mm^{-2}\,K^{-1}}$	$10\,\mathrm{MW\,m^{-2}}$	603 MPa	546 °C	941 °C
$T_{bulk} = 600\,^{\circ}\mathrm{C}$ $P_{bulk} = 4\,\mathrm{MPa}$ $h_{wall} = 0.02\,\mathrm{W\,mm^{-2}\,K^{-1}}$	$5\,\mathrm{MW\,m^{-2}}$	$250MPa$	899 °C	1095 °C
$T_{bulk} = 600\,^{\circ}\mathrm{C}$ $P_{bulk} = 4\,\mathrm{MPa}$ $h_{wall} = 0.02\,\mathrm{W\,mm^{-2}\,K^{-1}}$	$10\,\mathrm{MW\,m^{-2}}$	537 MPa	1029 °C	1485 °C

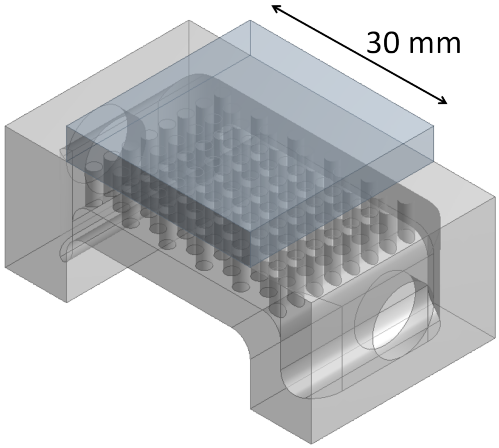

Figure 9: Pin fin array test geometry

power. The rear-fed small pipe concept has demonstrated this empirically, but for the pin-fin array this would need significant further design development, particularly given the lack of prior data for pin-fin arrays operating under divertor-relevant conditions. The increased internal surface area and increased heat transfer coefficients for a given flow rate both contribute to the potential to reduce flow velocity and/or pumping power, reducing erosion and increasing overall plant efficiency. By using tile, rather than monoblock, arrangements, both concepts employ significantly less tungsten armour; $5\,m^3$ of tungsten per m^2 of divertor target area vs $22\,m^3$ for ITER. The large internal volume compared to structural material means that overall material use is reduced reducing both manufacturing and decommissioning costs. The reduction in material also results in a reduced mass, easing remote handling requirements.

6. Conclusions

This paper has summarised the need for advanced divertor concepts for use in DEMO and subsequent fusion power plants. The advantages of AM for fusion divertor designs have been introduced, particularly that it is well suited to small, complex components made out of expensive or hard to manufacture materials and that complex cooling geometries and high temperature materials can be used to enhance their performance.

Two generic tile-based divertor concept models have been assessed. Each highlights geometric features enabled by AM and, in order to show the potential for high temperature operation using materials facilitated by AM, both employ tantalum as the structural material. Preliminary analytical comparisons are drawn, showing that these types of concepts are worthy of further investigation, showing performance, cost, and operational benefits, despite their preliminary nature.

The maturity of the additive manufacturing of refractory materials for fusion applications, a detailed assessment of the suitability of refractory metals such as tantalum as structural materials for divertor components, or the status of ongoing testing of additive manufactured divertor concepts have not been discussed as they are presented in parallel publications currently in preparation, although trial builds of test components have begun, as shown in 10.

Figure 10: Small-pipe concept test build in tantalum

Acknowledgements

This work has been part-funded by the European Union's Horizon 2020 research and innovation programme. The views and opinions expressed herein do not necessarily reflect those of the European Commission. This work has also been part-funded by the RCUK Energy Programme [grant number EP/P012450/1]. Additional support has been provided by FAU Erlangen and the University of Birmingham school of Metallurgy and Materials. To obtain further information on the data and models underlying this paper please contact publications-manager@ccfe.ac.uk.

References

[1] F. Romanelli, Fusion Electricity: A roadmap to the realisation of fusion energy, Tech. rep., EDFDA (2012). doi:ISBN978-3-00-040720-8.

[2] G. Federici, R. Kemp, D. Ward, C. Bachmann, T. Franke, S. Gonzalez, C. Lowry, M. Gadomska, J. Harman, B. Meszaros, C. Morlock, F. Romanelli, R. Wenninger, Overview of EU DEMO design and R&D activities, Fusion Eng. Des. 89 (7-8) (2014) 882–889. doi:10.1016/j.fusengdes.2014.01.070.

[3] A. Garofalo, M. Abdou, J. Canik, V. Chan, A. Hyatt, D. Hill, N. Morley, G. Navratil, M. Sawan, T. Taylor, C. Wong, W. Wu, A. Ying, A Fusion Nuclear Science Facility for a fast-track path to DEMO, Fusion Eng. Des. 89 (7-8) (2014) 876–881. doi:10.1016/j.fusengdes.2014.03.055.

[4] Y. Wan, J. Li, Y. Liu, X. Wang, V. Chan, C. Chen, X. Duan, P. Fu, X. Gao, K. Feng, S. Liu, Y. Song, P. Weng, B. Wan, F. Wan, H. Wang, S. Wu, M. Ye, Q. Yang, G. Zheng, G. Zhuang, Q. Li, Overview of the present progress and activities on the CFETR, Nucl. Fusion 57 (10) (2017) 102009. doi:10.1088/1741-4326/aa686a.

[5] J. H. You, E. Visca, C. Bachmann, T. Barrett, F. Crescenzi, M. Fursdon, H. Greuner, D. Guilhem, P. Languille, M. Li, S. McIntosh, A. V. Müller, J. Reiser, M. Richou, M. Rieth, European DEMO divertor target: Operational requirements

and material-design interface, Nucl. Mater. Energy 9 (2016) 171–176. doi:10.1016/j.nme.2016.02.005.

[6] G. Fishpool, J. Canik, G. Cunningham, J. Harrison, I. Katramados, A. Kirk, M. Kovari, H. Meyer, R. Scannell, MAST-upgrade divertor facility and assessing performance of long-legged divertors, J. Nucl. Mater. 438 (2013) S356–S359. doi:10.1016/j.jnucmat.2013.01.067.

[7] T. Barrett, S. McIntosh, M. Fursdon, D. Hancock, W. Timmis, M. Coleman, M. Rieth, J. Reiser, Enhancing the DEMO divertor target by interlayer engineering, Fusion Eng. Des. 98-99 (2015) 1216–1220. doi:10.1016/j.fusengdes.2015.03.031.

[8] T. Hirai, F. Escourbiac, S. Carpentier-Chouchana, A. Fedosov, L. Ferrand, T. Jokinen, V. Komarov, A. Kukushkin, M. Merola, R. Mitteau, R. Pitts, W. Shu, M. Sugihara, B. Riccardi, S. Suzuki, R. Villari, ITER tungsten divertor design development and qualification program, Fusion Eng. Des. 88 (9-10) (2013) 1798–1801. doi:10.1016/j.fusengdes.2013.05.010.

[9] A. R. Raffray, R. Nygren, D. G. Whyte, S. Abdel-Khalik, R. Doerner, F. Escourbiac, T. Evans, R. J. Goldston, D. T. Hoelzer, S. Konishi, P. Lorenzetto, M. Merola, R. Neu, P. Norajitra, R. A. Pitts, M. Rieth, M. Roedig, T. Rognlien, S. Suzuki, M. S. Tillack, C. Wong, High heat flux components—Readiness to proceed from near term fusion systems to power plants, Fusion Eng. Des. 85 (1) (2010) 93–108. doi:10.1016/j.fusengdes.2009.08.002.

[10] D. Brackett, I. Ashcroft, R. Hague, Topology optimisation for additive manufacturing, in: Proc. solid Free. Fabr. Symp., Austin, TX, 2011.

[11] D. Bourell, J. P. Kruth, M. Leu, G. Levy, D. Rosen, A. M. Beese, A. Clare, Materials for additive manufacturing, CIRP Ann. - Manuf. Technol. 66 (2) (2017) 659–681. doi:10.1016/j.cirp.2017.05.009.

[12] T. Weber, J. Aktaa, Numerical assessment of functionally graded tungsten/steel joints for divertor applications, Fusion Eng. Des. 86 (2-3) (2011) 220–226. doi:10.1016/j.fusengdes.2010.12.084.

[13] G. Pintsuk, S. Brünings, J.-E. Döring, J. Linke, I. Smid, L. Xue, Development of W/Cu—functionally graded materials, Fusion Eng. Des. 66-68 (2003) 237–240. doi:10.1016/S0920-3796(03)00220-5.

[14] M. Rieth, S. Dudarev, S. Gonzalez de Vicente, J. Aktaa, T. Ahlgren, S. Antusch, D. Armstrong, M. Balden, N. Baluc, M.-F. Barthe, W. Basuki, M. Battabyal, C. Becquart, D. Blagoeva, H. Boldyryeva, J. Brinkmann, M. Celino, L. Ciupinski, J. Correia, A. De Backer, C. Domain, E. Gaganidze, C. García-Rosales, J. Gibson, M. Gilbert, S. Giusepponi, B. Gludovatz, H. Greuner, K. Heinola, T. Höschen, A. Hoffmann, N. Holstein, F. Koch, W. Krauss, H. Li, S. Lindig, J. Linke, C. Linsmeier, P. López-Ruiz, H. Maier, J. Matejicek, T. Mishra, M. Muhammed, A. Muñoz, M. Muzyk, K. Nordlund, D. Nguyen-Manh, J. Opschoor, N. Ordás, T. Palacios, G. Pintsuk, R. Pippan, J. Reiser, J. Riesch, S. Roberts, L. Romaner, M. Rosiński, M. Sanchez, W. Schulmeyer, H. Traxler, A. Ureña, J. van der Laan, L. Veleva, S. Wahlberg, M. Walter, T. Weber, T. Weitkamp, S. Wurster, M. Yar, J.-H. You, A. Zivelonghi, Recent progress in research on tungsten materials for nuclear fusion applications in Europe, J. Nucl. Mater. 432 (1-3) (2013) 482–500. doi:10.1016/j.jnucmat.2012.08.018.

[15] S. A. Jahan, T. Wu, Y. Zhang, J. Zhang, A. Tovar, H. Elmounayri, Thermo-mechanical Design Optimization of Conformal Cooling Channels using Design of Experiments Approach, Procedia Manuf. 10 (2017) 898–911. doi:10.1016/j.promfg.2017.07.078.

[16] C. Baxi, Comparison of swirl tube and hypervapotron for cooling of ITER divertor, in: Proc. 16th Int. Symp. Fusion Eng., Vol. 1, IEEE, 1995, pp. 186–189. doi:10.1109/FUSION.1995.534199.

[17] K. Gadd, TRIZ for Engineers: Enabling Inventive Problem Solving, John Wiley & Sons, Ltd., 2011.

[18] D. Carfora, G. Di Gironimo, J. Järvenpää, K. Huhtala, T. Määttä, M. Siuko, Preliminary concept design of the divertor remote handling system for DEMO power plant, Fusion Eng. Des. 89 (11) (2014) 2743–2747. doi:10.1016/j.fusengdes.2014.07.016.

[19] D. Maisonnier, I. Cook, S. Pierre, B. Lorenzo, B. Edgar, B. Karin, D. P. Luigi, F. Robin, G. Luciano, H. Stephan, N. Claudio, N. Prachai, P. Aldo, T. Neill, W. David, The European power plant conceptual study, Fusion Eng. Des. 75-79 (SUPPL.) (2005) 1173–1179. doi:10.1016/j.fusengdes.2005.06.095.

[20] T. T. Wohlers, Wohlers Report 2015: Additive Manufacturing and 3D Printing State of the Industry: Annual Worldwide Progress Report, Tech. rep. (2015).

[21] M. A. Abdou, Exploring novel high power density concepts for attractive fusion systems, Fusion Eng. Des. 45 (2) (1999) 145–167. doi:10.1016/S0920-3796(99)00018-6.

[22] S. Zinkle, N. M. Ghoniem, Operating temperature windows for fusion reactor structural materials, Fusion Eng. Des. 51-52 (52) (2000) 55–71. doi:10.1016/S0920-3796(00)00320-3.

[23] R. Guschlbauer, S. Momeni, F. Osmanlic, C. Körner, Process development of 99.95% pure copper processed via selective electron beam melting and its mechanical and physical properties, Mater. Charact.doi:10.1016/j.matchar.2018.04.009. URL http://linkinghub.elsevier.com/retrieve/pii/S1044580317333703

[24] S. J. Zinkle, Thermophysical and mechanical properties for Ta-8% W-2% Hf, Tech. rep., Oak Ridge National Laboratory, Oak Ridge (1998).

[25] B. Tabernig, N. Reheis, Joining of Refractory Metals and its Application, in: 17th Plansee Semin., 2009.

[26] B. A. Jasperson, Y. Jeon, K. T. Turner, F. E. Pfefferkorn, W. Qu, Comparison of micro-pin-fin and microchannel heat sinks considering thermal-hydraulic performance and manufacturability, IEEE Trans. Components Packag. Technol. 33 (1) (2010) 148–160. doi:10.1109/TCAPT.2009.2023980.

[27] N. Tsuzuki, Y. Kato, K. Nikitin, T. Ishizuka, Advanced microchannel heat exchanger with S-shaped fins, J. Nucl. Sci. Technol. 46 (5) (2009) 403–412.

[28] R. Neugebauer, B. Müller, M. Gebauer, T. Töppel, Additive manufacturing boosts efficiency of heat transfer components, Assem. Autom. 31 (4) (2011) 344–347. doi:10.1108/01445151111172925.

[29] M. Wong, S. Tsopanos, C. J. Sutcliffe, I. Owen, Selective laser melting of heat transfer devices, Rapid Prototyp. J. 13 (5) (2007) 291–297. doi:10.1108/13552540710824797.

[30] N. Sahiti, A. Lemouedda, D. Stojkovic, F. Durst, E. Franz, Performance comparison of pin fin in-duct flow arrays with various pin cross-sections, Appl. Therm. Eng. 26 (11-12) (2005) 1176–1192. doi:10.1016/j.applthermaleng.2005.10.042.

[31] D. A. Olson, Heat Transfer in Thin, Compact Heat Exchangers With Circular, Rectangular, or Pin-Fin Flow Passages, J. Heat Transfer 114 (2) (1992) 373. doi:10.1115/1.2911285.

4

Paper: "Additive Manufacturing of High Temperature Materials for Fusion: A Review of Current Capabilities and Future Outlook"

Context within thesis

Having justified the use of refractory metals and the complex cooling geometries that AM enables, this paper presents a strategy for progressing the maturity of AM for fusion. It also seeks to contribute to the corpus of knowledge or maturity of the technology at each stage of the AM component manufacturing lifecycle across a range of materials. Core challenges are identified; particularly material choice, feedstock supply, and AM platform suitability; and steps are proposed for improving quality of built material and validating material properties and part performance.

Novelty

- a broader more holistic and through-lifecycle approach to AM component development
- new contributions to the AM of refractories

Lead author contributions

- formalising research strategy
- technical lead for the following UKAEA contributions to the AMAZE project:
  - design of AM test build plates
  - design of AMAZE test pieces including design of high heat flux demonstrators in copper
  - HIVE facility design and construction
  - manufacture and qualification of high heat flux demonstrators including HIVE testing and analysis
  - collating results of research
- contributor to remainder of UKAEA AMAZE deliverables including high heat flux concept generation and initial design, research strategy and partner management, and project reporting
- undertaking subsection of SLM tests of molybdenum and tungsten in Sheffield
- designing geometry test pieces in tungsten, molybdenum, and tantalum
- Ta powder qualification, AM builds, and density measurements in Birmingham, supported by co-authors
- small punch testing of all materials apart from vanadium
- directing remaining material testing and analysing results
- identifying needs to progress use of AM for fusion high heat flux components
- all writing

Publication status

This paper currently includes the full scope of PhD work to facilitate thesis submission. It will be modified (and possibly subdivided) to a more concise form suitable for journal submission, most likely "Additive Manufacturing". Part of this work was presented in oral and poster form in September 2017 at the EUROMAT conference in Thessaloniki, Greece. Work carried out under AMAZE was presented at a technology forum event at the MTC in Coventry, UK in July 2017 and is available to view online at `https://youtu.be/qJQAr_DT-wM` [cited 2018-06-25]

Approval status

Co-authors and supervisors:	Internal	(REVIEWED)	External	(REVIEWED)
UKAEA:	C. Waldon	(CLEARED)	E. Surrey	(CLEARED)
EUROfusion:	K. Gal	(ENDORSED)	T. Donne	(CLEARED)
AMAZE (notification only):	D. Wimpenny	(RELEASED)	M. Holden	(RELEASED)

Approval process limited to thesis submission prior to editing for journal publication

Additive Manufacturing of High Temperature Materials for Fusion: A Review of Recent Work, Strategies, and Future Outlook

David Hancock[a,b,*], Iain Todd[b], Brad Wynne[a,b], David Homfray[a], Michael Porton[a], Elizabeth Surrey[a], Heather Lewtas[a], Amanda Field[c], Stewart Williams[d], Ralf Guschlbauer[e], Shahin Mehraban[f], Mike Curtis-Rouse[g]

[a] *United Kingdom Atomic Energy Authority, Culham Science Centre, Abingdon, Oxfordshire, OX14 3DB*
[b] *University of Sheffield Department of Materials Science and Engineering, Sir Robert Hadfield Building, Mappin Street, Sheffield, S1 3JD*
[c] *Department of Metallurgy and Materials, Pritchatts Road, Edgbaston Campus, University of Birmingham, B15 2TT*
[d] *School of Aerospace, Transport and Manufacturing, Building 46, Welding Engineering and Laser Processing Research Centre, Cranfield University, College Road, Bedfordshire, MK43 0AL*
[e] *Zentralinstitut für Neue Materialien und Prozesstechnik (ZMP), 90762 Fürth, Germany*
[f] *Materials Research Centre, College of Engineering, Swansea University Bay Campus, College of Engineering, Fabian Way, Swansea, SA1 8EN*
[g] *Science and Technologies Facilities Council, Rutherford Appleton Laboratory, Harwell, Didcot, OX11 0QX*

Abstract

The design of components able to extract high heat fluxes at high temperatures is critical for the realisation of commercial fusion power. Additive manufacturing (AM) has been identified as a means to facilitate the realisation of advanced concepts using cooled structures with complex internal geometries designed to optimise heat transfer performance. Tungsten is the leading candidate for plasma-facing armour for these components, but other refractory alloys show promise for use within the cooled substructure, allowing higher temperature operation than current water cooled designs.

To this end, several projects are working towards the AM of high heat flux components for fusion, both connected to and prompted by the recently concluded European FP7 "AMAZE" project (Additive Manufacturing Aiming Towards Zero Waste and Efficient Production of High-Tech Metal Products).

This paper introduces the context and scope of these projects including a brief review of related capability and applications. Details are then given of progress made on laser powder bed fusion of elemental tungsten, vanadium, molybdenum, and tantalum. The case is made for a broad and holistic approach to development with the aim of identifying key technological challenges throughout the manufacturing and qualification lifecycle. A brief introduction is also given to additional work on wire and arc additive manufacturing and electron beam melting.

For each process and material, an initial characterisation of the available feedstock has been carried out before progressing to parametric build trials seeking to optimise density and microstructure. Thermomechanical material testing has followed, with a focus on using small samples. The manufacture and testing of a number prototypes of representative geometry and scale is then described. Finally, the current state of the art is summarised and the perceived outlook for future work is presented.

Word count: 287

Keywords: refractory, additive manufacturing, fusion, high heat flux, divertor

1. Introduction

1.1. Fusion high heat flux components

The generation of electricity from the energy released by nuclear fusion promises abundant, clean, and inherently safe power to help meet an increasing global demand in the face of environmental and economic concerns. Magnetic confinement fusion employing a high-temperature deuterium-tritium plasma contained in a toroidal device known as a tokamak is currently the most mature technology for achieving fusion reactions at power-plant relevant scales [1].

The design, production, and qualification of plasma-facing components able to extract high heat fluxes at high temperatures is critical for the realisation of commercial fusion power using a tokamak. The most demanding of these, the divertor target, must be able to survive steady state heat fluxes of the order of $10\,\mathrm{MW\,m^{-2}}$ and transient loads of two to three times this value in the form of energetic particles while at the same time minimising contamination of the fusion plasma and without absorbing the tritium fuel essential for maintaining the reaction. In order to maximise plant availability and reduce maintenance costs and time, the lifetime of these components must be several years [2]. Demands on reliability, maintainability, and inspection are equally challenging,

*Corresponding Author
Email address: david.hancock@ukaea.uk (David Hancock)

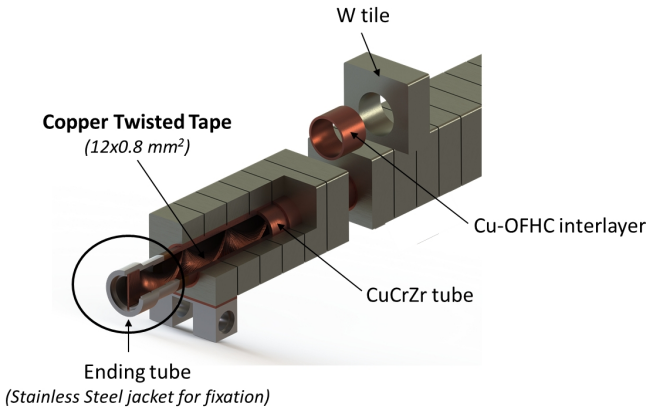

Figure 1: ITER-like tungsten and copper alloy "monoblock" design used in WEST [5]

particularly given the need to meet stringent nuclear design standards and satisfy the relevant regulatory bodies [3].

Current fusion experiments employ tungsten blocks joined to a dispersion strengthened copper alloy tube as their divertor target, as shown in figure 1. Irradiation induced material property degradation and the desire for improved performance as described above renders these concepts unsuitable for long-term use in a demonstration fusion power plant [4].

For advanced concepts, tungsten remains the leading candidate for the plasma-facing armour due to its high melting point, high sputtering resistance, vacuum compatibility, low activation, and low tritium absorption, but materials other than copper are being explored for use within the cooled substructure. Recent work has shown that previously discounted refractory alloys including those based on tantalum, molybdenum, and vanadium are worthy of re-evaluation when considering new technology and fresh priorities [6]. Additive Manufacturing (AM) has been identified as a means to facilitate the realisation of these concepts, allowing the inclusion of complex cooling geometries to further enhance performance [7].

1.2. Current status of refractory metal AM and AM for fusion

AM as a potential technology is gaining traction within the fusion community with two components already installed in JET [8, 9] and has been proposed as a possible manufacturing route for blanket and first wall components [10, 11] but these have been generally limited to materials more widely used outside fusion with an established processing route, such as steel and nickel alloys.

AM of tungsten for divertor applications has been proposed, though reported progress has been limited and the emphasis has been on deliberately creating porous material in which liquid lithium can be carried, rather than as a pressure-retaining structure [12]. Outside the fusion community, there are a significant number of reports of laser powder bed fusion of pure tungsten [13, 14, 15, 16, 17] and tungsten with small additions of tantalum for increased ductility [18]. Commercially, AM is inceasingly used to produce complex tungsten structures for shielding applications, for example collimators for medical imaging (e.g. [19]), although for these, once nearly full density has been achieved, little study has been carried out on thermal or structural properties.

Efforts to process molybdenum for fusion applications using a 200 W laser system have this far failed to achieve full density [20], but more recently Wang et al. have reported more success, including a degree of crack suppression using interlocking scanning strategies [21].

Vanadium alloys, regularly proposed as an alternative material for fusion structures, have also recently been processed with promising early results [22].

Among the refractory metals, the most success producing dense, crack free material has been reported with tantalum [23, 24, 25, 26]. Deliberately porous material has been produded as both components and coatings for biomedical applications [27] and complex solid tantalum propulsion components have been built for a space propulsion system [28]. Although other specific details are not published, defense and automotive applications are thought to be other active areas of development, particularly for high-temperature heat exchangers.

The bulk of work has been focussed on elemental material, although trials have been undertaken with WTaMoNb high entropy alloys [29].

Efforts to qualify AM for the fission industry are also ongoing, with engagement from ASME and ISO, though these are currently primarily limited to conventional materials.

1.3. Projects and scope

In the light of all this, work is being carried out towards the AM of prototype refractory metal high heat flux components for fusion applications. In order to strategically identify the most critical issues associated with deploying this technology, these projects have addressed multiple stages of the lifecycle in parallel from material supply to concept validation with the aim of both demonstrating the potential benefits of employing AM and identifying critical gaps in the supply and manufacturing chain. This paper aims to bring together a summary of some of these recent collaborative efforts and to determine the state of the art to identify the most significant research needs.

Much of this work was originated through the recently concluded European FP7 "AMAZE" project (Additive Manufacturing Aiming Towards Zero Waste and Efficient Production of High-Tech Metal Products); a collaborative research and development consortium aiming to deliver the technological capability for rapid production of large defect-free metallic components for use in high-tech sectors [30].

Within AMAZE, work was structured around the production and testing of a number of prototype parts. End-user consortium partners set requirements and provided a design for a component identified as suitable for AM. Other partners within the consortium variously focussed on theoretical and practical development of the AM processes themselves (including laser powder bed fusion (LPBF), electron beam melting (EBM) or wire-arc additive manufacturing (WAAM)), producing either material test coupons or the components themselves. Others carried out material characterisation including thermomechanical testing.

For the fusion-specific prototype, effort surrounded the production of a series of increasingly advanced high heat flux elements, introducing more complex geometry and challenging material combinations as the project progressed. Where possible, representative performance testing of these prototypes was carried out using a bespoke high heat flux facility as detailed in chapter 5.

In addition to work contributing to AMAZE and since the formal conclusion of that project, work has been undertaken to continue to explore alternative manufacturing techniques, materials, and geometries. In particular, initial comparative trials of LPBF of tungsten and molybdenum were carried out using pulsed and continuous laser systems before the start of AMAZE, and tantalum has been developed as an alternative promising candidate material subsequently. Investigations into underlying causes of grain boundary cracking of the more brittle materials are ongoing, with investigations of possible mitigation strategies and alloying solutions. Contributions to the corpus of material testing data for these materials are also ongoing, particularly focused on comparisons between as-built AM and conventional material. The production of a promising functionally graded interface between tungsten, molybdenum, and tantalum using WAAM during the latter stages of AMAZE is also prompting further investigation.

Full details of progress on EBM and WAAM are being reported elsewhere, and so this paper will be limited to focus on strategy and LPBF work.

2. Process Development

2.1. Rationale

When developing the AM processes, the method used here has been to characterise general attributes of the currently available feedstock, investigate build parameters for one or more combination of feedstock and AM platform, and then progress to representative size and shape parts, material test coupons, and prototype components immediately. This method provides a first pass at establishing feasibility, seeks to identify any previously unforeseen fundamental difficulties, and highlights critical areas for strategically targeted further development.

At this stage, the availability of refractory powders suitable for AM is limited to a very small number of suppliers and elemental metals. There has been significant investigative effort expended and much debate ongoing about the most important attributes for AM powder, but the avoidance of unwanted impurities and the need for powder to flow and spread well on the build platform are universally agreed. Given the relative paucity of supplier options, an in-depth characterisation of the available material beyond simple morphology and chemical analysis was deemed premature, pending maturation of the supply chain.

Likewise, the large variability between AM platforms and poor characterisation or definition of input settings (even when considering similar machines) renders absolute definition of "ideal" build parameters matched to theoretical modelling impractical without a much more extensive research programme which would duplicate ongoing work both in modelling (e.g. [31]) and in-situ monitoring [32]. This uncertainty is compounded by the well publicised effects of part size, geometry, orientation, location within the build envelope, and proximity to other components (e.g. [33, 34]).

The aforementioned overview approach, therefore, gives indication of feasibility of material processing at relevant part size and type in new materials with the available resources and without duplicating existing research.

2.2. Method

First, the feedstock was assessed for physical morphology. General size and shape has been qualitatively determined by optical and electron microscopy. Flow properties (as a metric for ease of spreading) have then been evaluated by Hall flow, Hausner ratio and Carr index.

Secondly, design of experiments (DoE) has been used to determine build parameters on increasingly representative parts, beginning with small 10 mm to 15 mm cubes. Starting parameters have been selected on the basis of prior experience as well as first principle estimates of the required energy density to achieve melting.

Two approaches for calculating energy density have been considered. The first calculates volumetric energy density (E_{vol}) as a function of laser power (P), scan speed (v_{scan}), layer thickness (l), and hatch spacing (h) as shown in equation 1.

$$E_{vol} = \frac{P}{v_{scan} \cdot l \cdot h} \tag{1}$$

The second approach takes into account laser spot radius (r_{beam}), and calculates a linear volumetric energy density ($E_{vol,linear}$) as shown in equation 2.

$$E_{vol,linear} = \frac{P}{v_{scan} \cdot \pi \cdot r_{beam}^2} \tag{2}$$

For pulsed laser systems such as those produced by Renishaw, an effective scan speed can be calculated as

shown in equation 3, allowing a degree of direct comparison with continuous beam systems.

$$v_{effective} = \left(\frac{exposure\ time}{point\ distance} + \frac{1}{idle\ speed} \right)^{-1} \quad (3)$$

Preliminary trials explored variations in scanning strategy, hatch spacing and layer thickness, as well as beam speed, power, and spot radius. Later builds reduced the number of variables, maintaining a consistent layer thickness of order powder size and hatch spacing of order twice beam diameter. Since hatch spacing and layer thickness were similar for most of the build trials, while spot size varied more significantly as outlined below, the second approach for calculating energy (equation 2) was used while determining a threshold for consolidation.

Part density has been used as the primary assessment metric for the DoE, using Archimedes and optical measurements on sections. Surface finish has been evaluated qualitatively as a secondary metric for overall build quality, where multiple combinations of parameters with similar energy densities produced similar part densities.

A custom Python package, SLMtools [35], has been created and used as a combined data organisation structure, visualisation tool, and predictive toolbox throughout this process. Written in Python 3, this is an extensible, hierarchical, object-oriented package with classes for buildset (multiple related builds to be compared), build parameters, material, and part details. This data can be written to and read from a range of data formats including Microsoft spreadsheets and the open, language-independent, JavaScript Object Notation (JSON) format [36]. Calculation tools included provide simple weld pool modelling, normalised and volumetric energy density calculations and parameter comparisons and conversions between pulsed and steady state laser systems to allow a degree of predictive capability. Input parameters and results such as part density can be visually plotted and tabulated using included methods.

Once density has been optimised and is more than 95% of parent material, more rigorous microscopy, including scanning electron microscopy (SEM), has been used to determine whether cracking has occurred, and if so, the process has been iterated.

Using the best parameters from this exercise, material testing coupons and more representative geometries have been built. For larger parts it has been found that a slight reduction in overall power density has improved build quality. This can be accounted for by the greater cumulative power and resulting higher temperature of the parts during the build process.

The limited powder quantities available, particularly of vanadium, heavily restricted the number of builds possible and placed very tight constraints on the number of tests that could be carried out. In order to make the most efficient use of the feedstock, to standardize (as far as possible) the builds between materials, and to streamline the procedures used in preparation for high heat flux testing, two standard build plates were proposed: the first produces a full set of material test coupon types, and the second includes a subset of coupons with one or more high-heat flux elements. Figure 2 shows labelled diagrams of the designs and photographs of two example builds. A pressure test "thimble" was used in early trials to determine leak tightness and structural integrity without the need for a larger part. Test builds in aluminium allowed trials of part removal and post-machining techniques and allowed modifications to be made to optimise these processes.

2.3. LPBF tungsten

Plasma spherodised powder from LPW[1] with a size distribution of 40 µm to 55 µm was used throughout the development of LPBF tungsten. Figure 3 shows its spherical shape, lack of satellites, and few fine particles.

The selection of this feedstock and initial build parameters drew significantly from prior (unpublished) work using a pulsed 200 W Renishaw SLM125[2]. These parameters are given in table 1, and the scan strategy used was a simple "meander" with a 60° rotation between layers.

Table 1: Renishaw tungsten build parameters

P	200 W
r_{beam}	25 µm
h	50 µm
l	30 µm
$v_{effective}$	135 mm s^{-1}

Initially promising indications of densities of over 90% for 10 mm cubes prompted an immediate attempt to demonstrate fusion-relevant geometries, as detailed in section 4. This proved unsustainable for larger parts without increased laser power, however, due to limited ability to reduce effective beam velocity. Subsequent laser profiling suggests actual power may have been as low as 170 W. Figure 4 shows a typical cross section for one of these early parts, showing high porosity and poor powder consolidation due to incomplete melting.

Subsequent work employed a continuous 400 W Concept Laser M2 Cusing[3]. Although using parameters given in table 2 with a 5 mm "checkerboard" scan strategy produced densities approaching 100% to be achieved, persistent grain boundary cracking was observed as shown in figure 5.

Ongoing work seeks to identify and suppress the underlying causes of this, while providing the material testing

[1] https://www.lpwtechnology.com/
[2] https:/www.renishaw.com
[3] https://www.concept-laser.de/

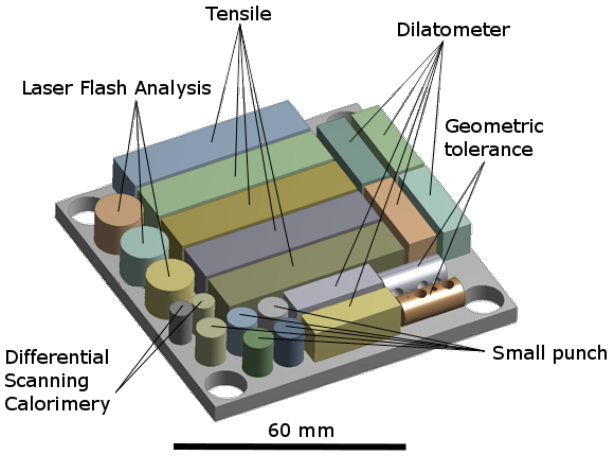

(a) Material testing test plate design

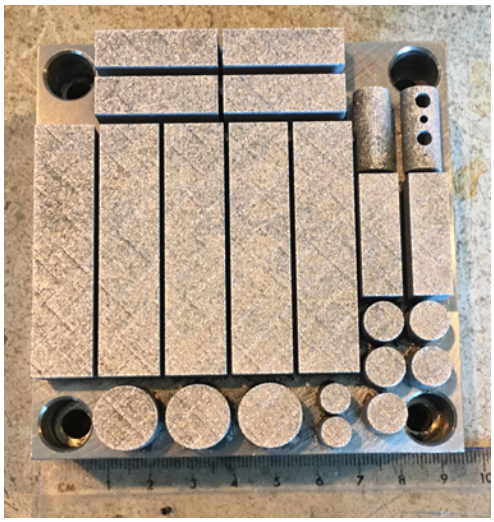

(b) Material testing test plate (Vanadium)

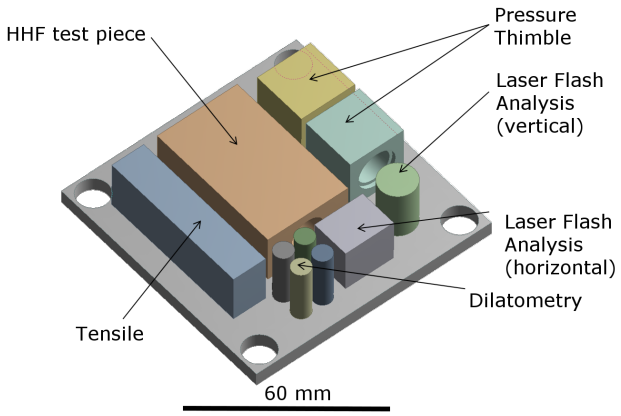

(c) High heat flux test plate design

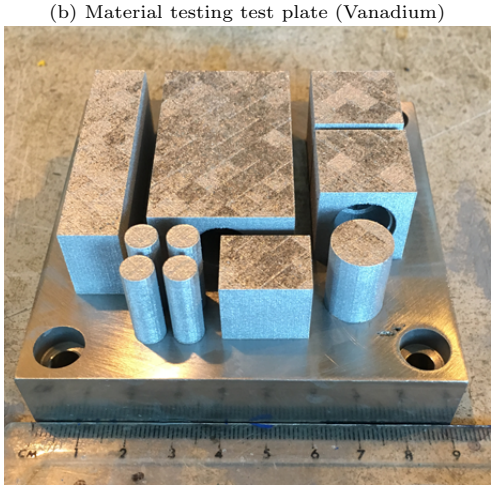

(d) High heat flux test plate (Molybdenum)

Figure 2: Material testing and high heat flux test build plates

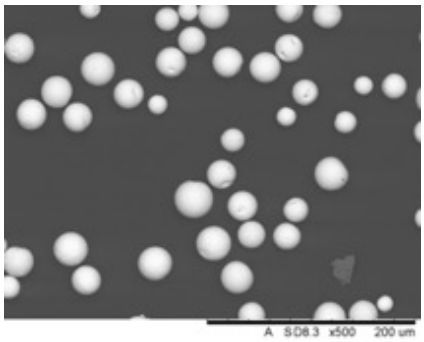

Figure 3: Optical micrograph of LPW tungsten powder

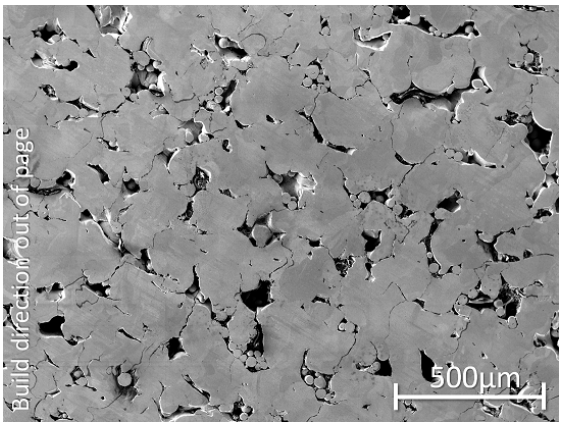

Figure 4: SEM image of typically porous tungsten achieved with Renishaw 125

Table 2: M2 tungsten build parameters

P	300 W
r_{beam}	42.5 µm
h	45 µm
l	30 µm
v_{scan}	950 mm s^{-1}

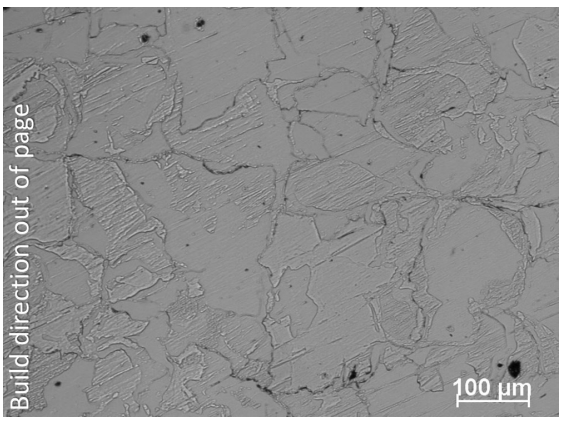

Figure 5: Dense but cracked tungsten achieved with Concept Laser M2 Cusing

samples described in section 3 as a baseline from which to measure improvements in properties. Three strategies in particular are being pursued: reducing the oxygen content in powder and build atmosphere which acts as a barrier to consolidation, raising bed temperature to reduce residual stresses causing cracking, and including small quantities of alloying material to enhance ductility.

Since this work was carried out, a number of other attempts to produce LBPF tungsten have been discovered. Similar results have been reported, i.e. achieving densities in excess of 97%, but with similar persistent grain-boundary cracking [16, 14]. Claims of crack-free material have not yet been supported by published data.

2.4. LPBF molybdenum

A wider range of powder sources was available for molybdenum, with two separate batches supplied by TLS with slightly different size distributions, one by Tekna[4], and a fourth by HC Starck[5]. Figure 6 shows electron microscopy images of these, showing the variability of size distribution and morphology.

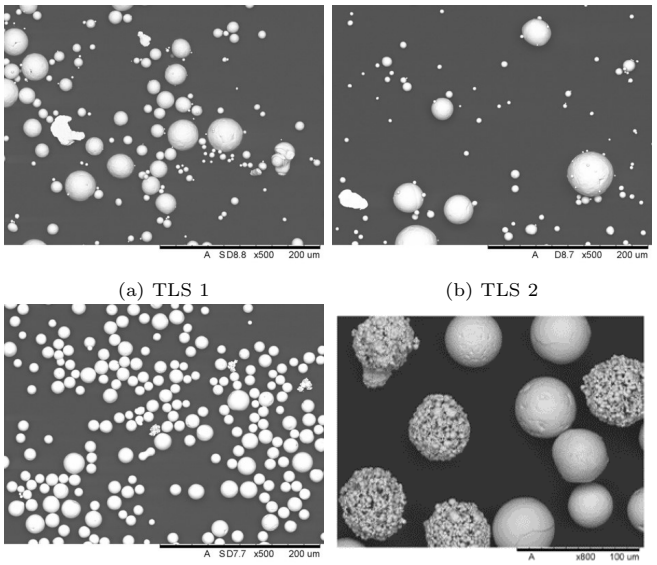

(a) TLS 1 (b) TLS 2

(c) Tekna (d) HC Starck

Figure 6: SEM images of molybdenum powders

Measurements of flow properties using apparent and tap densities showed similar behaviour between the TLS and Tekna powders, with Hausner ratios of approximately 1.1 and Carr indices between 7.4 and 8 respectively, suggesting good flowabilty across all the batches. A large number of agglomerated particles in the HC Starck powder led to it being excluded prior to the flow studies.

For molybdenum, preliminary trials were also carried out using the 200W pulsed laser Renishaw platform, but with limited success, achieving densities of approximately

[4] `https://www.tekna.com`
[5] `https://www.hcstarck.com`

90%, and with significant cracking. Subsequent testing was then carried out using the same Concept Laser M2 as above.

Figure 7 shows a graph of component density against volumetric energy density for the design of experiments parameter trials carried out using the M2.

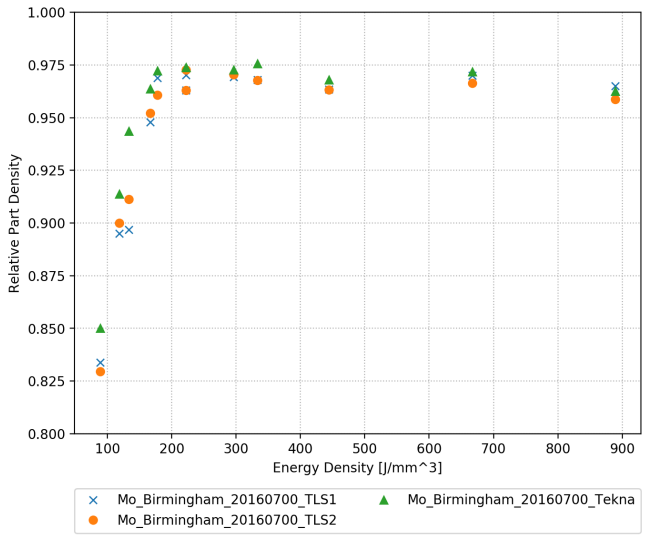

Figure 7: Molybdenum part density vs volumetric energy density

Uncertainties in laser absolute power for the Renishaw system and beam profile for the Concept Laser M2 render absolute interpretation of these figures impossible, but a consolidation threshold is clear at around 200 J mm^{-3} with a gradual reduction in density above this value.

Figure 8 shows a SEM image of the level of density and consolidation achieved using parameters given in table 3. Density is approximately 98% according to archimedes testing, but cracking continues to be evident along grain boundaries.

Table 3: M2 molybdenum build parameters

P	300 W
r_{beam}	75 µm
h	112 µm
l	30 µm
v_{scan}	600 mm s^{-1}

Oxidation and residual stress are again proposed as the primary causes of this cracking and so as well as improved atmosphere control and heated build chamber, a range of post build heat treatments have been explored. The open porosity caused by the crack network renders Hot Isostatic Pressing (HIP) challenging without canning components, and even if closed porosity could be achieved, the resulting high pressure inside pores would be likely to cause re-opening of voids at the elevated temperatures at which

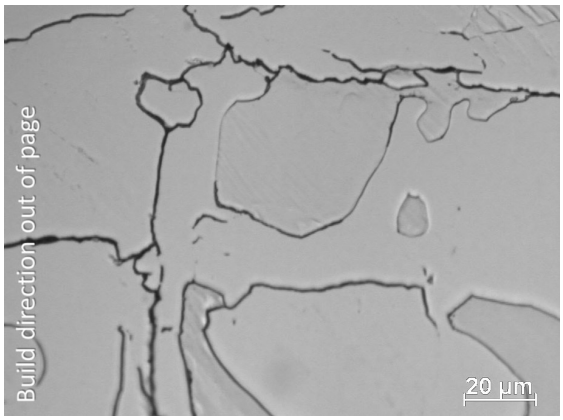

Figure 8: Optical micrograph of LPBF molybdenum

these components are likely to be operated. Microwave sintering has also been suggested as a means of post build heat treatment, though it would not be possible to achieve the penetration depth into larger parts needed for uniform heating at the high frequencies used.

2.5. LPBF vanadium

Initial process trials of pure vanadium under AMAZE, again using the Concept Laser M2 Cusing, were promising, with the parameters in table 4 producing material with high density and little cracking, as shown in figure 10.

Table 4: M2 vanadium build parameters

P	200 W
r_{beam}	75 µm
h	112 µm
l	30 µm
v_{scan}	1000 mm s^{-1}

A limited quantity of powder was available, however, and limited subsequent builds to a single design of experiments trial and two sets of material testing coupons. The latter builds were only partially successful due to powder leakage during build in one case and significant delamination between build plate and components in the other, as shown in figure 9.

A number of test coupons were successfully extracted retained and some small punch testing was carried out as reported in section 3.6.

2.6. LPBF Tantalum

Two tantalum powders were analysed. The first, supplied by HC Starck was a mechanically reduced powder with a size distribution of 20 µm to 40 µm. The second powder was spherodised and supplied by LPW using material produced by Metalysis[6] and had a size range

[6] https://www.metalysis.com

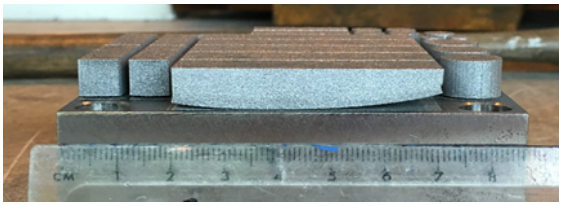

(a) Delamination of vanadium test build

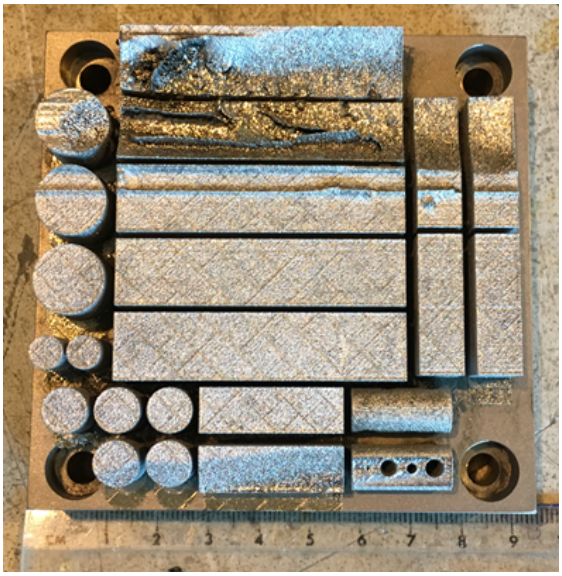

(b) Results of powder leakage from vanadium test build

Figure 9: Vanadium test plates

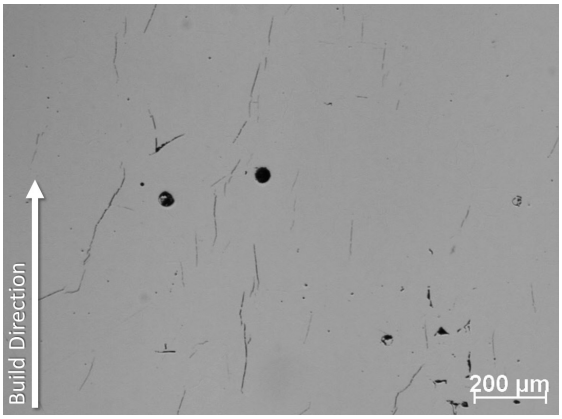

Figure 10: Optical micrograph image of LPBF vanadium

of 30 µm to 60 µm. Figure 11 shows optical micrographs of both, demonstrating the similar size distribution but significantly different morphologies.

Both powders showed very poor flow properties during Hall flow testing. This was as expected for the mechanically reduced morphology, but it is possible that the spherical powder had been subject to moisture contamination. After allowing the LPW powder to dry in an inert argon atmosphere, a Hausner ratio of 1.1, Carr index of 8.7 and Hall flow of 12 s per 50 g were recorded.

Despite the poor flow properties, initial trials with the

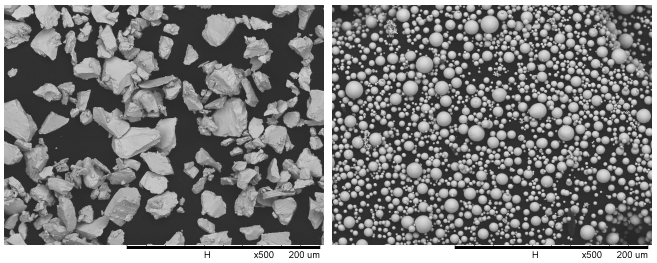

(a) HC Starck Ta powder (b) LPW Ta powder

Figure 11: SEM images of tantalum powders

mechanically reduced powder achieved densities of 97.5% with no obvious cracking. Higher densities (approaching 99%) were achieved with the spherical powder at slightly lower power, as shown in figure 12.

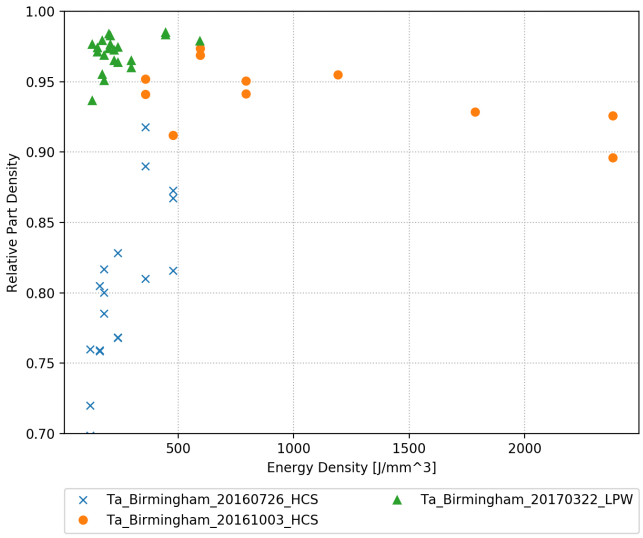

Figure 12: Density vs Energy Density Graph

Build trials varied power between 200 W and 400 W and scan speed between 50 mm s^{-1} and 1500 mm s^{-1}. A replacement of the laser optics partway through the project reduced the beam radius from 75 µm to 42.5 µm for later builds. Figure 13 shows an image of 98% dense tantalum, achieved using parameters given in table 5.

Table 5: M2 tantalum build parameters

P	400 W
r_{beam}	42.5 µm
h	45 µm
l	30 µm
v_{scan}	1500 mm s^{-1}

Unfortunately, problems with recoater blade damage reduced the number of successfully build components,

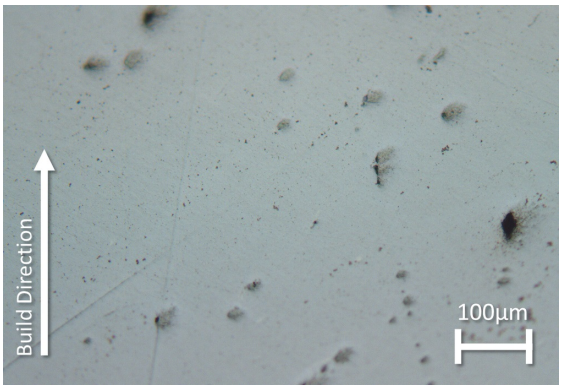

Figure 13: Optical micrograph of as-built tantalum

although some geometric trials were achieved as detailed in section 4.

2.7. EBM of copper and tungsten

In order to allow a direct performance comparison between conventional and AM material and demonstration parts, EBM was used to produce copper structural components and material testing coupons.

Full details of feedstock characterisation and process development are published elsewhere (including [37]), and so this paper will be limited to a report of component manufacture and testing as described in section 4. It is worth noting, however, that consistency of purity in supplied powder was poor, and so the success of builds was somewhat unpredictable.

Separate from AMAZE, parallel work to develop the EBM of tungsten has shown significant promise for producing dense, crack free material[7]. The process inherently operates at a higher temperature than laser powder bed fusion, reducing the residual stress between layers and remaining above the DBTT even for slightly oxidised material. By building entirely in a vacuum, the chance of oxidation is also significantly reduced.

3. Material Testing

3.1. Rationale

The limited quantity of material available and large amount of variability between builds has thus far prevented an extensive or statistically significant assessment of thermomechanical properties for AM refractories at their current state of development. Work has, nonetheless, begun to identify the most appropriate and strategic methods for characterising performance of these materials and to draw a metaphorical line in the sand from which progress can be made towards parent properties or which highlights the need to investigate alternative alloys.

A subset of critical properties has been investigated, focussing on those relevant for fusion high heat flux components. In particular, the desire was to understand basic thermal and mechanical behaviour at high temperature, namely strength, thermal conductivity, and thermal expansion. Given the small volume of material being produced, small scale testing has been used exclusively. This also allows the possiblity of including testing coupons for these techniques into build plates for components in the future or for addition of features into parts from which monitoring samples could be taken throughout the lifetime of a part.

In order to characterise the mechanical properties of these materials at high temperature, testing must be carried out in an inert atmosphere or vacuum to avoid oxidation. The limited availabilty of suitable testing equipment, the small volume of available material, and the desire to identify the most effective testing method has led to the trial of a number of techniques outlined below.

This material data has been collated and stored using a new python library (materialtools [38]), based around the MatML markup language [39]. This library allows comparison from different sources as well as automated import, interpretation and visualisation of raw data from a number of material testing machines used throughout the project.

3.2. Dilatometry

Thermal expansion measurements were carried out on a small number of 6 mm diameter × 20 mm long cylindrical samples of as-built LPBF tungsten, molybdenum, and tantalum using a NETZSCH DIL 402C dilatometer in a nitrogen atmosphere with a temperature ramp rate of $20\,^{\circ}\mathrm{C\,min^{-1}}$. The resulting strain and thermal expansion coefficient data are shown in figure 14.

These graphs show large variability in material properties even between parts built at the same time with the same parameters, and most samples show significant variation between the heating and cooling cycles. The samples were unpolished and it is likely that additional error was introduced by friction within the testing apparatus due to its horizontal orientation.

Despite the limited number of samples and poor quality of the data all three materials demonstrate similar bulk thermal expansion properties to ideal material, particularly on the cooling stroke, but there are consistently unexpected volume changes in the tungsten and tantalum which cannot be accounted for purely by friction.

The volume reduction in the tungsten after the first heating cycle (figure 14a) is of the order of the expected porosity in the as-built material and may be attributed to partial closing of pores, but the phenomenon begins at roughly 500 °C to 600 °C which is significantly lower than the temperature at which sintering would be expected to occur and will need further work to understand.

Conversely, there appears to be an increase in volume in the tantalum samples at a similar temperature (figure 14c). One possible cause is the presence of a non bcc phase,

[7] Results awaiting publication.

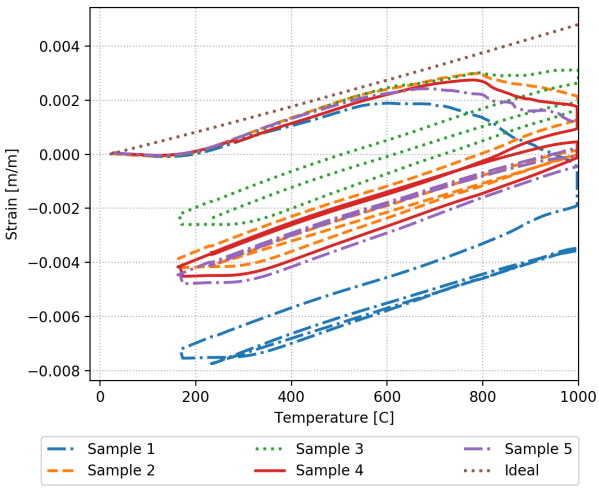

(a) Tungsten strain

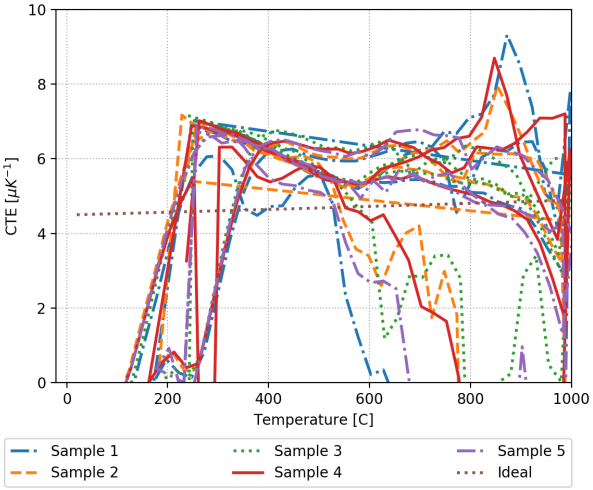

(b) Tungsten thermal expansion coefficient

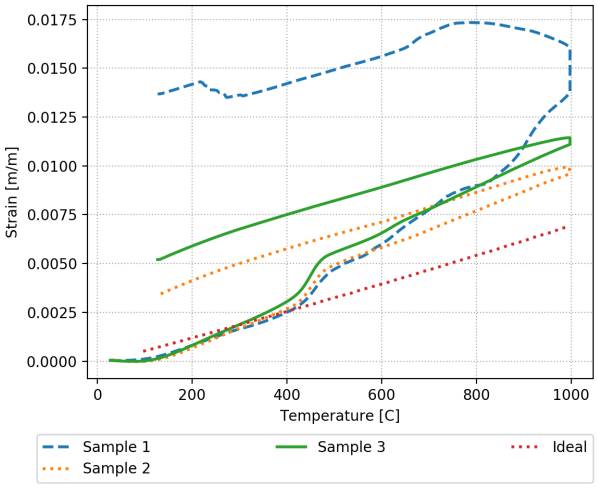

(c) Tantalum strain

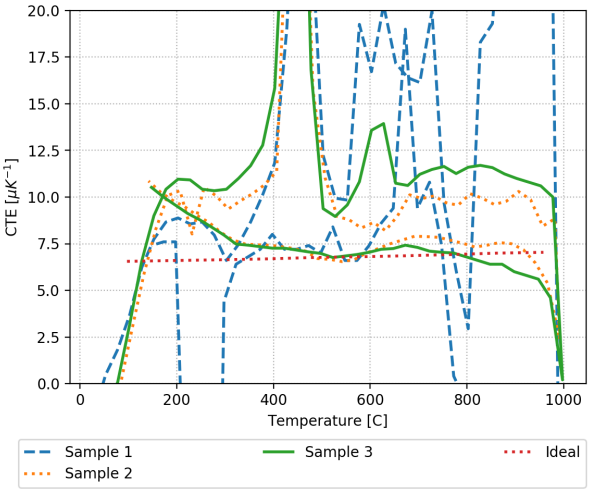

(d) Tantalum thermal expansion coefficient

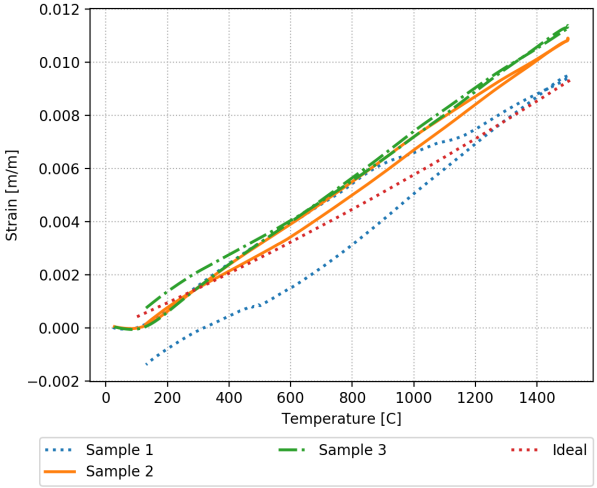

(e) Molybdenum strain

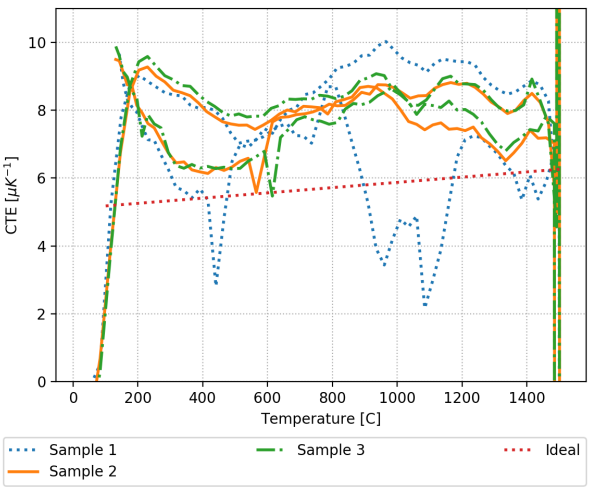

(f) Molybdenum thermal expansion coefficient

Figure 14: Results of thermal expansion measurements

e.g. the tetragonal β phase described in [40, 41] which is frequently produced by thin-film deposition or a hexagonal ω phase which has been produced under extreme laser deformation [42].

3.3. Laser Flash Analysis

Diffusivity measurements were carried out using a NETZSCH LFA 457 laser flash analyser on tungsten, molybdenum, and tantalum from the same builds as the dilatometry. Samples were coated with graphite to increase absorption and reduce reflection and measurements were made in an argon atmosphere. Measurements were made between 50 °C and 850 °C at 50 °C intervals with results from 5 shots at each interval averaged. Conductivity was calculated from diffusivity using a reference value for specific heat.

The small sample size (12.2 mm diameter, ≈2 mm thick discs) allowed a larger number of samples to be tested, but a similar level of variability in the data was seen, as shown in figure 15.

The tungsten showed a consistently lower thermal conductivity than ideal, with the closest values neither at the top nor bottom of the build volume. This is in keeping with the increased level of cracking seen in these regions. Partial densification would not be expected to have as significant effect on thermal conductivity as on the dilatometry results, and while there is some evidence of an increase in conductivity, this could be accounted for by the change in geometry affecting the calculation.

The large increase in calculated thermal conductivity of some of the tantalum at 600 °C, if caused by the phase change described above, can be accounted for by a combination of the higher actual conductivity of the bcc phase.

A larger number of molybdenum samples were tested, including four built in a horizontal orientation allowing testing perpendicular to the build direction. Significant anisotropy (as well as scatter) was seen as shown by figures 15c and 15d. Conductivity in the build direction was generally higher than the horizontal measurements, in keeping with observations of cracking anisotropy. Most samples showed slight increases in measured values above 600 °C similar to the tungsten and tantalum. A conventional pure molybdenum standard sample measured using the same equipment shows a similar trend, however, suggesting an underlying experimental anomaly at this point. Repeat measurements on the AM material showed increases in conductivity for all samples, however, suggesting a heat-treatment effect of some kind, unfortunately unverifiable due to lack of material.

3.4. Small scale tensile

Small scale tensile testing of SLM molybdenum was attempted using the sample geometry shown in figure 16 but the brittle and porous nature of the samples used caused them to fail before any significant load was applied or useful data gathered.

Small scale tensile testing would be more suitable for higher quality and more ductile materials, and should certainly be included in ongoing work, but further tests were deemed spurious pending processing improvements.

3.5. Small bending

Prompted by the brittle nature of the samples, small-scale four point bending tests were carried out on LBPF tungsten and tantalum using the bespoke jig shown in figure 17 in the same load frame as the small punch tests described below.

This used the same 2 mm x 2.5 mm x 30 mm sample dimensions used to probabilistically assess brittle tungsten for divertor applications [43], to allow for comparison. Unfortunately, equipment failures meant that the data are not valid and there was a lack of sufficient samples to repeat the testing.

3.6. Small punch

Small punch testing provides a means to test stress strain, creep, and brittleness behaviour of small material samples [44], and while the complex stress-state induced makes extraction of quantitative absolute material properties challenging, small punch testing gives an efficient means to test comparative performance between materials. In particular, the small sample size and cylindrical geometry lends itself well to inclusion in AM builds or in-service monitoring for nuclear applications (e.g. [45]).

Testing has therefore begun to be carried out comparing conventionally wrought off the shelf material and the additive materials under discussion. A selection of these results are shown in in figure 18. The limited volume of material as yet available prevents a comprehensive and statistically rigorous analysis of the results, but there is a clear trend towards higher hardness and brittleness in the AM material compared to wrought.

4. Component Manufacture

4.1. Geometry trials

Promising process development and a limited quantity of available powder prompted early trials of test geometries in vanadium, including the small pipe parts shown in figure 19. These were built with the small channels horizontal to deliberately demonstrate how a rougher surface could be induced in the region where the resulting convective heat transfer enhancement would be most beneficial. For AMAZE, subsequent work on vanadium was halted in favour of molybdenum and tungsten due to availability of powder and the requirement for a higher thermal conductivity for the specific designs being pursued.

Despite initially low densities and subsequent persistent cracking, complex parts were successfully produced in tungsten using the Renishaw SLM. Figure 20 shows an early concept for an enclosed pin-fin type heat exchanger structure and 21 shows a gyroid geometry which has high

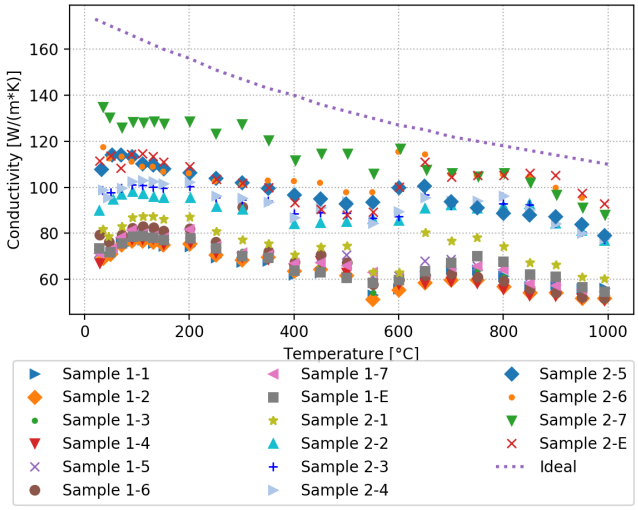

(a) Tungsten

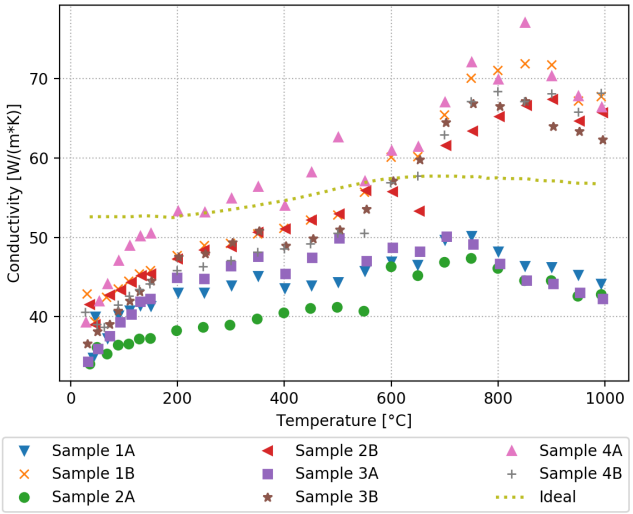

(b) Tantalum

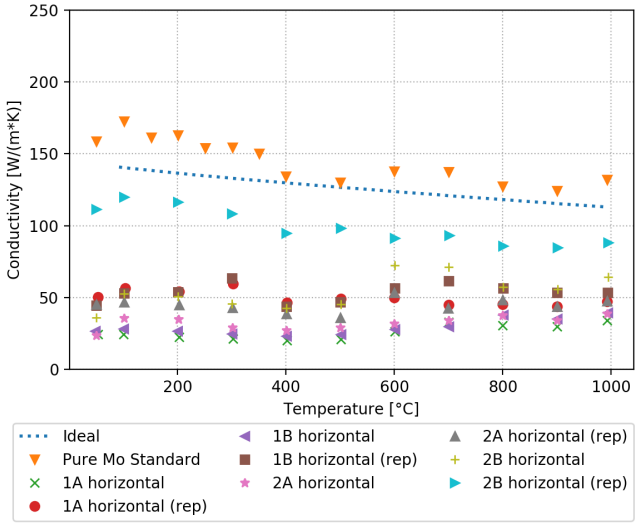

(c) Molybdenum (horizontal)

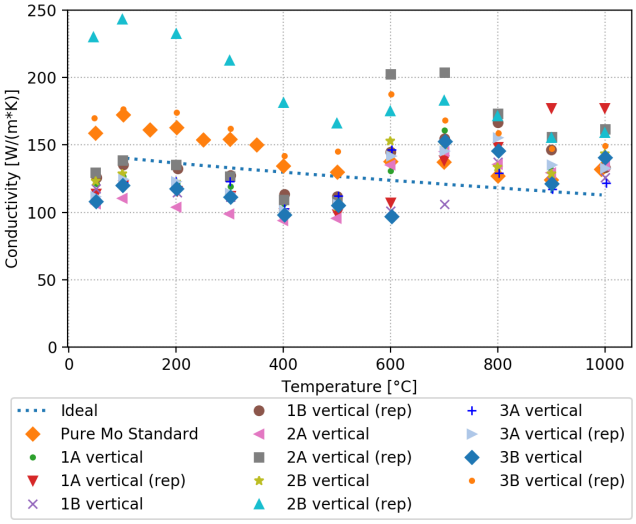

(d) Molybdenum (vertical)

Figure 15: Results of thermal conductivity measurements

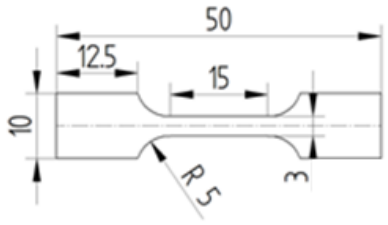

Figure 16: Sample geometry used for tensile testing

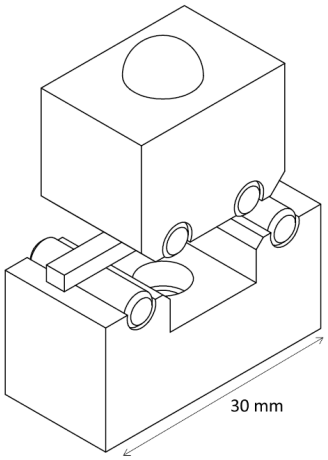

Figure 17: Small four-point bending test equipment

structural rigidity with open channels suitable for a more porous-type concept.

Figure 2d above shows the high heat flux test plate built in molybdenum. A simple block geometry, the dimensions for which are shown in 22, was to be used for comparative testing with conventional and AM copper components described below, but unfortunately the level of cracking prevented sufficient vacuum and water leak tightness for testing to proceed.

Figure 23 shows a tantalum build plate containing a series of small components used to test the production of thin-walled geometries at a range of radii, a selection of material testing coupons, and two pressure-thimble structures. Recoater blade damage towards the end of the build resulted in the rough surface and deep striations shown, but nonetheless some components with wall thicknesses of 0.5 mm were successfully produced and some dilatometer and laser flash samples were extracted for testing.

Figure 24 shows a concept geometry and as-built test part for a multiple small pipe high heat flux element using tantalum. This part shows the feasibility of complex internal geometries and associated thermomechanical analysis has shown that concepts of this type show promise for advantages over conventional concepts [7]. Slight modifications were made to the concept geometry shown in figure 24a to reduce overhangs in the larger voids and external radii were added to reduce overall material use and build time. Despite an interrupted build caused by a loss of power to the machine, the part completed successfully.

4.2. High Heat Flux Demonstrators

Successfully manufacturing subcomponents with the desired geometry and material properties using AM is not enough. These subcomponents must be successfully integrated with their various interfaces and their performance proven. In the case of fusion high heat flux components, the cooled substructure must be joined to armour, to coolant pipework, and possibly to support substructure. Where the cooling geometry employed cannot be manufactured via conventional techniques, analytical performance predictions must be validated experimentally. Under AMAZE, prototype demonstrator components were manufactured and a small experimental facility was designed and built for high heat flux testing with an explicit emphasis on rapid and cost-effective validation of advanced concepts and manufacturing processes.

Parts were built in copper using conventional machining and EBM using the geometry in figure 22. These copper components were then brazed to a conventional tungsten tile and copper pipework using a single-pass vacuum braze cycle. The prototype assemblies were then helium leak tested, hydrostatically pressure tested, and subjected to heat loads of order $5\,\mathrm{MW\,m^{-2}}$ using this facility, named HIVE (Heating by Induction to Verify Extremes). Temperature rises were monitored with embedded and surface mounted components and the results mapped to analytical values. One of the AM components is shown in HIVE under HHF testing in figure 25. The direct comparisons between AM and conventional components suggested that the rough surface of the AM parts enhanced convective heat transfer by as much as 20%, but that the lower thermal conductivity of the AM material counteracted this performance enhancement. Further details of the HIVE facility and these test results are given in [46].

A more complex cooled copper component was then produced (shown in figure 26). This geometry aimed to demonstrate the performance benefits of small pipe concepts generated under AMAZE, as well as integrating a LPBF tungsten tile to produce a "fully AM" prototype.

EBM requires a pre-heat cycle to partially sinter the powder before fully melting each layer, and the requirement to remove this pre-sintered powder limited the design to larger diameter cooling channels than initially intended and the design had to include near line-of-sight to these channels from each end to allow access for a small brush.

Unfortunately, while geometrical tolerances were good and the braze cycle appeared successful, the assembly as a whole failed to meet the vacuum leak tightness requirements for testing in HIVE.

5. Conclusions

5.1. Overview

This paper has presented a summary of a selection of recent work to progress the maturity of additive

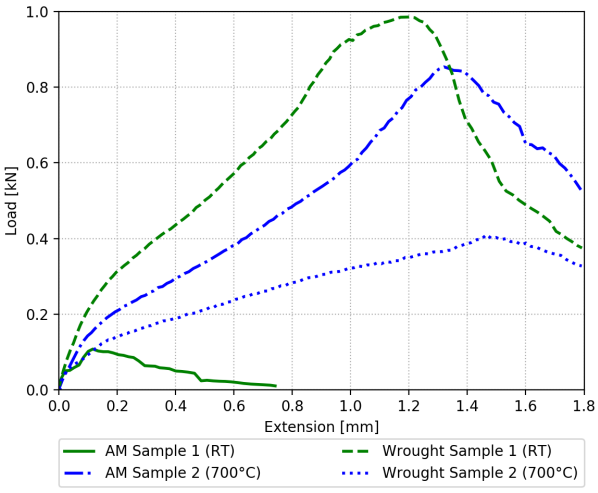

(a) Vanadium

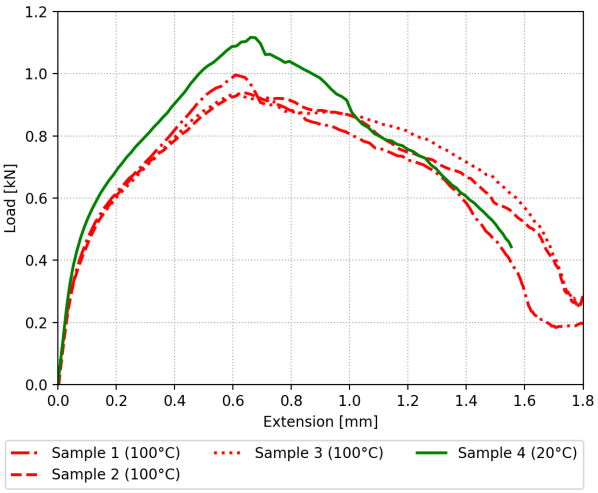

(b) Tantalum

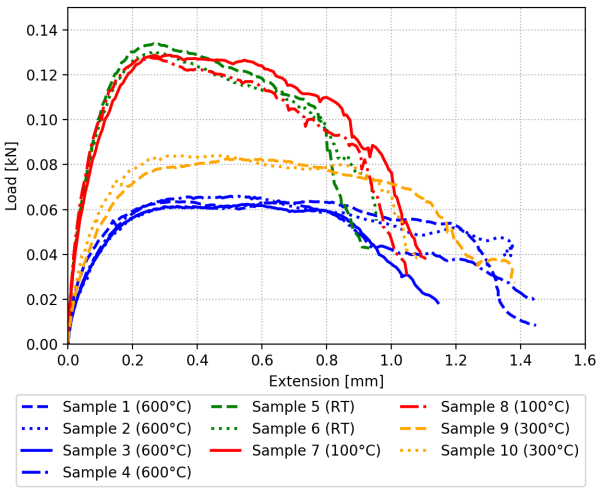

(c) Tungsten

Figure 18: Results of small punch testing

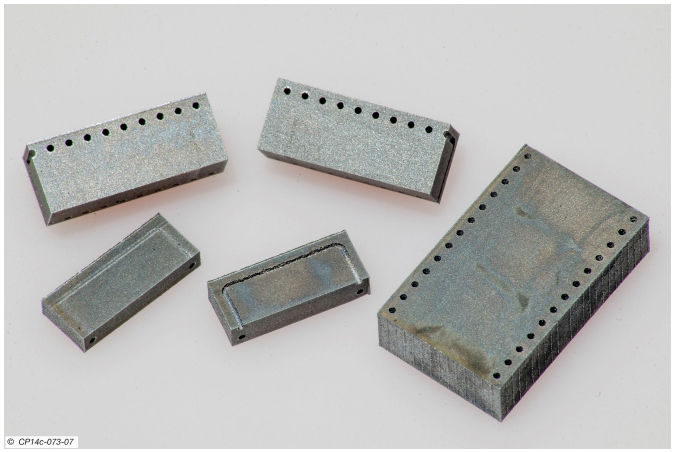

Figure 19: Vandadium small pipe test parts

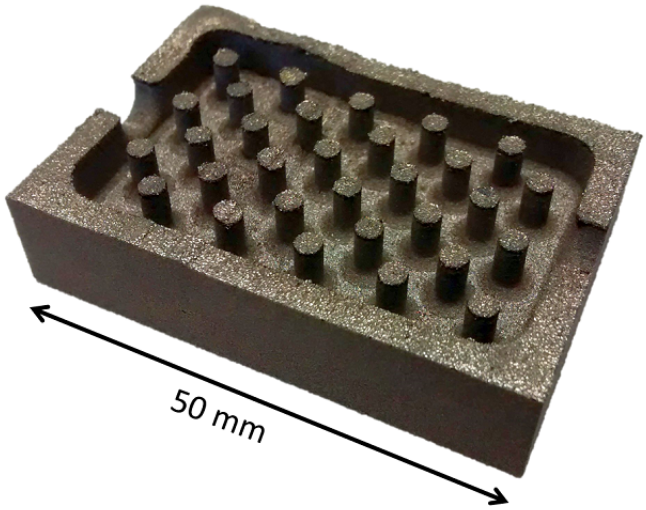

Figure 20: Tungsten pin-fin test part

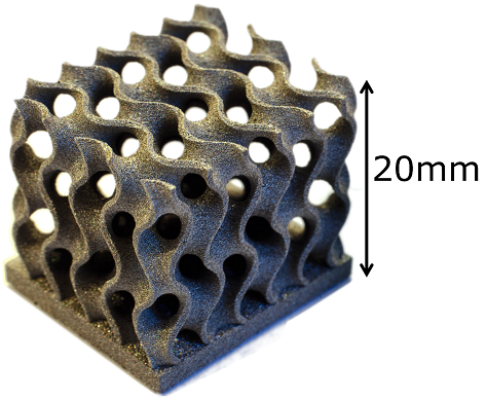

Figure 21: Tungsten gyroid test part

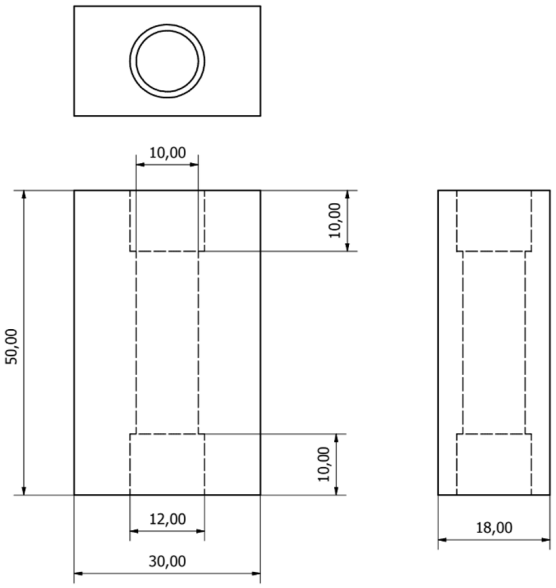

Figure 22: Simple high heat flux testpiece dimensions

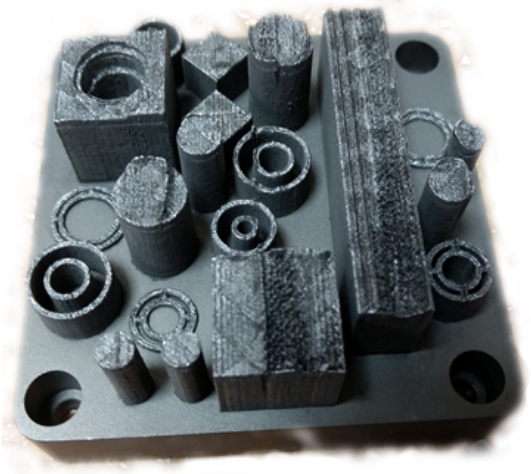

Figure 23: Tantalum geometry trial buildplate

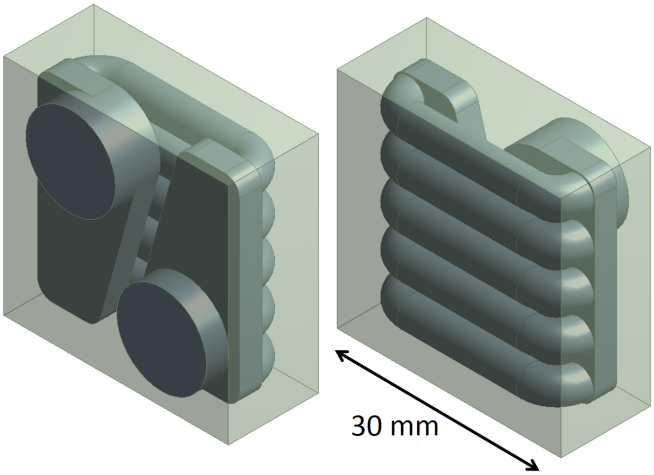

(a) Manifolded small pipe geometry

(b) Tantalum manifolded small pipe test part

Figure 24: Tantalum manifolded small pipe concept

Figure 25: EBM copper and wrought tungsten "simple" HHF demonstrator in HIVE

manufacturing of high temperature materials for high heat flux applications in fusion reactors, particularly focussed on LPBF of elemental refractory metals, with reference to related work using WAAM and EBM and to high heat flux testing of AM copper prototypes. The case has been made for a broad and holistic approach, addressing every phase of the AM process from feedstock supply to prototype testing, recognising that lessons learned upstream of a particular stage can usefully inform technological requirements and research priorities. This approach has been demonstrated through the examination of available powder feedstock for a number of materials, process development using these materials on two separate LPBF machines, limited but informative thermomechanical material testing, representative part manufacture, and component assembly and high heat flux testing.

5.2. State of the art

The field is a rapidly progressing one, rendering attempts to comprehensively or accurately identify the current state of the art challenging, but it is useful to record the authors' observations nonetheless:

As the leading candidate for plasma-facing armour material, tungsten will almost certainly be a significant part of any fusion power plant, and so interest in advanced manufacturing techniques is likely to remain high. Tungsten's high thermal conductivity, high melting point, ready oxidation, and brittleness render LPBF extremely challenging, however. With sufficient input energy, nearly fully dense material is relatively readily achievable, but cracking remains a persistent hurdle currently preventing use for cooled structures or complex shapes. EBM or alloying with more ductile elements may be promising alternatives, but results are preliminary. For bulk material deposition, WAAM produces attractive grain structure and may be a means to repair damaged armour tiles in-situ or provide a means to functionally grade joints during manufacture if cracking at the substrate can be overcome.

Progress with LPBF of molybdenum has been similar to that with tungsten; near ideal densities have been achieved, while cracking and oxidation remain issues. Molybdenum's lower melting point may mean that a heated bed in combination with better atmosphere control may improve matters, and reports to this effect are starting to informally emerge. In the meantime, molybdenum's high activation in a fusion neutron environment continue to render it a less than ideal candidate material, and unless molybdenum based alloys with vastly superior mechanical properties emerge, there is unlikely to be significant desire for further research.

Despite initially showing promise, development of LPBF vanadium suffered from a lack of available powder,

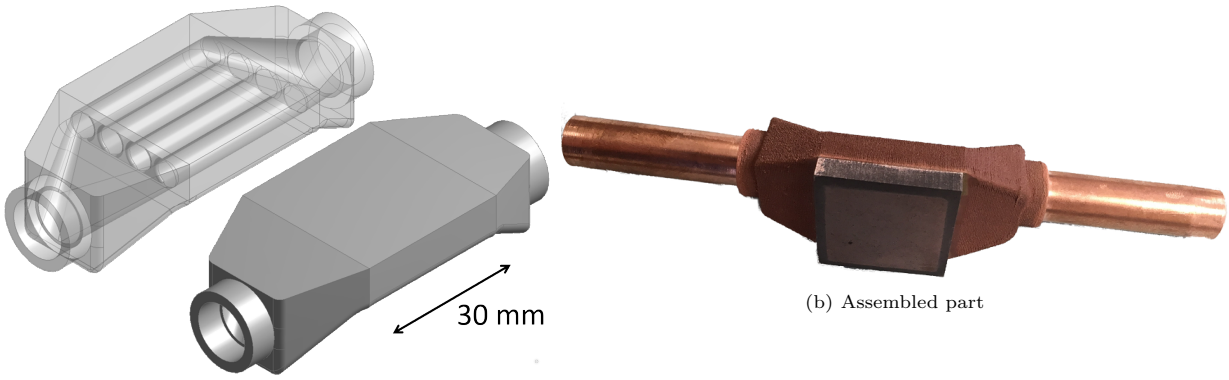

(a) Geometry

(b) Assembled part

Figure 26: AMAZE small pipe demonstrator

and was subsequently placed on hold in favour of materials with higher thermal conductivities. On the other hand, early results have been separately reported with more fusion-specific vanadium alloys [22, 47].

Results for LPBF tantalum are more encouraging, with early builds appearing nearly fully dense and crack free. Despite the limited number of builds carried out, complex geometries have been built and some early material testing has been carried out. The latter has shown that there may be non-bcc phases produced by the AM process which will need to be carefully considered for future work.

EBM of copper has primarily been used thus far to compare AM with conventional material in simple high heat flux trials, but the ability to produce complex cooled geometries in copper could prove of use where high performance but lower bulk temperature cooled components are needed. Reliability does not yet meet requirements for in service use, partly caused by uncertainty in powder quality, but in the future it could be a tool for characterising more complex cooling geometries prior to concept development in more challenging materials.

5.3. Outlook and future research needs

The argument for a broad and shallow approach has been justified in a number of ways and a clear list of challenges and opportunities for AM of fusion high heat flux materials are emerging. The current growth of interest in AM across industry sectors provides an opportunity for end-users with shared requirements to work with one another and with material and powder suppliers, AM platform manufacturers, and regulatory bodies to establish requirements and collaboratively undertake mutually beneficial research. Some of the key issues identified below are becoming more general consensus and "public knowledge" within the wider AM community, but others are more fusion and refractory specific:

Material choice.
In focussing on elemental materials, rather than alloys, progress has been limited by the inherent brittleness and propensity for oxidation of a number of candidates. Tungsten, tantalum, vanadium and molybdenum alloys have all been proposed for fusion applications, but few have specifically been designed for fusion, fewer are available in the form needed for AM, and none are specifically optimised for producing high quality AM parts.

An opportunity therefore exists for AM specific alloy development for fusion applications. This could, in the first instance be focussed on enhanced ductility and reduced oxygen pickup during manufacture. Unlike aerospace, where a large body of data already exists for baseline materials such as Ti-6Al-4V and renders the introduction of new alloys unattractive, no such body exists for fusion and the window remains (for the moment) open to the introduction of new candidates.

AM technology choice.
Each of the AM technologies discussed show separate strengths and weaknesses for use in fusion applications. LPBF has clear advantages for complex cooling geometries where conventional machining would not be feasible but significant work is needed to reduce cracking in brittle materials and improve consistency in material properties. EBM shows promise with tungsten and is relatively mature with copper but cooled structures need careful design to remove sintered powder which may counteract the benefits of using AM. WAAM, on the other hand, cannot currently produce complex internal geometries but may prove very effective for depositing armour material with favourable grain structure, for producing functionally graded joints between armour and cooled substructure, and possibly for in-situ repair.

Recognising that no single AM technology is perfect for all applications within fusion enables a more targeted and pragmatic approach to their deployment to support specific engineering needs.

Powder requirements and availability.
If AM is to be accepted as a viable technology for deploying in a future generation of fusion power plants, there must be a well established supply chain of consistently high quality powders suitable for AM in relevant materials at

economic cost and scale. In the meantime, there is a need to clarify to suppliers the materials and powder characteristics needed, which are likely to be application specific rather than universal.

Machine parameters.
It has become clear that in comparison to more established AM materials, the process window for successfully producing refractory metals is extremely narrow, particularly for LPBF, and achieving satisfactory results across build platforms and material batches may be impractical even if uncertainties in build parameters can be resolved.

It is possible to begin to identify a number of emerging requirements for AM of refractory metals: Details of laser parameters including power and scanning methodology must be extremely well understood and well controlled. The build chamber atmosphere must be free from contaminants, particularly oxygen. It is becoming evident that there is likely to be a need to pre-heat the substrate, ideally to a significant fraction of the melting temperature of the material. Finally, it may be necessary to vary the build parameters significantly over the duration of a build and for different sizes and orientations of parts to ensure a more consistent thermal history throughout the component.

This, in turn, will require close collaboration between AM platform manufacturers and end users, and unless this real-time tailoring of build parameters can be automatically carried out based on in-situ build monitoring, will require an openness which works counter to the trend of "AM as a package" where powder and set parameters are sold to an end user with the machine. In addition, the development of more stringent atmospheric monitoring and integration of high temperature build chamber heating would ideally be carried out in partnership with AM suppliers to produce platforms specifically designed for these high temperature materials.

Post build heat treatments.
The series of activities reported in this paper have made little effort to consider the use of post-build heat treatments. This decision was initially made anticipating that the goal of further sintering and densification would be difficult to achieve at temperatures possible in the vacuum furnaces available. The impact on material testing of this choice has been marked, however, with clear evolution of properties as samples have been thermally cycled. Extended and repeat testing has not been carried out on all material, both due to lack of volume of material and of resource availability within the projects.

It is clear that not only will a thorough investigation of the underlying causes of the material property evolution shown in section 3 be required, but it is possible that more favourable properties will be achieved with post-build heat treatment at even modest temperatures.

Testing techniques.
The thermomechanical material testing described in this paper sought to demonstrate the feasibility of characterising fundamental properties of AM material compared to conventional material using small samples well suited to inclusion in component builds or as in-service health monitoring tokens. The high degree of scatter in the data, while largely the result of inconsistency in the material due to unoptimised build processing, also highlights the need for both a more extensive testing programme to ensure statistical significance and to explore the underlying causes of a number of anomalous phenomena and the immaturity of some of the testing techniques themselves, particularly small punch testing.

Component design validation, performance testing, and qualification are also needed; this is particularly the case where AM introduces design features which cannot be duplicated using traditional manufacturing techniques. Small-scale validation facilities such as HIVE provide an efficient means to carry out design screening and optimisation during the development phase prior to more extensive qualification programmes.

Joining.
The joint between armour and cooled structure is typically the point of most frequent failure for fusion high heat flux components [48]. Using traditional methods such as brazing or welding to join AM and conventional material together has proven relatively straightforward within the scope of the work described here, but will require in-depth characterisation to confirm and qualify. On the other hand, the possibility of functionally grading this joint using AM provides a potential mitigation strategy for dissimilar metal joints and WAAM has already been demonstrated as a possible route, but will require more development to refine the technique.

The strategic nature of the integration of joining and advanced manufacturing has been identified as part of the recently launched UK National Fusion Technology Platform (NaFTeP) [49], and there will be a dedicated Joining and Advanced Manufacturing (JAM) laboratory within the new Fusion Technology Facility (FTF) designed for this purpose.

Codes and standards.
Codes and standards for AM are being actively developed (e.g. by ASTM Committee F42 and ISO/TC 261) but a more pro-active role must be taken to ensure fusion and nuclear specific needs are represented at every stage to ensure that relevant materials and particular requirements are included.

Acknowledgements:

This work has been carried out within the framework of the EUROfusion Consortium and has received funding from the Euratom research and training programme 2014-2018 under grant agreement No 633053. This project has also received funding from the European Union's

Seventh Framework Programme for research, technical development, and demonstration under grant agreement no 313781. The views and opinions expressed herein do not necessarily reflect those of the European Commission. This work has also been part-funded by the RCUK Energy Programme [grant number EP/P012450/1]. To obtain further information on the data and models underlying this paper please contact publicationsmanager@ccfe.ac.uk.

References

References

[1] F. Romanelli, Fusion Electricity: A roadmap to the realisation of fusion energy, Tech. rep., EDFDA (2012). doi:ISBN978-3-00-040720-8.

[2] D. Maisonnier, I. Cook, S. Pierre, B. Lorenzo, B. Edgar, B. Karin, D. P. Luigi, F. Robin, G. Luciano, H. Stephan, N. Claudio, N. Prachai, P. Aldo, T. Neill, W. David, The European power plant conceptual study, Fusion Eng. Des. 75-79 (SUPPL.) (2005) 1173–1179. doi:10.1016/j.fusengdes.2005.06.095.

[3] G. Federici, W. Biel, M. Gilbert, R. Kemp, N. Taylor, R. Wenninger, European DEMO design strategy and consequences for materials, Nucl. Fusion 57 (9) (2017) 092002. doi:10.1088/1741-4326/57/9/092002.

[4] T. Barrett, S. McIntosh, M. Fursdon, D. Hancock, W. Timmis, M. Coleman, M. Rieth, J. Reiser, Enhancing the DEMO divertor target by interlayer engineering, Fusion Eng. Des. 98-99 (2015) 1216–1220. doi:10.1016/j.fusengdes.2015.03.031.

[5] P. Ghendrih, E. Tsitrone, C. Bourdelle, S. Brémond, J. Bucalossi, Y. Corre, A. Ekedahl, G. Giruzzi, R. Guirlet, P. Maget, Y. Marandet, M. Missirlian, P. Moreau, E. Nardon, B. Pégourié, The WEST research plan (February).

[6] D. Hancock, D. Homfray, M. Porton, I. Todd, B. Wynne, M. Coleman, Refractory Metals as Structural Materials for Fusion High Heat Flux Components, (Article Prep.

[7] D. Hancock, D. Homfray, M. Porton, I. Todd, B. Wynne, Exploring Complex High Heat Flux Geometries for Fusion Applications Enabled by Additive Manufacturing, Fusion Eng. Des.doi:https://doi.org/10.1016/j.fusengdes.2018.02.097.

[8] Z. Vizvary, B. Bourde, A. Garcia-Carrasco, N. Lam, F. Leipold, R. Pitts, R. Reichle, V. Riccardo, M. Rubel, G. De Temmerman, V. Thompson, A. Widdowson, Engineering design and analysis of an ITER-like first mirror test assembly on JET, Accept. Publ. Fusion Eng. Des. Proc. 29th Symp. Fusion Technol. xxx. doi:10.1016/j.fusengdes.2016.12.016.

[9] V. Thompson, N. Lam, IN-VESSEL REPLACEMENTS (IVER) Development of SLM (Selective Laser Melting) as a Manufacturing Process for In-Vessel Parts for JET, Tech. rep., CCFE (2014).

[10] N. Ordás, L. C. Ardila, I. Iturriza, F. Garcianda, P. Álvarez, C. García-Rosales, Fabrication of TBMs cooling structures demonstrators using additive manufacturing (AM) technology and HIP, in: Fusion Eng. Des., Vol. 96-97, 2015, pp. 142–148. doi:10.1016/j.fusengdes.2015.05.059.

[11] Y. Zhong, L. E. Rännar, S. Wikman, A. Koptyug, L. Liu, D. Cui, Z. Shen, Additive manufacturing of ITER first wall panel parts by two approaches: Selective laser melting and electron beam melting, Fusion Eng. Des. 116 (2017) 24–33. doi:10.1016/j.fusengdes.2017.01.032.

[12] R. E. Nygren, D. L. Youchison, B. D. Wirth, L. L. Snead, A new vision of plasma facing components, Fusion Eng. Des. 109-111 (2016) 192–200. doi:10.1016/j.fusengdes.2016.03.031.

[13] S. Bai, J. Liu, P. Yang, M. Zhai, H. Huang, L.-M. Yang, Femtosecond Fiber Laser Additive Manufacturing of Tungsten, in: Proc. SPIE 9738, Laser 3D Manuf. III, 97380U, San Fransisco, 2016. doi:10.1117/12.2217551.

[14] D. Wang, C. Yu, X. Zhou, J. Ma, W. Liu, Z. Shen, Dense Pure Tungsten Fabricated by Selective Laser Melting, Appl. Sci. 7 (4) (2017) 430. doi:10.3390/app7040430.

[15] R. K. Enneti, R. Morgan, T. Wolfe, A. Harooni, S. Volk, Direct Metal Laser Sintering/Selective Laser Melting of Tungsten Powders, Int. J. Powder Metall. 53 (4) (2017) 23–31.

[16] A. T. Sidambe, P. Fox, Investigation of the Selective Laser Melting process with tungsten metal powder.

[17] C. Tan, K. Zhou, W. Ma, B. Attard, P. Zhang, T. Kuang, Selective laser melting of high-performance pure tungsten: parameter design, densification behavior and mechanical properties, Sci. Technol. Adv. Mater. 19 (1). doi:10.1080/14686996.2018.1455154.

[18] A. Iveković, N. Omidvari, B. Vrancken, K. Lietaert, L. Thijs, K. Vanmeensel, J. Vleugels, J.-P. P. Kruth, A. Ivekovic, N. Omidvari, B. Vrancken, K. Lietaert, L. Thijs, K. Vanmeensel, J. Vleugels, J.-P. P. Kruth, A. Iveković, N. Omidvari, B. Vrancken, K. Lietaert, L. Thijs, K. Vanmeensel, J. Vleugels, J.-P. P. Kruth, Selective laser melting of tungsten and tungsten alloys, Int. J. Refract. Met. Hard Mater. 72 (2018) 27–32. doi:10.1016/j.ijrmhm.2017.12.005.

[19] K. Deprez, S. Vandenberghe, K. Van Audenhaege, J. Van Vaerenbergh, R. Van Holen, Rapid additive manufacturing of MR compatible multipinhole collimators with selective laser melting of tungsten powder, Med. Phys. 40 (1) (2012) 012501. doi:10.1118/1.4769122.

[20] D. Faidel, D. Jonas, G. Natour, W. Behr, Investigation of the selective laser melting process with molybdenum powder, Addit. Manuf. 8 (2015) 88–94. arXiv:arXiv:1011.1669v3, doi:10.1016/j.addma.2015.09.002.

[21] D. Wang, C. Yu, J. Ma, W. Liu, Z. Shen, Densification and crack suppression in selective laser melting of pure molybdenum, Mater. Des. 129 (2017) 44–52. doi:10.1016/j.matdes.2017.04.094.

[22] Y. Jialin, Selective laser melting additive manufacturing of advanced nuclear materials V-6Cr-6Ti, Mater. Lett. 209 (2017) 268–271. doi:10.1016/j.matlet.2017.08.014.

[23] V. Livescu, C. M. Knapp, G. T. Gray, R. M. Martinez, B. M. Morrow, B. G. Ndefru, Additively manufactured tantalum microstructures, Materialia 1 (2018) 15–24. doi:10.1016/j.mtla.2018.06.007.

[24] L. Zhou, T. Yuan, R. Li, J. Tang, G. Wang, K. Guo, Selective laser melting of pure tantalum: Densification, microstructure and mechanical behaviors, Mater. Sci. Eng. A 707 (September) (2017) 443–451. doi:10.1016/j.msea.2017.09.083.

[25] G. T. Gray, C. M. Knapp, D. R. Jones, V. Livescu, S. Fensin, B. M. Morrow, C. P. Trujillo, D. T. Martinez, J. A. Valdez, Structure/property characterization of spallation in wrought and additively manufactured tantalum, AIP Conf. Proc. 1979. doi:10.1063/1.5044799.

[26] R. Wauthle, J. Van Der Stok, S. A. Yavari, J. Van Humbeeck, J. P. Kruth, A. A. Zadpoor, H. Weinans, M. Mulier, J. Schrooten, Additively manufactured porous tantalum implants, Acta Biomater. 14 (2015) 217–225. doi:10.1016/j.actbio.2014.12.003.

[27] L. Thijs, M. L. Montero Sistiaga, R. Wauthle, Q. Xie, J.-P. Kruth, J. Van Humbeeck, Strong morphological and crystallographic texture and resulting yield strength anisotropy in selective laser melted tantalum, Acta Mater. 61 (12) (2013) 4657–4668. doi:10.1016/j.actamat.2013.04.036.

[28] F. Romei, A. N. Grubišić, D. Gibbon, Manufacturing of a high-temperature resistojet heat exchanger by selective laser melting, Acta Astronaut. 138 (2017) 356–368. doi:10.1016/j.actaastro.2017.05.020.

[29] H. Zhang, W. Xu, Y. Xu, Z. Lu, D. Li, The thermal-mechanical behavior of WTaMoNb high-entropy alloy via selective laser melting (SLM): experiment and simulation, Int. J. Adv. Manuf. Technol. (2018) 1–14doi:10.1007/s00170-017-1331-9.

[30] AMAZE Website.

[31] M. Thomas, G. J. Baxter, I. Todd, Normalised model-based processing diagrams for additive layer manufacture of

engineering alloys, Acta Mater. 108 (September) (2016) 26–35. doi:10.1016/j.actamat.2016.02.025.

[32] S. K. Everton, M. Hirsch, P. Stravroulakis, R. K. Leach, A. T. Clare, Review of in-situ process monitoring and in-situ metrology for metal additive manufacturing, JMADE 95 (2016) 431–445. doi:10.1016/j.matdes.2016.01.099.

[33] C. J. Smith, M. Gilbert, I. Todd, F. Derguti, Application of layout optimization to the design of additively manufactured metallic components, Struct. Multidiscip. Optim. 54 (2016) 1297–1313. doi:10.1007/s00158-016-1426-1.

[34] E. Fitzgerald, W. Everhart, The Effect of Location on the Structure and Mechanical Properties of Selective Laser Melted 316L Stainless Steel.

[35] D. Hancock, https://github.com/adlhancock/SLMtools (2017).

[36] T. Bray, The javascript object notation (json) data interchange format.

[37] R. Guschlbauer, S. Momeni, F. Osmanlic, C. Körner, Process development of 99.95% pure copper processed via selective electron beam melting and its mechanical and physical properties, Mater. Charact.doi:10.1016/j.matchar.2018.04.009.

[38] D. Hancock, https://github.com/adlhancock/materialtools (2017).

[39] J. G. Kaufman, E. F. Begley, MatML: A Data Interchange Markup Language, Adv. Mater. Process. 161 (No. 11).

[40] L. A. Clevenger, A. Mutscheller, J. M. Harper, C. Cabral, K. Barmak, The relationship between deposition conditions, the beta to alpha phase transformation, and stress relaxation in tantalum thin films, J. Appl. Phys. 72 (10) (1992) 4918–4924. doi:10.1063/1.352059.

[41] A. Yohannan, Characterization of Alpha and Beta Phases of Tantalum Coatings, Ph.D. thesis, New Jersey Institute of Technology (2001). doi:10.3141/2100-07.

[42] C. H. Lu, E. N. Hahn, B. A. Remington, B. R. Maddox, E. M. Bringa, M. A. Meyers, Phase Transformation in Tantalum under Extreme Laser Deformation, Sci. Rep. 5 (2015) 1–8. doi:10.1038/srep15064.

[43] M. Lessmann, Non-Ductile Design Of DEMO Divertor Armour: Towards the Probabilistic Reliability Assessment of Brittle Tungsten Components in their Irradiated State, Ph.D. thesis, The University of Manchester (2016).

[44] European Committee of Standardization, CWA 15627:2007 (E) Small Punch Test Method for Metallic Materials (2007).

[45] A. Husain, R. Sharma, D. Sehgal, Small Punch and Indentation Tests for Structural Health Monitoring, Procedia Eng. 173 (2017) 710–717. doi:10.1016/J.PROENG.2016.12.157.

[46] D. Hancock, D. Homfray, M. Porton, I. Todd, B. Wynne, H. Robinson, H. Lewtas, R. Bamber, Testing Advanced Divertor Concepts for Fusion Power Plants Using a Small High Heat Flux Facility, (Article Prep.

[47] J. Yang, J. Li, Fabrication and Analysis of Vanadium-Based Metal Powders for Selective Laser Melting, J. Miner. Mater. Charact. Eng. 06 (01) (2018) 50–59. doi:10.4236/jmmce.2018.61005.

[48] M. Fursdon, T. Barrett, F. Domptail, L. M. Evans, N. Luzginova, N. H. Greuner, J.-H. You, M. Li, M. Richou, F. Gallay, E. Visca, The development and testing of the thermal break divertor monoblock target design delivering 20 MW m^{-2} heat load capability, Phys. Scr. T170 (2017) 014042. doi:10.1088/1402-4896/aa8c8e.

[49] United Kingdom Atomic Energy Authority, UKAEA launches National Fusion Technology Platform (2018).
URL https://www.gov.uk/government/news/ukaea-launches-national-fusion-technology-platform

5

Paper:
“Testing Advanced Divertor Concepts for Fusion Power Plants Using a Small High Heat Flux Facility”

Context within thesis

To meet the goal of establishing the viability of using AM for fusion HHF components, this paper presents contributions to the testing and qualification process.

Novelty

- developing and employing a new testing methodology and philosophy for fusion HHF components focussed on comparative validation prior to more comprehensive qualification
- comparative testing of AM and conventional fusion HHF components

Lead author contributions

- technical lead for design, build, commissioning, and testing of HIVE facility
- contributions to high heat flux concept generation and manufacture
- undertaking finite element analysis and 1D calculations to predict performance
- analysing results
- identifying future opportunities
- all writing

Publication status

This paper was submitted to "ASTM Journal of Testing and Evaluation" on 19$^{\text{th}}$ June 2018.
This paper has been re-typeset and additional material included for thesis submission

Approval status

Co-authors and supervisors:	Internal	(REVIEWED)	External	(REVIEWED)
UKAEA:	C. Waldon	(CLEARED)	E. Surrey	(CLEARED)
EUROfusion:	K. Gal	(ENDORSED)	T. Donne	(CLEARED)
AMAZE (notification only):	D. Wimpenny	(RELEASED)	M. Holden	(RELEASED)

Testing Advanced Divertor Concepts for Fusion Power Plants Using a Small High Heat Flux Facility

David Hancock[a,b,*], David Homfray[a], Michael Porton[a], Iain Todd[b], Brad Wynne[a,b], Rob Bamber[a], Kieran Flinders[a], Paul Jepson[a], Heather Lewtas[a], Harry Robinson[a]

[a] *United Kingdom Atomic Energy Authority, Culham Science Centre, Abingdon, Oxon, OX14 3DB*
[b] *University of Sheffield, Department of Materials Science and Engineering, Sir Robert Hadfield Building, Mappin Street, Sheffield, S1 3JD*

Abstract

The development of improved designs for components which will be subject to high heat fluxes has been identified as a critical challenge for the realisation of commercial fusion power. This paper presents details of a facility which allows early verification of thermofluid and thermomechananical performance of prototype components and enables comparison between concepts and manufacturing methods. This provides a validation step between in silico design and analysis and high-cost particle beam testing which is the usual qualification method for fusion high heat flux components.

As part of AMAZE, an European FP7 project aiming to grow confidence in additive manufacturing, prototype divertor structural and armour elements were manufactured in copper and tungsten respectively using both conventional machining and a range of AM techniques. In order to assess the comparative performance of these conventional and AM prototypes, a small high heat flux facility has been designed and built at the Culham Centre for Fusion Energy in Oxfordshire. This facility, HIVE (Heating by Induction to Verify Extremes), consists of a 45 kW high frequency induction heating system, 200 °C, 20 bar closed-loop water cooling, a 500 mm diameter vacuum vessel, and bespoke control and instrumentation system. Water flow, temperature, and pressure transducers provide calorimetry and thermofluid performance measurement, while embedded thermocouples and thermal imagery allow comparisons with finite element thermal models and between samples.

The design and key features of this facility and the results of testing carried out under AMAZE are presented, highlighting both the promise of AM as a manufacturing technique for fusion high heat flux components and the value of these low-cost, short-timescale tests in initial down-selection and preliminary validation of concepts. In addition, future plans for HIVE are presented, including other test campaigns post-AMAZE and associated diagnostic and operational upgrades.

Keywords: additive manufacturing, fusion, high heat flux, divertor, DEMO, testing

1. Introduction

The development of improved designs for components with higher heat flux handling capability (>20 MW m^{-2}), longer in-service lifetimes (2–3 full-power years), and better thermal efficiency has been identified as a critical challenge for the realisation of commercial fusion power [1]. To meet this need, concepts have been developed for the divertor target, which range from incremental modifications to the baseline solution to be used for the ITER tokamak experiment currently under construction [2], employing a CuCrZr pipe and W monoblock [3], to more novel concepts employing additive manufacturing (AM) of refractory metals as structural and armour materials and employing high temperature coolants [4]. This broad approach to concept generation ranging from conservative to advanced gives breadth to the community and balances the risks associated with novel designs with the potential for significant performance enhancement.

*Corresponding Author
Email address: david.hancock@ukaea.uk (David Hancock)

1.1. Current testing options

The qualification process for fusion high heat flux concepts must involve representative testing. Typically, this includes high heat flux testing using either an electron beam facility such as JUDITH II [5], IDTF [6], or FE200 [7] or an ion beam facility such as GLADIS [8], or Magnum-PSI [9]. Linsmeier et al. [10] give a thorough overview of these and more. These facilities simulate the particle fluxes to which the component is subjected in a fusion device and typically include water or gas cooling at high pressure and temperature. They are particularly well suited to provide detailed data about failure mechanisms in the armour material and damage due to plasma-surface interactions. They include thermal imagery to confirm performance and integrity, and have been used to qualify by experiment components for which design by analysis has not been feasible [11]. The rigour and scale of these tests, however comes at a significant cost and this inevitably impacts the scope for innovation and in some cases the ability to undertake large numbers of experiments either to cover the full range of load cases or to improve statistical significance of data gathered.

1.2. Objectives of the HIVE facility

This paper presents the details of the HIVE facility (Heating by Induction to Verify Extremes), designed to allow early verification of thermofluid and thermomechananical performance of high heat flux components and to allow comparison between concepts and manufacturing methods, typically prior to full component qualification or investigations of plasma surface interactions using the facilities described above.

This approach is particularly attractive when investigating concepts produced via additive manufacturing as it allows a rapid evaluation of concepts which can include novel features or materials and can quantitatively measure the impact of geometric or material property variation. In addition, the ability to carry out high numbers of thermal cycles allows the investigation of thermomechanically induced damage mechanisms, including the potential to carry out interrupted testing to explore the evolution of this damage. The primary goals of HIVE are as follows:

- to test components under fusion relevant surface heat fluxes in vacuum.
- to provide a high degree of flexibility of component architecture.
- to provide verification of the feasibility of concept designs which use advanced manufacturing processes — specifically to compare the thermal and mechanical behaviour of cooled components to modelling and to compare results from novel and conventionally manufactured components.
- to minimise facility capital and operational costs while allowing scope for future upgrades.

HIVE's initial function has been to assess the comparative performance of conventionally manufactured and AM prototypes produced as part of the AMAZE project[†]. This was a European FP7 project involving a wide range of industrial and academic partners aiming to grow confidence in AM. Prototype divertor structural elements were manufactured in copper using both conventional machining and electron beam melting (EBM), a powder based additive layer process. Tungsten armour tiles were also manufactured using laser powder bed and wire-arc (WAAM) techniques, with the aim of comparing their performance to rolled plate.

Details of the design and key features of the facility are given below as well as the results of testing carried out under AMAZE. This highlights both the promise of AM as a manufacturing technique for fusion high heat flux components and the value of these low-cost, short-timescale tests in initial down-selection and preliminary validation of concepts. In addition, future plans for HIVE are presented, including other test campaigns post-AMAZE and associated diagnostic and operational upgrades.

[†]http://amazeproject.eu

2. The HIVE facility

2.1. Overview

Central to the design rationale of HIVE has been the desire to employ commercial off-the-shelf systems as far as possible. This is to ensure robustness of performance and reliability, to reduce design overheads, and to provide access to ongoing maintenance and repair. Furthermore, capacity has been included wherever possible for upgrade and extension to allow increases in performance or alterations in usage in the future. Figure 1 shows an overview of the HIVE facility, the core elements of which are described in more detail in the following sections.

2.2. Location and infrastructure

HIVE is located within a building adjacent to the Joint European Torus (JET) on the Culham Science Centre site in Oxfordshire, UK, with existing power and services infrastructure, in close proximity to extensive specialist workshop facilities. This has not only provided significant capital cost savings during the procurement and commissioning phase of the facility, but will continue to ensure affordable and timely access to technical support for users in the periods leading up to and during operations.

Power is provided directly from the existing 415 V three-phase supply, with two dedicated feeds installed to supply the high-power requirements of heating and cooling systems and to support the remaining subsystems including the control cubicle and vacuum system. Steel support frames have been manufactured to support the vacuum vessel and heating workhead, and to provide a location for maintenance work to be carried out on the vessel lid assembly, including installation of the sample, coil, and instrumentation.

2.3. Vacuum vessel and sample mounting

The heart of HIVE is a small, bespoke 500 mm diameter by 500 mm high vacuum vessel shown in figure 2. Designed and tested to a leak rate less than 10^{-9} mbar l s^{-1} it is also rated to a positive test pressure of 2 bar absolute, due to the need to retain integrity in the case of sample failure and coolant leak.

A 0.5 bar burst disk with an outlet to the building exterior provides passive protection limiting the possible overpressure in the event of such a failure. Pumping is provided by a 240 l s^{-1} turbomolecular pump with the aim of providing sufficiently high vacuum to duplicate differential pressures and to minimise oxidation of components at elevated temperatures. Without baking the vessel, HIVE currently operates at 2×10^{-7} mbar.

Three 100 mm diameter and one 200 mm diameter equatorially-located ports provide a range of viewing angles through optical and IR transparent windows, while vacuum pumping and monitoring are located on a further two ports.

Figure 3 shows how the test piece and associated service connections are all mounted on the removable

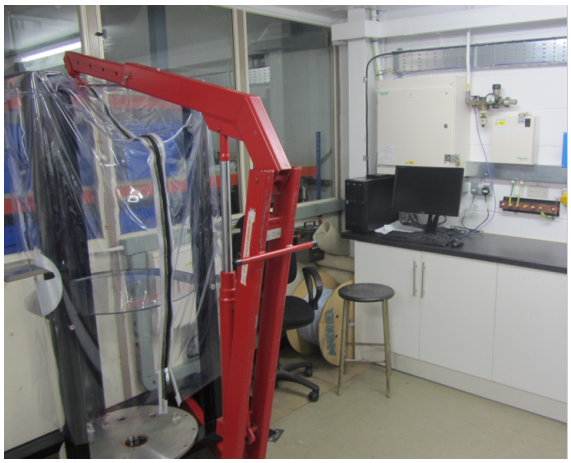

(a) Maintenance frame and control PC

(b) (from left to right) water supply, induction heating, vacuum vessel, and control cubicle

Figure 1: Overview of the HIVE facility

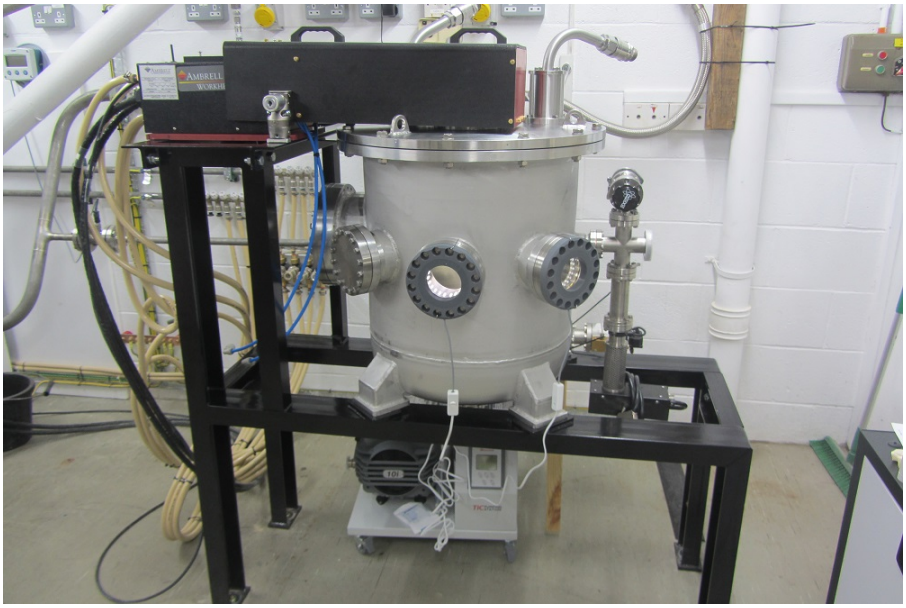

Figure 2: The HIVE vacuum vessel

vacuum vessel lid, allowing maintenance and assembly to be carried out on a conveniently located maintenance frame located adjacent to the vacuum vessel itself.

2.4. Heating

Heating is provided by a 45 kW, 50 kHz to 150 kHz induction heating system supplied by Ambrell Induction Heating Ltd.*. As currently configured, this system provides up to approximately 8 kW of heating power at 80 kHz to the test sample via direct coupling, using a pancake coil arrangement as shown in figure 4.

Coupling efficiency of this kind of coil arrangement is theoretically 25 % – 30 % [12], and factory acceptance testing has confirmed performance at this level achieving to up to 12 kW delivered, equating to 30 MW m^{-2} for an uncooled 20 mm square tungsten piece, but power and pulse length is limited by the current cabling and feedthrough arrangements.

Coils for this system have been designed and procured for a range of sample sizes between 20 mm and 50 mm square, leading to incident heat fluxes between 5 MW m^{-2} for the largest samples and 20 MW m^{-2} for the smallest, allowing for modest transmission losses.

Operation at high frequency ensures that induced current density in the sample surface penetrates less than 1 mm into the surface, simulating a surface heat load similar to divertor and first wall conditions. If acceptable uniformity of heat flux at the armour-structure inter-

*https://www.ambrell.com

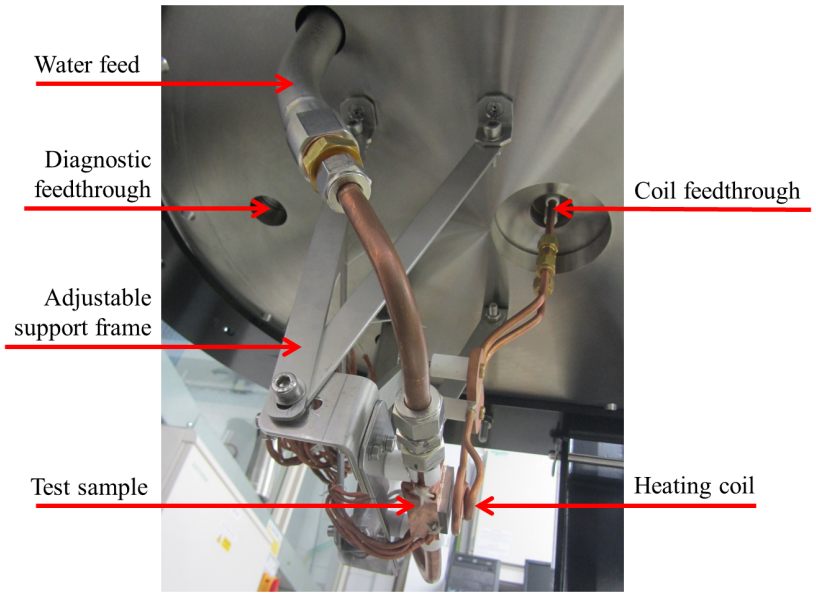

Figure 3: View of vacuum vessel lid from below showing coil and sample mounting arrangement

face of a particular concept cannot be achieved by careful coil shaping and placement, increasing the tungsten thickness slightly will provide a more uniform heat distribution at this interface due to the tungsten's high conductivity, though consideration will need to be made of any resulting impact on component stresses. In addition, this will prevent the direct measurement of peak tungsten temperatures and surface temperature distributions. Alternatively, indirect heating can be employed, as has been used elsewhere [13], though this will significantly reduce the heat flux available.

2.5. Cooling

Water is supplied at up to 80 l/ min between ambient pressure and temperature and 200 °C at 20 bar by a closed-loop Temperature Control Unit (TCU) from ICS Cool Energy Ltd[†] coupled with an external 20 kW chiller. Flow is controlled manually using a combination of in-line and bypass valves. DN40 stainless steel pipework provides low pressure drop between the TCU and flexible quick-release connections to the interface with the test sample. Pneumatically actuated shut-off valves minimise water loss and steam generation in the event of sample failure and pressure relief in the TCU provides additional protection against overpressure. Water temperature, pressure, and flow rate are monitored as described in section 2.6 to provide calorimetry and flow characterisation. The site-supplied water used in the system is chemically monitored and replaced regularly as required.

[†]https://www.icscoolenergy.com

2.6. Instrumentation and control

Instrumentation and control are managed through a local cubicle containing a National Instruments[‡] RIO with a range of modules to handle the digital and analogue inputs and control signals needed. This, in turn, is controlled via a custom LabView^{TM} GUI on a local PC. Installed capacity is larger than current requirements giving scope for further expansion as upgrades occur.

Safety aspects of the facility are designed to be exclusively passive, but plant protection logic is included on the inbuilt FPGA giving low latency, deterministic protection. The cubicle has full control of the heating, cooling, and vacuum systems, as well as the ability to control shut-off valves in the water line and a gate valve between the vacuum vessel and turbo pump.

Water flow-rate and inlet and outlet pressure and temperature measurements from the TCU are supplemented by high-accuracy transducers placed in-line close to the sample. Sample temperatures are monitored by a combination of IR thermography and K-type thermocouples mounted externally and percussion welded into drilled pockets using well established JET practice. Heating power and frequency are recorded from the RF generator itself. Vacuum monitoring employs a combination Pirani and inverted magnetron wide range gauge for pressure measurement and a residual gas analyser for leak testing and detection of outgassed material has recently been installed.

[‡]http://www.ni.com

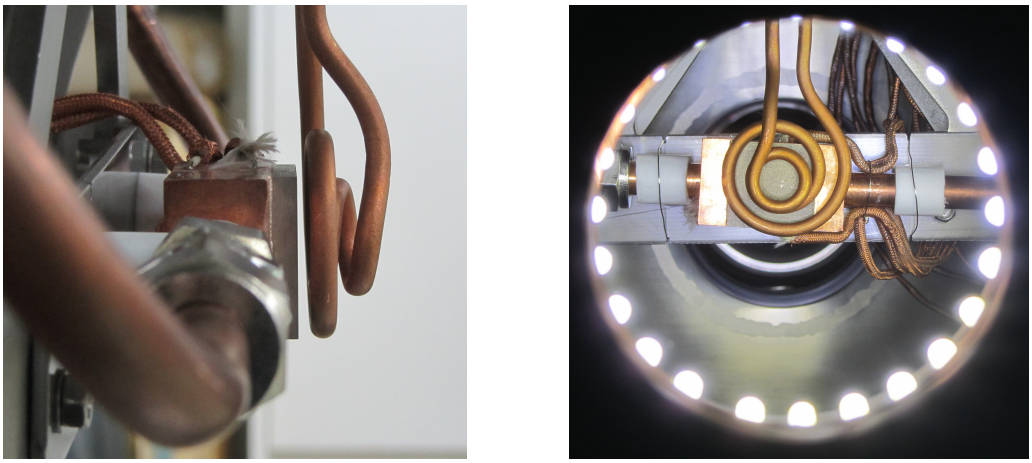

(a) side view (b) front view

Figure 4: Coil and sample arrangement side and front views

3. Commissioning and first results

As outlined in section 1, the motivation for creating HIVE was primarily driven by the desire to test AM high heat flux components for the AMAZE project. However, in order to allow safe commissioning, characterisation of the performance of HIVE, calibration of transducers, and direct comparisons between AM and conventional technology, a stepwise approach was taken to test component design, beginning with a well understood combination of materials, cooling geometry, and manufacturing techniques before aiming to progress to a fully AM refractory component with complex cooling geometry. Unfortunately, due to limitations of the additive processes used and project time constraints, only the first steps along this progression have been completed to date. Further details of the design and manufacture of the additive components for AMAZE are included in [4] and chapter 4.

3.1. Sample design and manufacture

First, a simple, conventionally manufactured "commissioning" sample was tested to the rear and sides of which a number of thermocouples were percussion welded. This was subsequently followed by a similar component with embedded rather than surface mounted thermocouples and finally a component in which the copper block was manufactured by researchers at FAU Erlangen using electron beam melting on an ARCAM system [14]. These parts, the geometry of which is shown in figure 5, consisted of a 30 mm × 20 mm × 50 mm copper block brazed to 10 mm internal diameter copper feed pipes and 30 mm × 30 mm × 5 mm tungsten armour.

The vacuum brazing technique developed for this component and tested on both AM and conventional material allowed the joining of both pipes and armour to the central copper block in a single brazing cycle.

Prior to installation in HIVE, these components were helium leak tested to 10^{-9} mbar l s^{-1} and hydraulically

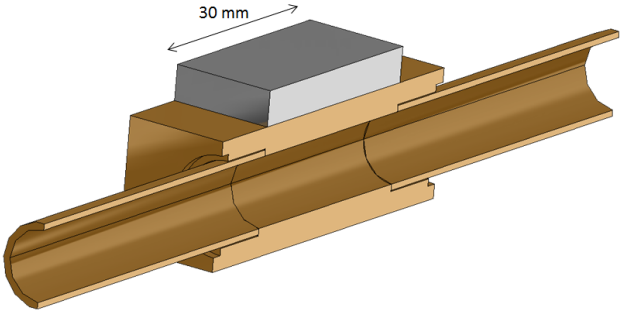

Figure 5: Geometry used for HIVE commissioning and AMAZE testing

pressure tested to 40 bar at room temperature. The calculation of test pressure (Equation 1) is drawn from the ITER structural design criteria for in-vessel components [15],

$$P_t = 1.25 P_d \frac{S_m(T_t)}{S_m(T_d)} \tag{1}$$

where P_t and P_d are test pressure and design pressure respectively and $S_m(T_t)$ and $S_m(T_p)$ are the allowable stresses at test and design temperatures. This allows verification of component integrity at elevated temperature with testing at room temperature.

It is important to note that, in contrast to the final AMAZE concepts, the geometry chosen for comparison is not optimised for high performance and is limited by the low operational window of the pure copper structure, the simple pipe cooling geometry, and the high thermal mismatch stress at the copper-tungsten interface.

3.2. Testing method

An operational window was defined for test components based on finite element analysis and heat transfer correlations in accordance with established methods for

ITER components [16]. In this case, conservative limits were applied using margins to critical heat flux and plastic strain in the copper component. These limits were then converted to operational limits defined by coolant parameters and measured temperatures in both structure and coolant.

Samples were subjected to heat fluxes up to $3\,\mathrm{MW\,m^{-2}}$ with coolant at 20 °C and 50 °C and the resulting temperature distributions were compared to one another and to empirical calculations and the aforementioned finite element models. Figure 6 shows indicative thermal and visual imagery of one such component under test in HIVE.

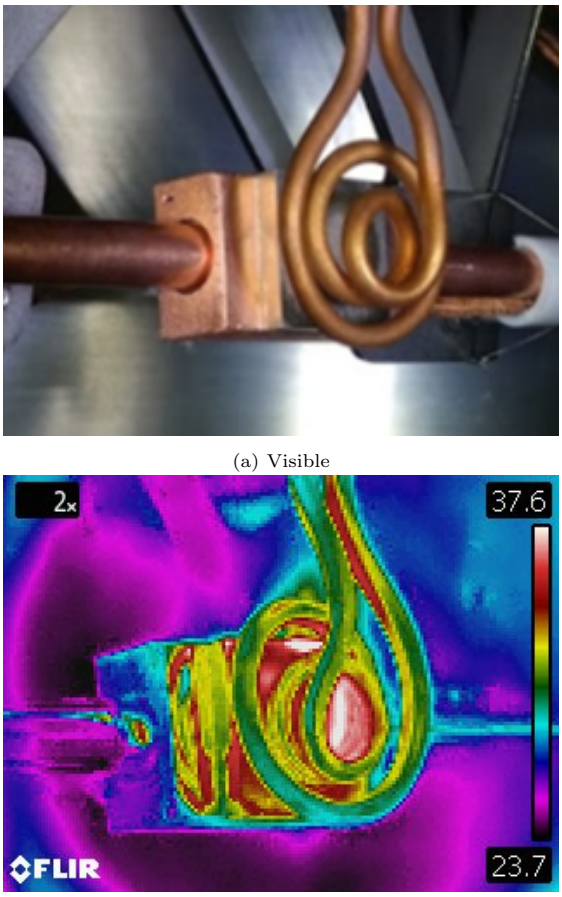

(a) Visible

(b) IR

Figure 6: Visible and IR images of AMAZE AM component being tested in HIVE under low heat flux

Data was recorded from a total of six K-type thermocouples: four embedded in pockets in the copper and two mounted on the rear surface. Figure 7 shows the location of the thermocouple used for comparison of maximum sample temperature.

Figure 8 shows a representative signal plot during a typical HIVE pulse, including thermocouple readings and supplied power[§].

[§]Thermocouples here are given a three letter designation describing location within the sample: (t)op, (m)iddle, (b)ottom; (i)nlet, (m)iddle, (o)utlet; and (f)ront or (b)ack. Power is as reported at the generator, before transmission losses which, in this case, were as much as 90%.

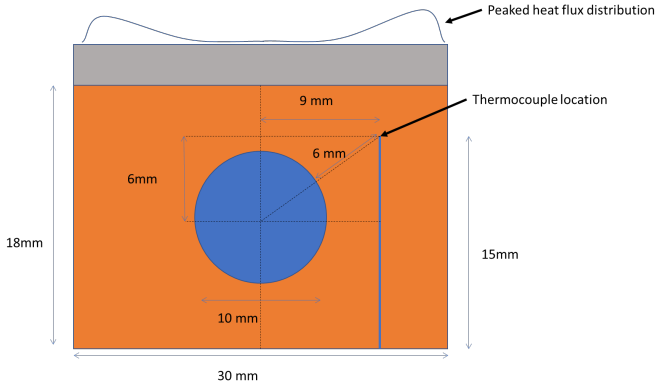

Figure 7: Thermocouple location and illustration of heat flux peaking (midplane cross section)

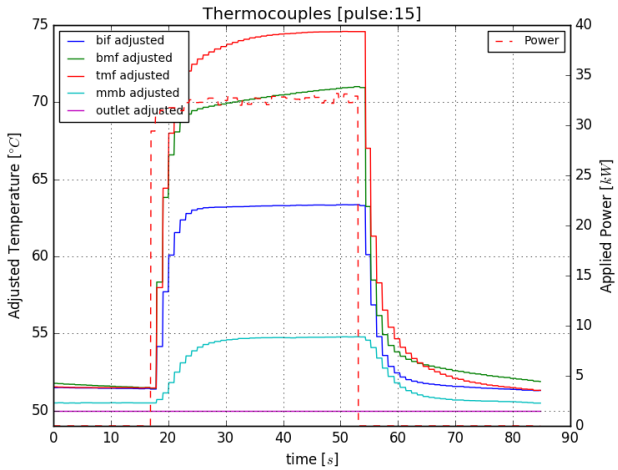

Figure 8: HIVE pulse graphs

3.3. Results

Figure 9 shows the maximum temperature in the copper structure at the point described above with varying power, given the same coolant conditions for each sample (in this case 50 °C water with a flow rate of 40 l/ min). 1D analytical calculations varying copper thermal conductivity and heat transfer coefficient were used to plot structural temperature vs input power and were compared with the experimental data to determine the driving mechanisms for performance differences between the AM and conventional components. An additional correction factor was used to take into account the non-uniformity of the applied heating.

The increased peak structural temperature of up to 15 °C shows that the AM sample does not perform as well as the conventional. The modelling suggests that the primary cause of this degradation is likely to be significant decrease in the thermal conductivity of the component by

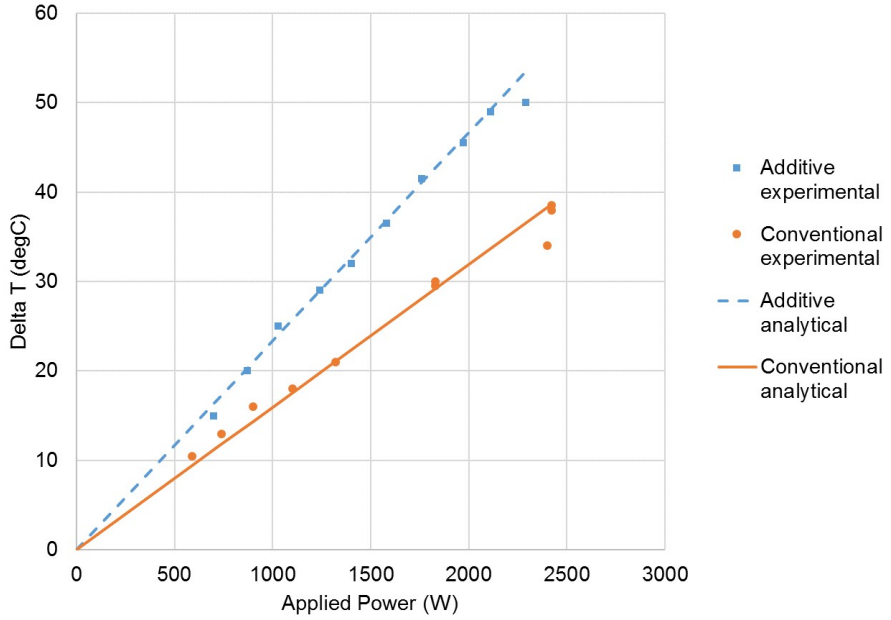

Figure 9: Maximum temperature increase in AM and conventional high heat flux samples with delivered power, compared to 1D analytical estimates

approximately 60 %. This reduction in thermal conductivity has yet to be compared with material property testing but although near ideal properties have previously been reported when sufficiently pure raw material is used[17], in this case significant phosphorous impurities were found to be present in the powder used, and this is likely to be a contributing factor to a reduction in the conductivity of the copper. Impurities cannot completely explain the degree of reduction, however. The vacuum-tightness and low outgssing of the sample suggests there is not signifcant porosity, and so there are likely to be additional factors involved. The most likely candidate is poor braze wetting at the copper-tungsten interface — to be confirmed by post-test sectioning and examination.

Applying a 20 % increase in the heat transfer coefficient between additive and conventional samples to the analytical calculation results in a further improvement in the correlation between modelling and experiment. This corresponds reasonably well to analytical estimates based on surface roughnesses of around 50 µm, similar in magnitude to the size of powder used, but will need to be verified by further testing. The difference in temperature readings between top and bottom thermocouples shown in figure 8 is the result of misalignment in the heating coil for this particular sample and improved coil design and placement have been shown to improve this significantly in subsequent tests. Uncertainties in calculating the applied heating distribution are the subject of an ongoing investigation and effects such as variation in braze joint quality are not included in the modelling, so will need to be resolved before the conclusions presented above can be considered more than preliminary.

4. Future work

4.1. Castellated tiles

Divertor tile armour is typically castellated to reduce thermal stress and to lengthen paths for induced currents during disruptions. A test programme is therefore underway to investigate the impact of such castellations on induction heating efficiency and homogeneity of heat flux with the existing coil design in HIVE. Figure 10 shows images of this testing.

4.2. Ongoing proposals

Water cooled tests were the primary goal of HIVE, but uncooled tests during commissioning highlighted the usefulness of in-vacuum thermal cycling and plans are in place to investigate a number of tungsten coating technologies including vacuum plasma spraying, cold spray, and electrodeposition. The modular nature of the cooling system has also prompted proposals for CFD validation experiments and tests using alternative coolants, including nanofluids.

4.3. Upgrades and inclusion in new facilities

Future work will be supported by more detailed virtual engineering modelling and enhanced diagnostics, including high resolution IR thermography, digital image correlation measurements of strain, and spectroscopy of any outgassing from samples. A wider programme of upgrades, including integration into a newly announced Fusion Technology Facility (FTF) at UKAEA Culham, itself part of the more significant National Fusion Technology Platform (NFTP), includes the potential for duplicating the core concept of HIVE as a small component validation

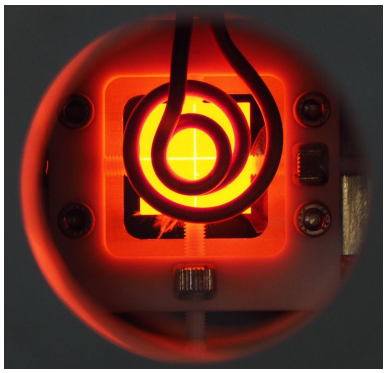

(a) Visible

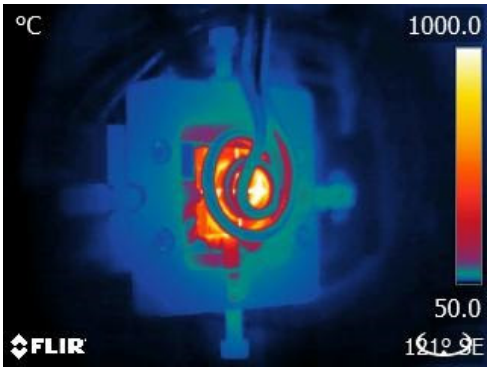

(b) IR

Figure 10: Visible and IR images of an uncooled castellated tungsten tile being tested at 1000 °C

platform to allow parallel and extended duration testing under a range of conditions.

5. Conclusions

HIVE, a new small high heat flux facility has been designed and built at the Culham Centre for Fusion Energy. This facility provides a strategic resource, lying between in silico design and analysis and full scale particle beam or plasma-surface interaction testing. In particular, HIVE has demonstrated low operational and capital cost, high flexibility, and rapid sample turnover. HIVE has been used to test the first fully additively manufactured divertor target element prototype as part of the AMAZE project. These tests have provided direct comparison between additive and conventional components, using a simple, well-understood cooling geometry.

Performance degradation in the additive sample has been attributed to 60 % lower thermal conductivity in the EBM copper compared to the conventional material, though evidence from empirical calculations points towards up to 20 % increased convective heat transfer due to the rough internal surfaces. Further research is required, however, to verify these conclusions.

Future upgrades to HIVE, in part facilitated by its key role in the UK fusion technology research programme, are planned to extend its capability and a number of experimental campaigns are planned to demonstrate HIVE's potential contribution to a range of fusion and related applications.

Acknowledgements

This work has been carried out within the framework of the EUROfusion Consortium and has received funding from the Euratom research and training programme 2014-2018 under grant agreement No 633053. This project has also received funding from the European Union's Seventh Framework Programme for research, technical development, and demonstration under grant agreement no 313781. The views and opinions expressed herein do not necessarily reflect those of the European Commission. This work has also been part-funded by the RCUK Energy Programme [grant number EP/P012450/1]. To obtain further information on the data and models underlying this paper please contact publicationsmanager@ccfe.ac.uk.

References

References

[1] F. Romanelli, Fusion Electricity: A roadmap to the realisation of fusion energy, Tech. rep., EDFDA (2012). doi:ISBN978-3-00-040720-8.

[2] N. Holtkamp, et al., An overview of the iter project, Fusion Engineering and Design 82 (5-14) (2007) 427–434.

[3] J. H. You, G. Mazzone, E. Visca, C. Bachmann, E. Autissier, T. Barrett, V. Cocilovo, F. Crescenzi, P. K. Domalapally, D. Dongiovanni, S. Entler, G. Federici, P. Frosi, M. Fursdon, H. Greuner, D. Hancock, D. Marzullo, S. McIntosh, A. V. Müller, M. T. Porfiri, G. Ramogida, J. Reiser, M. Richou, M. Rieth, A. Rydzy, R. Villari, V. Widak, Conceptual design studies for the European DEMO divertor: Rationale and first results, Fusion Eng. Des. 109-111 (PartB) (2016) 1598–1603. doi:10.1016/j.fusengdes.2015.11.012.

[4] D. Hancock, D. Homfray, M. Porton, I. Todd, B. Wynne, Exploring Complex High Heat Flux Geometries for Fusion Applications Enabled by Additive Manufacturing, Fusion Eng. Des. in press.

[5] P. Majerus, R. Duwe, T. Hirai, W. Kühnlein, J. Linke, M. Rödig, The new electron beam test facility JUDITH II for high heat flux experiments on plasma facing components, Fusion Eng. Des. 75-79 (2005) 365–369. doi:10.1016/j.fusengdes.2005.06.058.

[6] V. Kuznetsov, A. Gorbenko, V. Davydov, A. Kokoulin, A. Komarov, I. Mazul, B. Mudyugin, I. Ovchinnikov, N. Stepanov, R. Rulev, A. Volodin, Status of the IDTF high-heat-flux test facility, Fusion Eng. Des. 89 (7-8) (2014) 955–959. doi:10.1016/j.fusengdes.2014.04.064.

[7] P. Gavila, B. Riccardi, S. Constans, J. L. Jouvelot, I. B. Vastra, M. Missirlian, M. Richou, High heat flux testing of mock-ups for a full tungsten ITER divertor, Fusion Eng. Des. 86 (9-11) (2011) 1652–1655. doi:10.1016/j.fusengdes.2011.02.012.

[8] H. Greuner, H. Bolt, B. Böswirth, T. Franke, P. McNeely, S. Obermayer, N. Rust, R. Süß, Design, performance and construction of a 2MW ion beam test facility for plasma facing components, Fusion Eng. Des. 75-79 (2005) 345–350. doi:10.1016/j.fusengdes.2005.06.021.

[9] G. De Temmerman, M. van den Berg, J. Scholten, A. Lof, H. van der Meiden, H. van Eck, T. Morgan, T. de Kruijf, P. Zeijlmans van Emmichoven, J. Zielinski, High heat flux capabilities of the Magnum-PSI linear plasma device, Fusion Eng. Des. 88 (6-8) (2013) 483–487. doi:10.1016/J.FUSENGDES.2013.05.047.

[10] C. Linsmeier, B. Unterberg, J. Coenen, R. Doerner, H. Greuner, A. Kreter, J. Linke, H. Maier, Material testing facilities and programs for plasma-facing component testing, Nucl. Fusion 57 (9) (2017) 092012. doi:10.1088/1741-4326/aa4feb.

[11] G. Pintsuk, M. Bednarek, P. Gavila, S. Gerzoskovitz, J. Linke, P. Lorenzetto, B. Riccardi, F. Escourbiac, Characterization of ITER tungsten qualification mock-ups exposed to high cyclic thermal loads, Fusion Eng. Des.doi:10.1016/j.fusengdes.2015.01.037.

[12] S. L. Semiatin, Elements of Induction Heating: Design, Control, and Applications, ASM International, 1988.

[13] S. A. Musa, B. Zhao, S. I. Abdel-Khalik, M. Yoda, Reversed Heat Flux Study of Impinging-Jet Water Cooling for Helium-Cooled Finger-Type Divertors, Fusion Sci. Technol. (2017) 1–6doi:10.1080/15361055.2017.1333829.

[14] M. A. Lodes, R. Guschlbauer, C. Körner, Process development for the manufacturing of 99.94% pure copper via selective electron beam melting, Materials Letters 143 (2015) 298–301. doi:10.1016/j.matlet.2014.12.105.

[15] Structural Design Criteria for In-Vessel Components (SDC-IC), ITER Doc. G 74 MA 8 01-05-28 W0.2.

[16] T. Barrett, S. McIntosh, M. Fursdon, D. Hancock, W. Timmis, M. Coleman, M. Rieth, J. Reiser, Enhancing the DEMO divertor target by interlayer engineering, Fusion Eng. Des. 98-99 (2015) 1216–1220. doi:10.1016/j.fusengdes.2015.03.031.

[17] S. J. Raab, R. Guschlbauer, M. A. Lodes, C. Körner, Thermal and Electrical Conductivity of 99.9% Pure Copper Processed via Selective Electron Beam Melting, Adv. Eng. Mater.doi:10.1002/adem.201600078.

6

Conclusions: Summary and Future Research

1 Conclusions

Improved high heat flux component design and realisation is one of the most keenly felt challenges on the path to commercialisation of fusion energy. AM is an emerging technology with the potential to facilitate novel designs and the use of new materials. This project has aimed to address the former need with the latter solution. Recognising that both fusion high heat flux component design and additive manufacturing are highly multidisciplinary and integrated problems, the project has adopted a broad and holistic approach addressing as many aspects of the problem as possible in parallel. To achieve this, the core research activities have been material selection, geometry design, AM process development, and concept validation and testing. New approaches for undertaking each of these have been proposed and demonstrated and tools and methodologies developed for future use while simultaneously adding to the general corpus of knowledge at each stage. Detailed conclusions have been given at the conclusion of each of the previous chapters, and so rather than duplicate those explanations, a collection and summary of more general outcomes are given here:

Material choice
Baseline high heat flux designs for current and future fusion devices draw from a limited palette of materials; principally the result of historical inertia and a linear approach to selection criteria with an emphasis on avoiding brittleness and activation. By systematically listing these criteria (including practical considerations including cost, availability, and manufacturability), then re-evaluating and applying a more parallel approach with more of an emphasis on high temperature operation, compatibility with tungsten armour, and advanced manufacturing techniques including AM, new alternatives have presented themselves. In particular, a number of refractory metals including those based on tungsten, tantalum, molybdenum and vanadium have emerged or re-emerged as potential candidates worthy of consideration.

This process has focussed on elemental and unirradiated materials, but has highlighted the potential performance increases that could be achieved by developing refractory alloys specifically tailored for fusion and AM applications and has shown the inevitable compromises that must be made in the absence of an ideal solution, particularly (and most controversially) when it comes to choosing materials on the basis of their activation under irradiation. An additional compromise that is likely to be necessary is acknowledging the inevitability of embrittlement under irradiation and exposure to hydrogen and helium, and recognising that high performance designs are likely to require new design and analysis tools to accommodate this. The lack of fusion relevant (i.e. 14 MeV neutron) irradiated data for current candidate materials is not news to anyone designing for fusion, but it is hoped that even with the limited time and resources available space is made within the various research programmes for including some of the refractory alloys proposed here.

Geometry design
The freedom of geometry that AM provides, while by no means unlimited, vastly widens the potential range of concepts available to high heat flux designers. Although currently a costly alternative to traditional techniques in many cases, the materials under consideration have very high melting points and are generally very difficult to machine, forge, or cast. In addition, AM (and LPBF in particular) enables complex internal geometries with the potential of improved heat transfer and thermohydraulic performance over current designs. Beyond these, additional potential gains include the possibility of functionally grading joints between dissimilar materials, the inclusion of integrated manifolding to reduce joints overall, and the reduction of total material used which in turn reduces raw material cost, wastage, and the weight of parts which must be manipulated by remote handling.

This project has aimed to demonstrate that such freedom of material and geometry can indeed lead to higher performance and/or provide these additional benefits. Rather than present a complete prototype, two sample geometries have been developed representing two different concept families. The first uses multiple small cooling channels to provide higher heat transfer, more even cooling, and lower structural stress. The second uses a pin-fin heat exchanger concept with similar goals. The analysis has shown the need for optimisation, design refinement, and experimental validation of heat transfer coefficients and pressure drop relationships before significant heat flux handling improvements from these concepts can be claimed, but has demonstrated their potential nonetheless, particularly in the areas of high temperature operation. The benefits of reduced overall material use, reduced stress between armour and substructure, and reduced joint number have been much more clearly shown.

AM process development
Industrial confidence in AM is growing apace in the aerospace and medical fields and to a lesser extent in the automotive industry but, with a few notable exceptions, the AM of refractory metals as structural materials has yet to be extensively developed. Having identified the potential for their use in fusion high heat flux components, this project has contributed to the effort to develop refractory AM prototypes both as part of collaborative efforts and independently. This project has primarily focussed on LPBF of tungsten, molybdenum, and tantalum, while partners have progressed LPBF of vanadium, EBM of copper and tungsten, and WAAM of tungsten, molybdenum, and tantalum. The state

of the art of these technologies has been summarised, and key research needs identified. A broad approach has been adopted examining each aspect of the process from feedstock to prototype testing.

Each AM technology (namely LPBF, EBM, and WAAM) have been shown to have different strengths and weaknesses with differing potential applications as a result. The ability to produce complex internal geometries with fine tolerances makes LPBF most attractive for cooled structures. For depositing armour material quickly both for initial manufacture and repair, WAAM shows promise. EBM has been a useful tool for producing test geometries in copper and may prove more successful than LPBF with tungsten if a method can be found for removing powder from small channels.

The lack of a robust refractory powder supply chain has hampered progress, but by attempting to undertake build trials, material testing, geometry trials, and component testing even with the limited quantity and variable quality of the powder available, it has been shown that simply having high quality powder will not immediately facilitate high quality AM material. Persistent cracking in molybdenum and tantalum has been an ongoing challenge for this project and similar difficulties have been reported elsewhere. Strategies for preventing this have been identified, including heating the build platform to reduce residual stresses, improving atmosphere control to reduce oxidation, and including alloying elements to improve ductility. The desire for a higher temperature heated bed and better atmosphere control suggest the need for an AM platform more specifically tailored for high temperature materials. This is further supported by the mounting evidence that these materials have a particularly narrow processing window and are less forgiving of variable laser parameters than e.g. titanium alloys or steel. An AM platform focussed on high temperature materials would, therefore, also need very well defined and fine grained build parameter control.

The scope of this project prevented investigation of post build heat treatment. There is some evidence from preliminary results in this project that even relatively low temperature heating may be of use in improving density, though the data is sparse. Tantalum, in particular, also showed evidence of unexpected phases present in as-built material and care will needed to take this into account for future work.

The adoption of AM across industries is being supported by corresponding work to develop applicable codes and standards. This is not yet the case for AM for nuclear fusion, though nuclear fission has begun to consider AM in some cases. If AM parts are to be included in DEMO or subsequent commercial fusion power plants, early inclusion in standards is vital, best achieved by pro-active involvement by fusion researchers in existing standards committees.

Concept validation and testing

Concepts introducing complex cooling geometries, new materials, and new manufacturing techniques all together require some kind of experimental feasibility testing and validation before they can begin to be considered as serious candidates and effort can be expended to progress their technology readiness level through more extensive representative testing and comprehensive qualification. In addition, AM lends itself well to quick turnover of concept prototypes and experimental validation alongside analytical predictions.

This project has sought to build confidence in fusion high heat flux concepts employing AM by developing and demonstrating a small high heat flux testing facility specifically designed for this purpose. The HIVE facility employs a combination of largely off-the shelf subsystems to provide a robust and cost-effective technology and component validation tool for evaluating water-cooled high heat flux components in vacuum. Comparison tests between conventional and AM copper and tungsten components have been undertaken, using simple well-understood geometries. Analytical calculations have been used to show that the rough surface of the AM parts has improved convective heat transfer by as much as 20%, though the reduced thermal conductivity of the AM material compared to the conventional reduced overall heat flux handling capability.

2 Project Proposals

To assist with meeting the strategic needs identified above, a selection of brief project descriptions are given below to act as a resource on which to draw for future research.

Development of Refractory Alloys Tailored for use with Additive Manufacturing for Fusion Applications
Work to develop additive manufacturing (AM) of refractory metals for fusion high heat flux applications has thus far been limited to elemental materials. Other alloys have been identified, including TZM, V-4Cr-4Ti, and several Ta alloys developed for space reactor applications such as T-111 and T-222. These (or variants on these) may have significant advantages over their elemental parents, particularly high temperature ductility, oxidation resistance, and strength which may improve their suitability both for AM and for use in fusion. This project builds on the experience of the partners to produce feedstock in the relevant materials and undertake AM process trials. If feasible, modifications to the alloys will be tried.

AM Process Sensitivity to Feedstock Specification
"Traditional" size, chemistry, and morphology requirements for AM powder are usually "best effort" rather than defined as windows. Vigorous debate exists about whether these are all equally important and the extent to which they are wide windows. This project will take a range of powders (possibly for more than one material) with a range of characteristics and compare the impact of varying parameters. The controlled and tailored production of these powders may be facilitated by the proprietary capability at partner organisations.

Thermo-fluid optimisation and validation of complex cooling geometries for high heat flux components enabled by additive manufacturing
Advanced HHF concepts have been suggested as part of AMAZE and other PhD work. Some development and testing has been carried out but they have not been fully optimised or characterised. This project would employ CFD, prototyping, and HIVE testing to further develop these advanced HHF concepts.

Development of an additive manufacturing platform for high temperature materials
The majority of commercial interest in LPBF has, thus far, been focussed on aerospace titanium alloys, nickel superalloys and steel. More recently, AM of refractory alloys including those based on tungsten, molybdenum, vanadium, and tantalum has been identified as a potential tool for high temperature applications including fusion reactor high heat flux components and satellite propulsion. The high melting point, inherent brittleness, and propensity for oxidation of these materials make it challenging to achieve full densification while simultaneously suppressing of cracking induced by thermal stress and powder surface contamination. In addition, it has become clear that the processing window for build parameters may be significantly smaller. Lastly, the high density and cost of refractory powders means that processing is usually carried out at a smaller scale than, for example titanium.

Overcoming these challenges would be significantly helped by the provision of an AM platform more specifically tailored to these requirements, perhaps focussing on one or more of the following features: It has been shown that a heated build platform can be used to suppress residual stress and cracking, but this has been limited to a few hundred degrees whereas approaching 1000 °C would both ensure the ductility of the materials and reduce the thermal gradients through parts. The degree of atmospheric monitoring and atmosphere control varies between AM manufacturers and platforms, and improving this or even operating in partial vacuum could contribute to prevention of oxidation. Small build volume machines are currently available, but these generally come with lower power heating and are more focussed on precious metals rather than experimental development work. A smaller machine with the capacity for dense powders and with design features to enable easy cleaning between different materials would further facilitate refractory metal research.

This project would aim to work either with an AM platform manufacturer or independently to verify the efficacy of these features and to integrate them into a dedicated AM machine for high temperature materials.

Development of functionally graded refractory metal joints for fusion high heat flux applications using additive manufacturing
WAAM and powder work under AMAZE to produce a functionally grade joint has shown some promise, but only preliminary work has been carried out. In particular, the Ta/Mo/W joint at Cranfield could feasibly be optimised. This project would further support the argument for using refractory metals as structural components and could also provide some input to the use of WAAM for in-situ repair.

Qualification of additive manufacturing processes for fusion energy applications
Additive manufacturing (AM) has been identified as a promising tool for developing components for fusion energy applications. AM (particularly of refractory metals) is at a very low technology readiness level (TRL) and to be

employed for fusion power plant high heat flux components both knowledge and experience of using the technology in relevant environments must be significantly advanced. AM includes a chain of highly interdependent steps; from raw material and powder production to component assembly and integration. There are ongoing activities to develop codes and standards for AM for other industries, including considerations for fission applications. Fusion has its own distinct needs, particularly relating to the different neutron spectrum, additional vacuum and fusion gas environment, magnetic fields, and extreme temperatures. This project will develop a proposed series of standards and processes, identifying similarities between and differences from current work.

Appendix A

Software

Materialtools

Description
Materialtools is a set of modules, objects, and functions to import, export, manipulate, and visualise material property data written in Python3. Following the MatML standard for material property data, there is a class for material data, with subclasses for material, property, and parameter. Additional modules provide import-export, visualisation, and calculation tools including the figures of merit used in chapter 2.

Repository: `http://github.com/adlhancock/materialtools`

DOI: `https://doi.org/10.15131/shef.data.6463043`

SLMtools

Description
SLMtools is an extensible, hierarchical, object-oriented package written in Python3 with classes for buildset (multiple related builds to be compared), build parameters, material, and part details. This data can be written to and read from a range of data formats including Microsoft spreadsheets and the open, language-independent, JavaScript Object Notation (JSON) format. Calculation tools included provide simple weld pool modelling, normalised and volumetric energy density calculations and parameter comparisons and conversions between pulsed and steady state laser systems to allow a degree of predictive capability. Input parameters and results such as part density can be visualised and tabulated using included methods and these have been used to support the work reported in chapter 4.

Repository: `http://github.com/adlhancock/SLMtools`

DOI: `https://doi.org/10.15131/shef.data.6463046`

HHFtools

Description
HHFtools is a set of modular calculation tools written in Python3 which can be used to provide first order estimates of thermofluid performance including convective heat transfer and pressure drop for simple high heat flux components. Heat transfer coefficients are calculated using the same set of equations as has been used for ITER divertor and first wall design with parameters for simple tubes, swirl tape inserts, rectangular channels, and hypervapotrons. Similar tools are partially developed for pin-fin arrays and multiple small channels in parallel. These tools were used for scoping designs described in chapter 3 and also to support the design of HIVE and preliminary testing as described in chapter 5.

Repository: `http://github.com/adlhancock/HHFtools`

DOI: `https://doi.org/10.15131/shef.data.6463049`